INTERACTION OF TACKIFIER RESINS WITH WATER-BASED AND OLEFINIC POLYMERS

A Dissertation
Submitted to the Graduate Faculty
of the
North Dakota State University
of Agriculture and Applied Science

By

Puthenkovilakom Rajesh Raja

In Partial Fulfillment of the Requirements
for the Degree of
DOCTOR OF PHILOSOPHY

Major Department:
Coatings and Polymeric Materials

December 2011

Fargo, North Dakota

North Dakota State University

Graduate School

Title

INTERACTION OF TACKIFIER RESINS WITH

WATER-BASED AND OLEFINIC POLYMERS

By

PUTHENKOVILAKOM RAJESH RAJA

The Supervisory Committee certifies that this ***disquisition*** complies with North Dakota State University's regulations and meets the accepted standards for the degree of

DOCTOR OF PHILOSOPHY

SUPERVISORY COMMITTEE:

Dr. Stuart Croll

Chair

Dr. Mark Peters

Dr. Dean Webster

Dr. Chad Ulven

Approved by Department Chair:

01/06/2012 — Date

Dr. Stuart Croll — Signature

ABSTRACT

The objective of this research was to investigate the interaction of tackifier resins in water-based and olefinic polymers for potential pressure sensitive adhesive applications. The first part of this research work was focused on evaluating the usefulness of olefinic block copolymer blends with two amorphous polyolefins (atactic propylene homopolymer and ethylene-propylene copolymer) as potential base polymers for hotmelt pressure-sensitive adhesives. Unsaturated and saturated hydrocarbon resins were studied as potential compatibilizing agents and rheology modifiers. Results show that the chemistry of hydrocarbon resins definitely influence the miscibility of the olefinic block polymer and amorphous polyolefin blends. Ethylene-propylene amorphous copolymer based blends seems to show better miscibility characteristics. Based on the learning from blend miscibility studies, it has successfully made pressure-sensitive adhesives for disposable diaper construction application with olefinic block copolymer/ethylene-propylene amorphous copolymer blends, containing unsaturated hydrocarbon resins and saturated hydrocarbon resins. These olefinic adhesives showed good sprayability characteristics, when applied using air assisted spiral spray equipment (Acumeter Spray Coater) and they showed good adhesive peel properties, which were comparable to the SBS based control.

The second part of the study was focused on the evaluation of natural rubber latex-based pressure-sensitive adhesives (PSA) containing three different C5 aliphatic tackifier dispersions with different softening points. Natural rubber-based, water-borne PSA wet rheology (rheology in liquid state) was correlated to morphological analysis on

a coating and converting stand point. Dry adhesive rheology was also studied and was then correlated to adhesive properties at different conditions. It has been learned that the type and amount of dispersing agents in tackifier dispersions has a major influence in wet rheology of the PSA formulations. Softening point of the dispersion seems to influence the dry adhesive rheology and adhesive properties such as peel, tack and shear.

ACKNOWLEDGMENTS

I express a deep sense of gratitude to my supervisor, Dr. Stuart Croll and my co-adviser Dr. Mark Peters, for their eminent guidance, support, encouragement and valuable advice throughout the course of my studies and research.

I am extremely grateful to Dr. Dean Webster, and Dr. Chad Ulven, of my graduate advisory committee, and Dr. Stephen Orth, Dr. Peter Dunckley, Dr. Brendan Boyd, and Dr. Dawn Mason of Eastman Chemical Company for their support, advice, helpful suggestions and encouragement throughout my research.

I owe sincere thanks to Andrea Hagood, Jill Wilson, Debbie Moroney and Chris Jones of Eastman Chemical Company for helping me to carry out the research work. I am thankful to the analytical support staff of Eastman Chemical Company, especially, George Caflisch, Arved Harding, Kab Sik Seo, Peter Shang, Yuqing Zhou, Dianne Buchanan and Sunny Bhat for their support in obtaining some of the data and analysis. I am also thankful to Scott Payne of USDA-Fargo for TEM evaluations.

Sincere thanks to my colleagues and friends, especially Tim Williams, Allen Crain, Lois Taylor, Alicia Powers, David Arnold, Johnson Thomas, A.J. Pasquale, Carl Eilo, Daniel Klosiewicz, Gary Robe, and Dilhan Fernando for their support, help, and pleasant association throughout the course of this work.

It would be most appropriate at this juncture to express my special thanks to Jacinda Wollan and Carol Johnson for their help and whole-hearted cooperation throughout the course of my studies and work.

DEDICATION

To the almighty god.

To my grandparents, parents, brother, sister, sister-in–law and to my loving and supporting wife, Krishna.

To the enriching scientific community around the world.

TABLE OF CONTENTS

LIST OF TABLES

LIST OF FIGURES

CHAPTER - 1. INTRODUCTION TO PRESSURE-SENSITIVE ADHESIVES AND APPLICATIONS

Introduction

Pressure-sensitive adhesives (PSAs) are a class of soft materials that adhere to different substrates without a chemical reaction under light pressure and short contact times.[1] Even though PSAs are dominated by packaging applications (tapes and labels), they are also widely used for medical applications, baby and feminine hygiene applications, and also for a wide range of office and household applications. Natural rubber-based pressure-sensitive type adhesives have been used for medical applications since 1845, when Day and his colleague improved adhesive plaster using India rubber, turpentine and pine gum.[2] In the 1880s, Robert Johnson, founder of Johnson & Johnson Company, started the commercial manufacturing of natural rubber-based pressure-sensitive medical tapes.[1] 3M pioneered the industrial applications of natural rubber-based pressure-sensitive adhesives in the 1910s starting with masking tapes for automobile painting.[3, 4] In the early 1900s, most of the medical pressure-sensitive tapes based on natural rubber were calendered onto the substrate (thick films), while industrial pressure-sensitive adhesives from 3M were solvent coated onto the backing.[1, 4] Until the 1940s, solvent-borne natural rubber-based pressure-sensitive adhesive technology dominated the market. Most of the early natural rubber-based pressure-sensitive adhesives formulations contained natural rubber as the polymer, petroleum derived and/or rosin-based resin as a plasticizer or tackifier, and a solvent. In 1940 Eustis *et al.* of Kendall Company reported the use of natural rubber latex-based pressure-sensitive adhesive technology with low volatility solvents.[5] Eustis used natural

rubber latex as the polymer, rosin and/or hydrogenated rosin-based resin dispersion as a plasticizer and casein/gum arabic/karaya gum as the protective colloid to improve adhesion of the adhesive to the backing.[5] It is interesting to note that the natural rubber latex-based pressure-sensitive adhesive formulators still depend on some of the above mentioned key ingredients today. According to a 2008 EPA report, 11% of the pressure-sensitive adhesive market is still based on natural rubber[1] and 3% of the total adhesives manufacturing segment remains based on natural rubber.[6]

During World War II, the shortage of natural rubber created a need for synthetic polymers and emulsions. Styrene butadiene rubber, butyl rubber and acrylic rubber emulsions were the prominent technologies in the 1950s and 1960s as synthetic polymers for pressure-sensitive adhesives. Pressure-sensitive adhesive technologies using solvent-based, polyacrylate, synthetic polymers became more popular than the natural rubber-based technologies especially in the medical market[1, 7, 8] because they caused less skin irritation and had superior tack without additives.

By the late 1960s and 1970s, the advent of emulsion-based pressure-sensitive adhesive technologies and 100% solids hotmelt PSA technology surpassed solvent-based technologies due to more stringent health and environmental restrictions.[7, 8, 9] Natural rubber emulsion-based technologies dominated other emulsion technologies until the late 1970s.[9] Availability and economics combined with the technical benefits of water-based acrylic PSAs popularized them in label applications and some medical applications in the early 1980s, and this is still the dominant technology used in water-based PSAs

today.[8] On the other hand, 100% solids hotmelt pressure-sensitive technology was getting more and more popular for pressure-sensitive tape applications in the early 1970s after the development of A-B-A block copolymers by Shell in 1966.[10]

Solvent, hotmelt and water-based pressure-sensitive adhesives are formulated with three major components, polymer, tackifying resins and other additives (plasticizers, stabilizers etc.). The polymer imparts strength and cohesive characteristics to the pressure-sensitive adhesive. Tackifier resins are low molecular weight, high T_g amorphous materials of petroleum origin or naturally derived (pine chemicals). A good tackifier resin should have low molecular weight, sufficient compatibility with polymer type, and have a glass transition temperature (T_g) higher than the base polymer to effectively impart pressure-sensitive adhesive characteristics.[1, 11] In the case of water-based PSAs, the tackifier resin is dispersed in water with the aid of surfactant. Since the late 1970s, the use of rosin-based tackifier resins dispersed into water without the use of solvent has been reported.[1, 9]

Until the late 1960s, much of the art of formulating pressure-sensitive adhesives were known and was considered a trade secret to some of the global adhesive manufacturers. Several text books and publications since then resulted into the promotion and teaching of the technology especially after the introduction of acrylics and A-B-A hotmelt PSA technologies. Harlen[10] reported the first pressure-sensitive adhesive formulation using styrenic block copolymers in 1966. However, the commercial use of 100% solids PSAs did not start until the commercialization of some of the styrene-butadiene-styrene and styrene-isoprene-styrene copolymers, generally known as

styrenic block copolymers (SBCs) in 1972.[12] The main advantage of the SBC polymers is that above the glass-transition temperature (T_g) of styrene, the SBC loses its cohesive strength and can be melt processed. Below this temperature, the styrenic domains greatly increase the cohesion of the system.[12] In 1974, Park[13] reported a hotmelt PSA adhesive composition blend using amorphous polyolefins, styrene-isoprene-styrene block copolymer and polyisobutylene polymer, which improved the low temperature application properties. Crossland and Harlen[30] of Shell Oil Company again reported in 1975 about the manufacture of PSAs using partially hydrogenated A-B-A block copolymer, in which the B block was an elastomeric, hydrogenated block copolymer of conjugated dienes. PSA formulations with improved thermal stability and different molecular weight versions of A-B-A block polymers were then reported by Korpman[31, 32] of Johnson & Johnson Company. There has been a lot of work reported by several researchers since then, and the majority of the hotmelt pressure-sensitive adhesive market (especially tapes and hygiene applications) is still dominated by styrenic block copolymer based systems.

PSAs can be used in a variety of applications such as labels, tapes and nonwoven adhesives applications. Tape applications can be further broken down into masking tape, box sealing tape, protective film tape, and tape in medical applications. Given the wide range of applications involved, the PSAs formulated should withstand different environmental and physical conditions. Therefore, understanding the adhesive properties and mechanical behavior of a PSA in a variety of operating conditions and temperatures is critical.[1]

Normally, pressure-sensitive adhesive properties are characterized in three ways: peel, tack and shear strength (hold power). Evaluation of these properties is critical, since a PSA should adhere to different substrates with no more than finger pressure and should be removed from the substrate surface without leaving a residue. It has been demonstrated that PSA peel adhesion measurements provide more information on expected adhesive performance characteristics than tack or shear measurements. Peel is measured as the force required to remove a PSA. Interfacial and bulk properties of PSAs normally contribute to peel. Separating each element's contributions to the peel is very difficult. Therefore peel force, as reported, are normally the combined effect of these factors. Different models have been established to explain the peel of a PSA. The most commonly used models include a dash-pot model proposed by Voigt, representing the viscous response to stress and a spring model suggested by Maxwell, representing the elastic response to stress. Complex models using the Voigt-Maxwell concepts with various configurations have also been established by other researchers to represent the true viscoelastic behavior of PSA peel.[14-17] The strength of the bond formed between an adhesive and substrate is characterized by measurement of peel strength, the force per unit width required to pull apart two strips of substrate held together by the adhesive as a function of temperature and the rate at which the strips are separated.

Tack can be defined as the ability of the material to adhere instantaneously to a solid surface when brought into contact under very light pressure. Tack is the composite response of the PSA's bulk and surface properties. Tack is normally

measured by the energy required to break the bond.[1, 14-16] Shear or hold power is the force required to pull the PSA from a parallel substrate and is normally reported as a function of holding time. Tack and peel represent the adhesive response of a PSA, while shear represents the cohesive characteristics of the PSA.[14-16] These properties are directly related to pressure-sensitive adhesive response to stress, so tack, peel and shear can be correlated to the stress-strain response of a PSA as explained by Dahlquist in the late 1960s.[18] Many reports followed, correlating viscoelastic performance of PSAs obtained through rheological measurements to adhesive properties such as tack, peel and shear of a PSA.[18-22] The shear modulus (*G'*) of a PSA at room temperature typically ranges between 10^3 and 10^6 Pa, and the T_g of a PSA is typically below 10°C.[23, 24]

Styrenic block copolymers have a T_g that is too low and a shear modulus that is too high at room temperature, and thus the properties of styrenic block copolymers as such is not suitable for most PSA applications. Previous studies have shown that viscoelastic processes and surface wetting characteristics of a PSA can only be activated if the T_g is close to the application temperature. Therefore, for pressure-sensitive adhesive applications, styrenic block copolymers are always formulated with tackifier resins and plasticizers to achieve the surface wetting characteristics and final adhesive properties.[25] Figure 1 shows the typical viscoelastic window (T_g and storage modulus (G')) for different pressure-sensitive adhesive applications.

Sheriff *et al.* and Class and Chu correlated the viscoelastic properties of PSAs containing tackifier resin with adhesive properties, and reported that tackifier resin structure, molecular weight and concentration have significant influence in determining

the viscoelastic characteristics of the PSA and thus, the adhesive properties.[20-22] The surface energy characteristics and viscoelastic behavior of a PSA formulation determines the coating application parameters and final adhesive performance characteristics.[1]

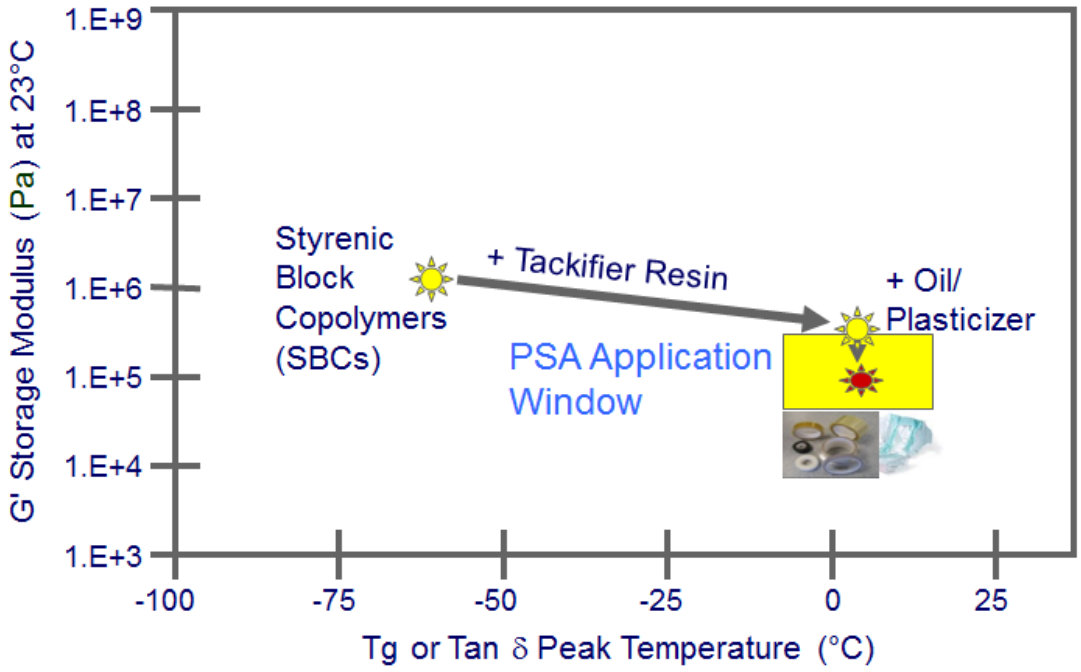

Figure 1. T_g and storage modulus (G') window for typical pressure-sensitive adhesive applications

Although there is much reported literature on hotmelt pressure-sensitive adhesives based on styrenic block copolymers, recent styrenic block copolymer availability issues are forcing more and more formulators to look for alternate technologies, especially olefinic polymer based PSAs. Yuan *et al.* studied[34] the effect of hydrogenated tackifier resins on amorphous polyolefins based PSAs and revealed that tackifiers can increase the T_g and reduce the shear modulus into pressure-sensitive adhesive region. However, one of the biggest disadvantages of most of the amorphous

polyolefin (atactic or random copolymers) based PSAs is the lack of elastomeric character resulting in lower peel and cohesive properties of the final adhesive compared to the styrenic block copolymer based PSAs. Thus, since 1974, most of the commercially available amorphous polyolefin based pressure-sensitive adhesives are blends of amorphous polyolefins with styrenic block copolymers[13, 35] or blends with polyisobutylene.[13, 33, 36] In 2006 Arriola *et al.* reported an olefinic block copolymer based on copolymerization of ethylene with octene, using a novel chain shuttling polymerization process.[26] The chain shuttling catalyst agent promotes a blocky polymer structure that combines the attributes of high density poly(ethylene) with an olefin elastomer. Even though there have been several polyolefin based polymers, this polymer is of particular interest due to its similarity in rheological performance characteristics to some of the styrenic block copolymers used in hotmelt pressure-sensitive adhesive applications.[27-29]

In 2007 Li Pi Shan *et al.* first reported[29] PSAs using high melt-index (15 and 21 at (190°C, 2.16 Kg)) developmental olefinic block copolymers (OBCs) based on ethylene and octene. Even though these developmental OBCs had similar T_g to styrene-isoprene-styrene block copolymer (15 wt% styrene), they had comparably high G' with higher slope (temperature ramp) than styrene-isoprene-styrene block copolymer (15 wt% styrene). Thus the resulting PSA formulation with developmental OBCs showed high stiffness and required significant amount of oil and tackifier, resulting in a soft adhesive with inferior adhesive performance compared to the styrene-isoprene-styrene block copolymer (15 wt% styrene) based formulation.[29] Recently Dow has commercialized a 5

melt index (190°C, 2.16 Kg), 0.866 g/cm^3 density ethylene-octene based olefinic block copolymer (OBC). The G' for this OBC is still higher than the typical styrenic block co-polymer and correlates well with reported[29] developmental OBCs. We believe that blending this polymer with amorphous polyolefin polymers will increase the T_g and reduce the G', resulting in similar G' to a styrenic block copolymer. Further modifying this blend with tackifier resins and oil will make a pressure-sensitive adhesive with comparable adhesive properties to styrenic block copolymers. Therefore, the first part of this research work is to evaluate olefinic block copolymer (OBC) blends with two amorphous polyolefins (atactic propylene homopolymer (PP) and ethylene-propylene copolymer (PE-PP)) as potential base polymers for hotmelt pressure-sensitive adhesives.

In addition, recent acrylic-based emulsion availability issues are prompting more and more formulators to go back to natural rubber latex-based PSAs. Unfortunately, most of the reported literature correlating the viscoelastic performance of natural rubber-based PSAs with adhesive properties was based on solvent-borne PSAs. In the second part of this study, a correlation of natural rubber-based, water-borne PSA rheology with adhesive properties at different conditions will be reported.

Next chapter (Chapter 2) describes the blend miscibility studies of OBC/PP and OBC/PE-PP polymer blends using dynamic mechanical analysis (DMA) and transmission electron microscopy (TEM). Chapter 3 and 4 are based on the interaction of olefinic block copolymer-amorphous polyolefin blends with different tackifier resins. The effect of three unsaturated hydrocarbon resins (with varying aromatic content) on miscibility

characteristics of OBC/PP blends and OBC/PE-PP blends are being discussed in Chapter 3. The effect of two saturated hydrocarbon resins on miscibility characteristics of OBC/PP blends and OBC/PE-PP blends are being discussed in Chapter 4. The fifth chapter covers the hotmelt pressure-sensitive adhesive formulations based on olefinic block copolymer-amorphous polyolefin blends.

Chapter 6 and 7 are based on the interaction of water-based aliphatic hydrocarbon tackifier dispersions with natural rubber-based latex for water- borne pressure-sensitive adhesive applications. Hydrocarbon resin dispersion effect on wet-rheology and morphology of natural rubber latex-based water-borne pressure- sensitive adhesive is discussed in Chapter 6. Chapter 7 describes the correlation of viscoelastic behavior with adhesive properties of the hydrocarbon resin dispersion containing natural rubber latex-based water-borne pressure sensitive-adhesives. An overall summary and possible future work is given in Chapter 8.

References

1. D. Satas (Ed.), *Handbook of Pressure Sensitive Adhesive Technology (Third edition),* Satas & Associates, Warwick, RI (1999)
2. W. H. Sheout and H. H. Day, US Patent No. 3965 (1845)
3. R. G. Drew, GB Patent 311,610 (1930)
4. R. G. Drew, GB Patent 405,163 (1934)
5. W. Eustis and G.R. Orrill, US Patent 1,419,113 (1947)

6. *Natural Rubber Latex Adhesives*, Economics and Policy Analysis Branch and Economics, Exposure and Technology Division , Office of Pollution Prevention and Toxics, USEPA – Washington DC, May-7 2008
7. T. Sanderson, *Adhesives Age*, 31 (Dec. 1978)
8. W. Demarteau and J. M. Loutz, *Progress in Organic Coatings*, 17, 33 (1996)
9. C. Oldack, R. E. Bloss, *Adhesives Age*, 38 (Apr. 1979)
10. J. T. Harlan Jr., US Patent No. 3,239,478 (1966)
11. N. Nakajima et al., *J. Appl. Polym. Sci.,* 44, 1437 (1991)
12. I. Skeist (Ed.), *Handbook of Adhesives (Second edition)*, Van Nostrand Reinhold Company, New York (1977)
13. V. K. Park, US Patent No. 3,239,478 (1974)
14. I. Benedek and L.J. Heymans, *Pressure Sensitive Adhesive Technology*, Marcel Dekker Inc., New York (1997)
15. D. H. Kaelble, *Physical Chemistry of Adhesion*, pp. 248-254, 471-480, Wiley-InterScience, New York (1971)
16. D. J. Yarusso, in: *The Mechanics of Adhesion*, A. V. Pocius and D. A. Dillard (Ed.), pp. 499-533. Elsevier, New York (2002)
17. D. Satas, in: *Hand Book of Pressure Sensitive Adhesive Technology 2nd ed.,* D. Satas (Ed.), pp. 61-96. Van Nostrand Reinhold, New York (1989)
18. C. A. Dahlquist, in: *Hand Book of Pressure Sensitive Adhesive Technology 2nd Ed.,* D. Satas (Ed.), pp. 97-114. Van Nostrand Reinhold, New York (1989)
19. G. Kraus et al., *Journal of Adhesion*, 8, 235 (1977)

20. M. Sheriff et al., *J. Appl. Polym. Sci.*, 17, 3423 (1973)

21. J. B. Class and S. G. Chu, *J. Appl. Polym. Sci.*, 30, 805-842 (1985)

22. S. G. Chu, in: *Hand Book of Pressure Sensitive Adhesive Technology 2nd ed.,* D. Satas (Ed.), pp. 159-203. Van Nostrand Reinhold, New York (1989)

23. E. P. Chang, *J. Adhesion,* 34, 189–200 (1991)

24. E. P. Chang, *J. Adhesion,* 60, 233–248 (1997)

25. P. M. Dunckley, *Adhesives Age*, 17 (Nov. 1993)

26. D. J. Arriola et al., Science*.,* 312, 714-719 (2006)

27. H. P. Wang et al., *Macromolecules*, 40, 2852-2862 (2007)

28. D. U. Khariwala et al., *Polymer*, 49, 1365-1375 (2008)

29. C. Li Pi Shan et al., *30th International PSTC Technical Seminar Orlando-FL* (May 2007)

30. R. K. Crossland and J. T. Harlan Jr., US Patent No. 3,917,607 (1975)

31. R. Korpman, US Patent No. 3,932,328 (1976)

32. R. Korpman, US Patent No. 4,028,292 (1977)

33. J. R. Trotter and F. D. Petke, US Patent No. 4,022,728 (1977)

34. B. Yuan et al., *J. Appl. Polym. Sci.*, 99, 2408-2413 (2006)

35. J. S. Lindquist et al., US Patent No. 5,869,562 (1999)

36. C. L. Ives et al., US Patent Application No. US2003/0232905 A1 (2003)

CHAPTER - 2. EVALUATION OF OLEFINIC BLOCK COPOLYMER BLENDS WITH LOW MOLECULAR WEIGHT PROPYLENE AND ETHYLENE-PROPYLENE AMORPHOUS POLYOLEFIN POLYMERS

Abstract

Blends of ethylene-octene based olefinic block copolymers with two amorphous polyolefins polymers (atactic propylene homopolymer and ethylene-propylene copolymer) were evaluated at three different ratios. Compatibility and polymer miscibility of the blends was evaluated using Dynamic Mechanical Analysis (DMA), and the morphology of the blends was analyzed using Transmission Electron Microscopy (TEM). Viscoelastic properties of both ethylene-octene olefinic block copolymer blends with amorphous polypropylene polymer, and ethylene-octene olefinic block copolymer blends with amorphous ethylene-polypropylene blends showed incompatibility. Analysis revealed that both blends formed two phase morphologies. The OBC matrix formed the continuous phase, while the amorphous polymers (polypropylene or ethylene-propylene) formed the dispersed phase of the blend morphology. The amount of dispersed phase increased as the amount of amorphous polymer in the blend increased.

Introduction

Polyolefins are a very important class of polymers being used in a wide range of adhesive applications. Even though Carothers[1] reported different methods of producing polyolefins in the 1930s, the commercial production of polyolefins did not start until the 1940s when ICI introduced the high pressure polymerization process.[2] Further development of high quality commercial production of polyolefin materials started after

the advent of olefin polymerization using the catalyst system introduced by Ziegler and Gellert[3] in 1950s, which resulted in the manufacture of linear polyethylene. The introduction of stereoregular polyolefin polymers by Natta[4] led to the development of a wide range of polyolefin polymer manufacturing including materials such as polypropylene and poly-1-butene. In 1970 Elaston reported the synthesis of homogeneous, random, partially crystalline copolymers of ethylene and alpha-olefin.[5] Until the late 1980s, Ziegler-Natta based catalyst chemistry dominated most of the commercial polyolefin manufacturing processes. Kaminsky[6] of Germany and Ewen[7] of EXXON chemicals reported the use of metallocene (zirconium) based catalyst systems to produce isotactic and syndiotactic polypropylene respectively. This gas phase reaction technology provided better enabled higher comonomer incorporation with narrower molecular weight distribution. Later, Dow introduced a solution process using a metallocene based catalyst technology named constrained geometry catalysis technology, which enabled high activities for ethylene and alpha-olefin copolymerization, resulting in long chain branching and thus improved processablity.[8-10]

As can be seen, most of the developments in polyolefin polymer systems were based on new catalyst developments. Recently, in 2006, Arriola *et al.* reported an olefinic block copolymer based on ethylene-octene, using a novel chain shuttling polymerization process.[11] The chain shuttling catalyst technology promotes a “blocky” polymer structure that combines the attributes of high density poly (ethylene) plastic and a polyolefin elastomer. Even though there have been several polyolefin based polymers, this polymer is of particular interest due to its similarity in rheological

performance characteristics to the styrenic block copolymers used in hotmelt pressure-sensitive adhesive applications.[12-14] In 2007 Li Pi Shan *et al.* first reported[14] PSAs using high melt-index (15 and 21 at (190°C, 2.16 Kg)) developmental olefinic block copolymers (OBCs) based on ethylene and octene. Even though these developmental OBCs had similar T_g as styrene-isoprene-styrene block copolymer (15 wt% styrene), they had comparably high G' with higher slope (temperature ramp) than styrene-isoprene-styrene block copolymer (15 wt% styrene). Thus the resulting PSA formulation with developmental OBCs showed high stiffness and required a significant amount of oil and tackifier, resulting in soft adhesive with inferior adhesive performance compared to the styrene-isoprene-styrene block copolymer (15 wt% styrene) based formulation.[14]

Recently, Dow has commercialized a 5 melt index (190°C, 2.16 Kg), 0.866 g/cm^3 density ethylene-octene based olefinic block copolymer (OBC). However, the G' for this OBC is still higher than the typical styrenic block co-polymer and correlates well with reported[14] developmental OBCs. We believe that blending this polymer with amorphous polyolefin polymers will increase the T_g and reduce the G', resulting in similar G' to a styrenic block copolymer. In this chapter, olefinic block copolymer blends with two amorphous polyolefins (atactic propylene homopolymer and ethylene-propylene copolymer) was studied as potential base polymers for hotmelt pressure-sensitive adhesives. Even though there have been several studies and reviews[2, 15, 16] of polyolefin blends for the improvement of different properties and processing characteristics, there has not been any known reported literature describing blends of OBCs and amorphous polyolefins (APOs).

Materials and Methods

A commercially available (INFUSE 9507) 5 melt index (190°C, 2.16 Kg), 0.866 g/cm^3 density ethylene-octene based olefinic block copolymer (OBC) was obtained from Dow Chemical Company. Atactic propylene homopolymer amorphous polyolefin and ethylene-propylene amorphous polyolefin copolymers were obtained from Eastman Chemical Company. Properties of the amorphous polyolefins (atactic propylene homopolymer and ethylene-propylene copolymer) are given in Table 1.

Table 1. Properties of polymers

Name	Penetration Hardness (ASTM D5)	Viscosity (190°C) mPa.S (ASTM D3236)	T_g (°C)
PP (Propylene homopolymer)	18	2300	-10
PE-PP (Ethylene-propylene copolymer)	35	5700	-20

Blends containing 30 wt%, 50 wt% and a 70 wt% OBC with PP or PE-PP were prepared using a Plasticorder Brabender at 150°C using roller blades. The formulations were blended for 20-45 minutes until the torque became constant. Formulations evaluated are given in Table 2.

Table 2. Polymer blend formulations in wt%

Formulation Description	30/70 (OBC/PP)	50/50 (OBC/PP)	70/30 (OBC/PP)	30/70 (OBC/PE-PP)	50/50 (OBC/PE-PP)	70/30 (OBC/PE-PP)
OBC	30	50	70	30	50	70
PP	70	50	30	-	-	–
PE-PP	–	-	–	70	50	30

Compatibility and polymer miscibility of the blends was evaluated using Dynamic Mechanical Analysis (DMA) and morphology of the blends was analyzed using Transmission Electron Microscopy (TEM). There have been several reports describing the effectiveness of determining the polymer compatibility and miscibility characteristics of polymer blends using dynamic mechanical analysis and describing morphological analysis using microscopic techniques.[16-20]

Dynamic Mechanical Analysis (DMA) of the blends was performed using a TA Instruments Ares RDA3® Rheometer in a parallel plate geometry. The diameter of the plates was 8 mm and the gap was set at 2.33 mm. Temperature sweep experiment was performed between -80°C and 300°C with a heating rate of 6°C/min, by keeping the frequency at 10 Hz and the maximum strain at 5%.

TEM images were taken after the blends were microtomed into 50 nm thickness using a Leica EM UC6 cryo-microtome with a knife temperature at -110°C and sample temperature at -120°C. These thin sections were then transferred onto TEM grids. TEM evaluation was performed using a Philips CM12 Microscopy with an accelerating voltage of 100 kV. No chemical staining has been applied to the sections. The contrast in the images is mainly created by density differences between the different structures.

Results and Discussion

OBC/PP blends will be discussed first followed by OBC/PE-PP blends. Figure 2 shows the viscoelastic characteristics of OBC, PP and PE-PP polymers.

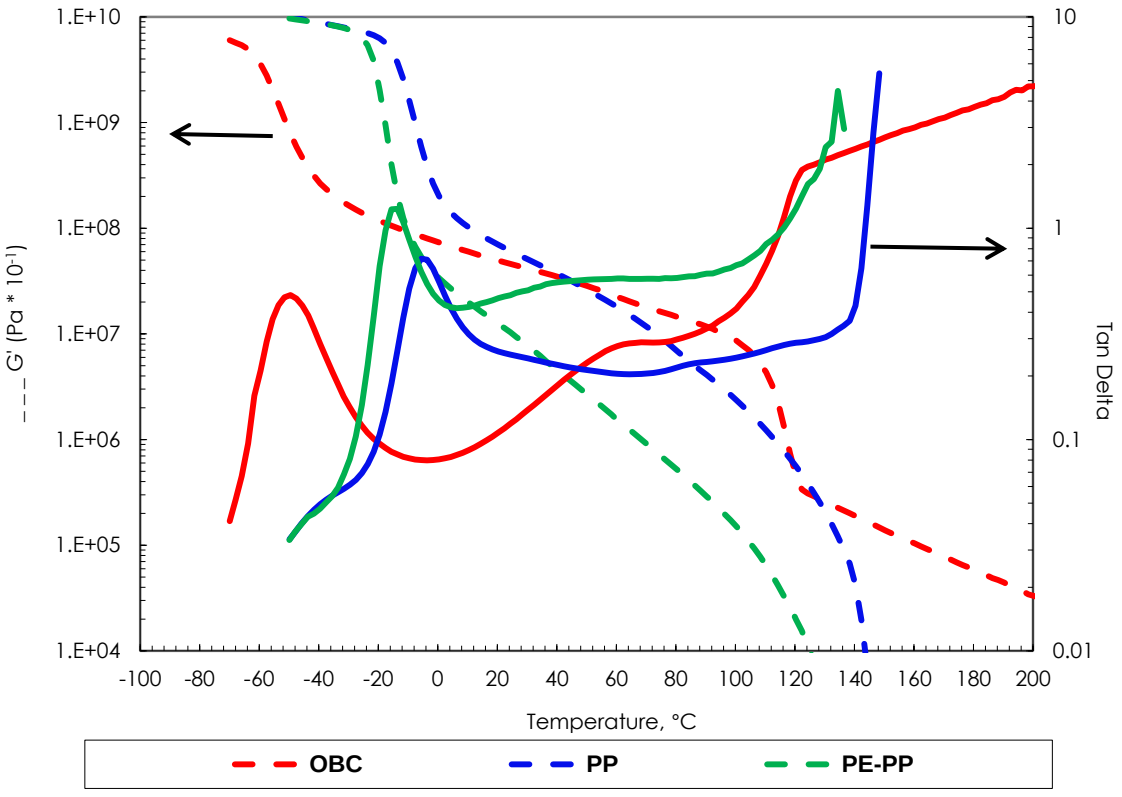

Figure 2. DMA plots for OBC, PP and PE-PP polymers

As can be seen from the tan δ peak of Figure 2, the OBC copolymer shows a T_g of -49°C. PE-PP copolymer has a lower T_g and lower modulus than that of the PP homopolymer. The storage modulus (G') of OBC at room temperature (25°C) is higher than that of PE-PP amorphous polymer, but little lower compared to PP homopolymer. Even though the elastic modulus of OBC decreases as the temperature increases, the decrease is not as pronounced as for the PP and PE-PP polymers. This shows the lack of elastic properties (strength) for PP and PE-PP polymers compared to OBC. Therefore PP and PE-PP polymers cannot be used as such for pressure-sensitive adhesives (PSA) applications due to the lack of elastic strength needed over a wide application temperature range, before it starts to flow. Morphological characterizations of the polymers were also evaluated using TEM. Figure 3 shows the TEM micrographs of the polymer.

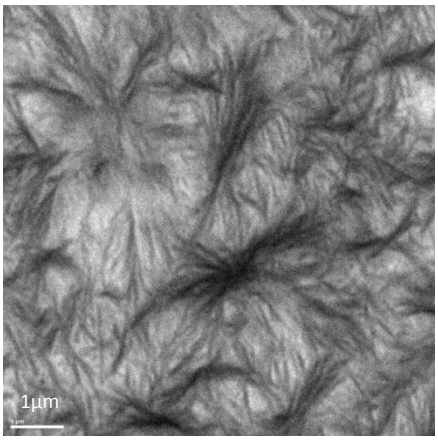

Figure 3. TEM micrograph of the OBC polymer

The dark crystalline regions and light amorphous regions of OBC are clear from Figure 3. The dark lamellar worm like regions correspond to crystalline domains

embedded in a light continuous amorphous matrix. Unfortunately, due to predominant amorphous characteristics of PP and PE-PP amorphous polymers, it was unable to obtain good TEM micrographs, since they formed transparent films due to the lack of heterogeneity or phase contrast. As mentioned earlier, the G' for this OBC is still higher than the typical styrenic block co-polymer used in PSA applications.[14] Therefore OBC/PP and OBC/PE-PP blends were prepared to reduce the elastic modulus of OBC polymer. Figure 4 shows the viscoelastic characteristics of OBC/PP blends at three different ratios as specified in Table 2.

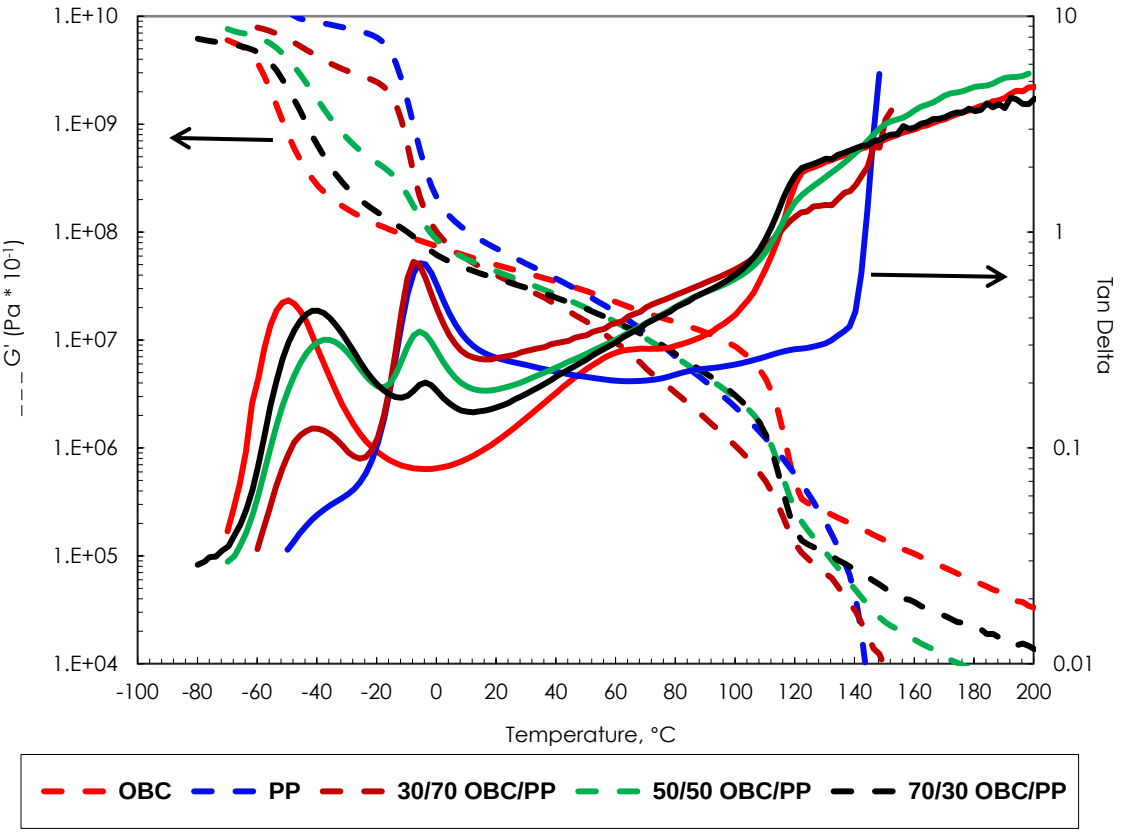

Figure 4. DMA plots for the OBC/PP blends

It is clear from Figure 4 that the OBC/PP blends show two tan delta peaks (two glass transitions) at 30%, 50% and 70% addition levels, which is a clear indication of immiscibility. There is a first transition around -40°C and a second transition around -10°C. The second glass transition for 30/70 OBC/PP corresponds to the PP glass transition temperature. All three blends show similar second glass transition temperatures (T_g) as for the parent PP homopolymer. While the first glass transition for all three blends are almost 10°C higher than that of the parent OBC polymer. The change in the first thermal transition associated with the OBC is an indication of limited miscibility of the PP homopolymer in OBC matrix. Tan delta peak height also correlate with the level of OBC and PP in the blend. Morphological characterization of the OBC/PP blends was also evaluated using TEM. Figure 5 shows the TEM micrographs of the OBC/PP blends.

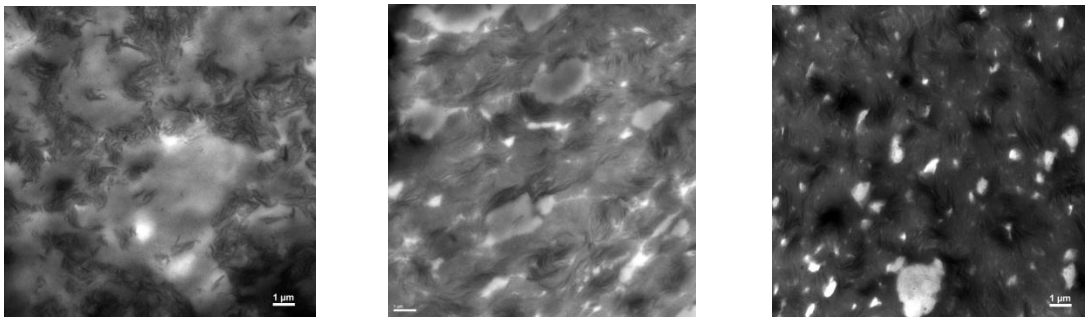

(a) (b) (c)

Figure 5. TEM micrographs of OBC/PP blends (a) 30/70 OBC/PP, (b) 50/50 OBC/PP, (c) 70/30 OBC/PP

As can been seen from the above TEM micrographs (Figure 5), all the blends show a two phase blend morphology. Immiscibility of the blends is very obvious. It can

be observed that at 30 wt% OBC addition level, OBC forms the dispersed phase (Dark worm-like regions) and PP forming the continuous phase, but as the OBC concentration in the blend increases to 50 wt%, phase inversion happens resulting in OBC matrix forming the continuous phase and the PP polymer forming the dispersed phase of the blend morphology. At 50 wt% and 70 wt% APO addition level, the amount of dispersed phase increases as the amount of amorphous polyolefin content increases. Even though we can see some dark crystalline phases of OBC, they are not as well defined as for the OBC homopolymer, indicating some loss of crystalline architecture. This is more pronounced as the amount of PP increases in the blend composition (50 and 70 wt%).

Figure 6 shows the viscoelastic characteristics of OBC/PE-PP blends. OBC/PE-PP blends also show similar glass transition behaviors as for OBC/PP blends. It is interesting to note that the elastic modulus of the blends show a different behavior for OBC/PE-PP blends. In this case the elastic modulus at room temperature gradually decreases as the amount of PE-PP amorphous polymer increases in the blend. The 50/50 OBC/PE-PP polymer blend shows an elastic modulus (at room temperature) in the middle of the respective OBC and PE-PP polymers, indicating some miscibility between the polymers.

Morphological evaluation of the OBC/PE-PP blends was also performed and can be seen in Figure 7. As discussed earlier in the case of OBC/PP polymer, OBC/PE-PP (Figure 7) also shows a two-phase morphology. At 30 wt% OBC addition level, OBC forms the dispersed phase and PE-PP forming the continuous phase. However, as the OBC concentration increases to 50 wt%, the phase inversion happens, resulting in OBC

becoming the continuous phase and the PE-PP amorphous polymer forming the dispersed phase.

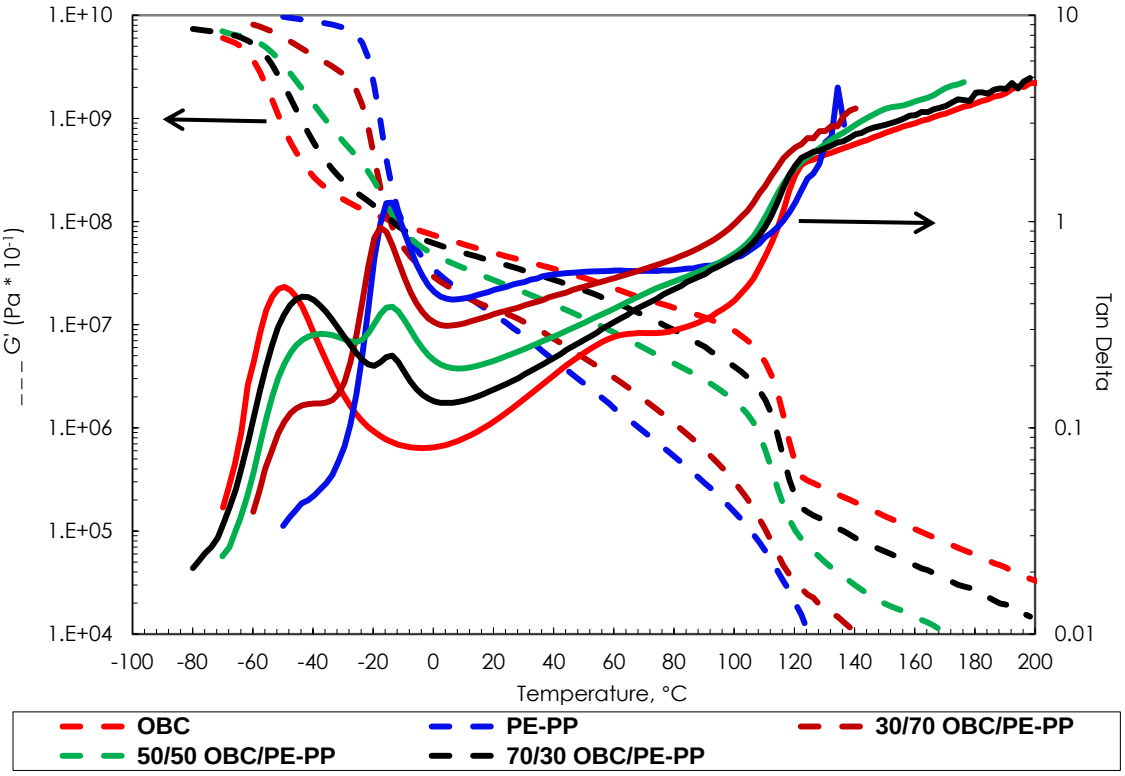

Figure 6. DMA plots for the OBC/PE-PP blends

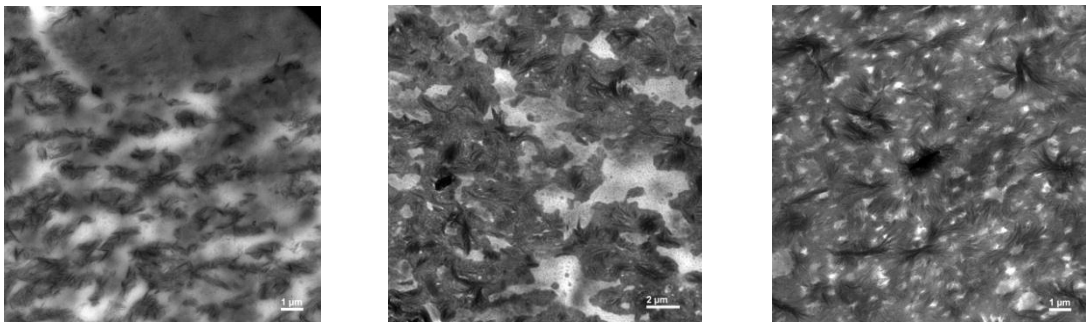

(a) (b) (c)

Figure 7. TEM micrographs of OBC/PE-PP blends (a) 30/70 OBC/PE-PP, (b) 50/50 OBC/PE-PP, (c) 70/30 OBC/PE-PP

Summary and Path Forward

- Both OBC/PP blends and OBC/PE-PP show two glass transitions at 30%, 50% and 70% addition levels. In both cases, the glass transition temperatures correspond to their parent polymers, which is a clear indication of incompatibility.
- Interestingly, the elastic modulus (at room temperature) of OBC/PE-PP blends decreased as the amount of PE-PP amorphous polymer increased in the blend and was in between both the parent polymers, indicating some interaction between the polymer phases. On the other hand for OBC/PP blends, the elastic modulus (at room temperature) was a little lower than that of the two parent polymers, but did not show a significant effect on modulus (G') indicating no interaction between the phases.
- Morphological evaluation of both blends (OBC/PP and OBC/PE-PP) again verified the immiscibility characteristics of the blends. In case of both blends (OBC/PP and OBC/PE-PP), it has been observed that at 30 wt% OBC addition level, OBC forms the dispersed phase, but as the OBC concentration in the blend increases to 50 wt%, phase inversion happens resulting in OBC matrix forming the continuous phase and the PP polymer or the PE-PP polymer forming the dispersed phase of the blend morphology respectively. At 50 wt% and 70 wt% APO addition level, the amount of dispersed phase increased as the amount of amorphous polyolefin content increased.
- Since OBC/PP and OBC/PE-PP polymer blends were immiscible, each exhibiting the T_g of pure blend components and a heterogeneous morphology, a

compatibilizing agent is needed to improve the miscibility characteristics of the polymer system. The effect of different low molecular weight hydrocarbon resins was evaluated as compatibilizing and tackifying agents to improve the interfacial adhesion (miscibility) characteristics between the two polymers and also to effectively tackify the polymer system to improve the pressure-sensitive adhesive characteristics. The next two chapters describe the effect of five different hydrocarbon resins with different chemistries as compatibilizing agents.

References

1. W. H Carothers et al., *J. Am. Chem. Soc.*, 52, 5279 (1930)
2. J. L. White and D. Choi (Ed.), *Polyolefins: Processing, Structure Development, and Properties,* Hanser Gardner Publications Inc., Cincinnati (2005)
3. K. W. Ziegler and H. G. Gellert, US Patent No. 2,699,457 (1955)
4. G. Natta, *J. Am. Chem. Soc.*, 77, 1708 (1955)
5. C. T. Elaston, US Patent 3,645,992 (1970)
6. W. Kaminsky et al., *Angew. Chem. Int. Ed. Eng.*, 24, 507 (1985)
7. J. Ewen et al., *J. Am. Chem. Soc.*, 110, 6255 (1988)
8. S. Y. Lai et al., US Patent 5,272,236 (1993)
9. J. C. Stevens, *Stud. Surf. Sci. Catal.*, 89, 277 (1994)
10. J. Minick et al., *J. Appl. Polym. Sci.*, 58, 1371 (1995)
11. D. J. Arriola et al., *Science.,* 312, 714-719 (2006)
12. H. P. Wang et al., *Macromolecules*, 40, 2852-2862 (2007)

13. D. U. Khariwala et al., *Polymer*, 49, 1365-1375 (2008)

14. C. Li Pi Shan et al., *30th International PSTC Technical Seminar Orlando-FL* (2007)

15. C. Vasile (Ed.), *Handbook of Polyolefins, Second edition,* Marcel Dekker Inc., New York (2000)

16. L. M. Robeson (Ed.), *Polymer Blends*, Hanser Gardner Publications Inc., Cincinnati (2007)

17. S. Krause, *Pure & Applied Chemistry*, 58 (12), 1553 (1986)

18. S. N. Yau and E. M. Woo, *Macromol. Rapid Commun.*, 17, 615 (1996)

19. S. Hamden et al., *Journal of Polymer Research*, 7 (4), 237 (2000)

20. A. K. Kulshreshtha and A. K. Vasile (Ed.), *Handbook of Polymer Blends and Composites*, Rapra Technology Limited, Shawbury-UK (2003)

CHAPTER - 3. EFFECT OF UNSATURATED ALIPHATIC AND ALIPHATIC/AROMATIC HYDROCARBON RESINS ON BLENDS OF OLEFINIC BLOCK COPOLYMER AND LOW MOLECULAR WEIGHT PROPYLENE AND ETHYLENE-PROPYLENE AMORPHOUS POLYMERS

Abstract

Blends of OBC with APO's have been studied and found to be incompatible at all concentrations. One way to improve the performance of these blends would be to introduce a material that could help compatibilize the different components in the blend. This chapter will explore the effect of three unsaturated aliphatic hydrocarbon resins with varying aromatic content on the performance of OBC/PP and OBC/PE-PP blends. One aliphatic and two aliphatic/aromatic unsaturated resins with varying aromatic content (5% and 14%) were selected for the study. A 1:1 polymer blend ratio of OBC/PP and OBC/PE-PP was selected for this study to better understand the influence of resin addition at three different levels 20 wt%, 30 wt% and 40 wt%. Dynamic mechanical analysis and transmission electron microscopy evaluations were performed to determine the blend miscibility characteristics. The fully aliphatic resin seems to improve the miscibility of the OBC/PP blends at higher resin addition levels. No improvement was observed for the OBC/PP/resin blends as the aromatic content of the resin increases. However, OBC/PE-PP blends showed improved miscibility with increasing aromatic content. A ternary phase morphology was particularly observed for both OBC/PP and OBC/PE-PP blends with highly aromatic (14%) unsaturated hydrocarbon resin, in which OBC formed the continuous phase, and PP, PE-PP and

unsaturated hydrocarbon resins formed the dispersed phase. The Harkins spreading coefficient concept was used to better understand the ternary blend dispersed phase morphology. Spreading coefficients indicate that the free unsaturated hydrocarbon resin is encapsulated by the amorphous PP or amorphous PE-PP polymer in the dispersed phase for the respective blend compositions. Overall it has been observed that OBC/PE-PP blend showed better miscibility when unsaturated hydrocarbon resins were used as compatibilizers than that of the OBC/PP blends with the same unsaturated hydrocarbon resins.

Introduction

Compatibilization techniques to improve the miscibility of polymer blend systems have been well studied. Extensive reviews, including several books on compatibilization of different polymer system already exist.[1-6] Compatibilizing agents improve the interfacial adhesion between the polymer system by reducing the interfacial tension. Compatibilizing agents can range from low molecular weight additives to high molecular weight polymers.[3] The heterogeneous blend morphologies and limited miscibility behavior of olefinic block copolymer blends with amorphous polypropylene and polyethylene-propylene amorphous polymers are explained in the previous chapter. In this chapter the influence of aliphatic and aliphatic/aromatic unsaturated hydrocarbon resins on the dynamic mechanical properties and morphology of OBC/APO blends were studied. Hydrocarbon resin compatibilizers are of particular interest due to the fact that as early as 1845, natural or petroleum derived hydrocarbon resins are used to improve tack and processing characteristics of pressure-sensitive

adhesives.[7-13] Hydrocarbon resins are low molecular weight, high T_g, amorphous materials of petroleum origin. As Class and Chu explained,[10] a good tackifier resin should have low molecular weight, sufficient compatibility with polymer type, and have a glass transition temperature (T_g) higher than the base polymer to effectively impart sufficient pressure-sensitive adhesive characteristics such as tack and peel.[13] The hydrocarbon resins added to OBC/APO blends may not only modify individual phases or distribute between the different phases resulting in better miscibility, but also may improve the adhesive properties of the blends. One aliphatic unsaturated hydrocarbon resin (mainly based on piperylene or C5) and two aromatically-modified C5 hydrocarbon unsaturated resins (styrene modified C5 hydrocarbon resin) with different aromatic content were selected for this study. Hydrocarbon resins evaluated in this study are derived from crude raw material C5 feedstock. The simplified structure given in Figure 8 is an idealized structure, rather than a particular actual one.

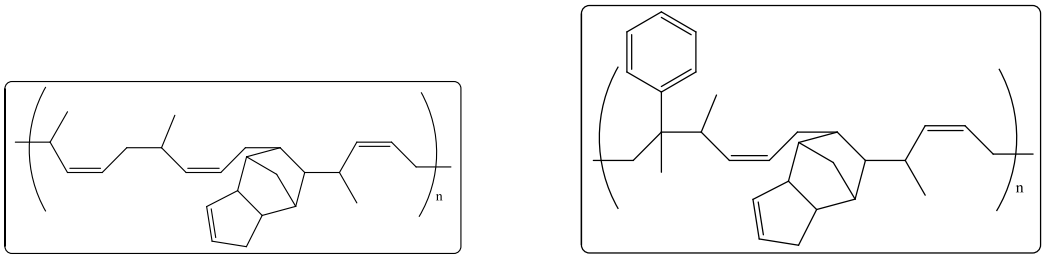

(a) (b)

Figure 8. Ideal structures of a C5 hydrocarbon resin. (a) An ideal unsaturated aliphatic C5 resin structure, (b) An ideal unsaturated aromatically modified aliphatic C5 resin structure

Influence of hydrocarbon resins on the effect of morphology (phase modification) and viscoelastic properties have been investigated in this study.

Materials and Methods

A commercially available (INFUSE 9507®) 5 melt index (190°C, 2.16 Kg), 0.866 g/cm^3 density ethylene-octene based olefinic block copolymer (OBC) was obtained from Dow Chemical Company. Atactic propylene homopolymer amorphous polyolefin and ethylene-propylene amorphous polyolefin copolymers were obtained from Eastman Chemical Company. Properties of the amorphous polyolefins (atactic propylene homopolymer and ethylene-propylene copolymer) are given in Table 3. Properties of the unsaturated hydrocarbon resins selected for this study are given in Table 4.

Table 3. Properties of polymers

Name	Penetration Hardness (ASTM D5)	Viscosity (190°C) mPa.S (ASTM D3236)	T_g (°C) (DMA tan δ peak height)
PP (Propylene homopolymer)	18	2300	-10
PE-PP (Ethylene-propylene copolymer)	35	5700	-20

Table 4. Properties of the unsaturated hydrocarbon resins

Resin	Type	Ring & Ball Softening Point (°C)	% Aromatic content (1H NMR)	Molecular Weight Mn/Mw/Mz (Daltons)
Resin 1 (R1)	Aliphatic	95	0.5	800/1700/3500
Resin 2 (R2)	Aliphatic/ Aromatic	95	5	850/2200/5500
Resin 3 (R3)	Aliphatic/ Aromatic	95	14	800/1700/4000

Ring & Ball Softening Point of hydrocarbon resin was measured using the Herzog Ring & Ball Tester. The softening point is defined as the temperature at which a disk of the sample held within a horizontal ring is forced Downward a distance of 25.4 mm (1 inch) under the weight of a steel ball as the sample is heated at 5°C/min in a silicon bath (400 ml). The temperature is recorded, when the resin sample passes through the sensors of the unit (ASTM D-6493-99).

To determine the aromatic hydrogen content of each hydrocarbon resin, the ratio of the integration area of aromatic hydrogen relative to the total integration area of hydrogen on the resin's NMR spectrum was determined via ^{1}H NMR analysis. The

NMR analysis was performed using a JEOL 600 MHz Eclipse NMR system with a pulse interval of 15 seconds, acquisition time of 3.6 seconds, pulse angle of 90°, X resolution of 0.27 Hz, and number of scans set at 16. The resin NMR samples were prepared by dissolving a known amount of each of hydrocarbon resins in methylene chloride-d2. The total integration value was normalized to 100. The results were reported in area percent.

Molecular weights (Mn, Mw, and Mz) of hydrocarbon resins were determined via gel permeation chromatography (GPC) with THF as a solvent. Each resin was analyzed at ambient temperature in Burdick and Jackson GPC-grade THF stabilized with BHT, at a flow rate of 1 ml/min. Sample solutions were prepared by dissolving about 50 mg of each resin in 10 ml of THF and adding 10 microliters of toluene thereto as a flow-rate marker. An auto sampler was used to inject 50 microliters of each solution onto a Polymer Laboratories PLgel™ column set consisting of a 5 micrometer Guard, a Mixed-C™ and an Oligopore™ column in series. The eluting polymer was detected by differential refractometry, with the detector cell held at 30°C. The detector signal was recorded by a Polymer Laboratories Caliber™ data acquisition system, and the chromatograms were integrated with software developed at Eastman Chemical Company. A calibration curve was determined with a set of eighteen nearly monodisperse polystyrene standards with molecular weight from 266 to 3,200,000 g/mole and 1-phenylhexane at 162 g/mole. The molecular weight distributions and averages were reported either as equivalent polystyrene values.

Surface tension measurements of hydrocarbon resins and polymers were obtained through contact angle measurements. Contact angle measurements were performed using VCA2500 XE video contact angle system (AST Products Inc. MA). Contact angle measurements were performed on a 0.5mil thick coated film of hydrocarbon resins and polymers on a glass plate. Contact angle of the solid surface with two liquids of known surface energy (distilled water and methylene iodide) was used to obtain the information about the surface free energy of the solid substrate. A sessile drop of liquid (distilled water followed by methylene iodide) was placed on the coated glass substrate surface. This created a specified contact (tangent) angle at the solid, liquid, air interface. A photograph of the drop profile was used to calculate the contact angle. Calculations of the wetting parameters were derived from thermodynamic principles based on Young's equation, which describes the stable equilibrium at a three-phase boundary between a solid, liquid and a vapor system (VCA software). Surface energy calculations were performed using Harmonic calculation with the help of SE2500 software.

A 1:1 polymer blend ratio of OBC/APO (where the APO is either PP or PE-PP) was selected for this study to better understand the influence of resin addition in three different levels 20 wt%, 30 wt% and 40 wt%.

Blends were prepared using a Plasticorder Brabender at 150°C using roller blades, and blended for 20-45 minutes until the torque became constant. OBC/PP/Resin

Formulations evaluated are given in Table 5 and OBC/PE-PP/Resin Formulations evaluated are given in Table 6.

Table 5. OBC-PP-Resins blend formulations in wt%

Formulation Description	OBC	PP	Resin 1	Resin 2	Resin 3
40/40/20(OBC/PP/R1)	40	40	20	-	-
35/35/30(OBC/PP/R1)	35	35	30	-	-
30/30/40(OBC/PP/R1)	30	30	40	-	-
40/40/20(OBC/PP/R2)	40	40	-	20	-
35/35/30(OBC/PP/R2)	35	35	-	30	-
30/30/40(OBC/PP/R2)	30	30	-	40	-
40/40/20(OBC/PP/R3)	40	40	-	-	20
35/35/30(OBC/PP/R3)	35	35	-	-	30
30/30/40(OBC/PP/R3)	30	30	-	-	40

Table 6. OBC-(PE-PP)-Resin blend formulations in wt%

Formulation Description	OBC	PE-PP	Resin 1	Resin 2	Resin 3
40/40/20(OBC/PE-PP/R1)	40	40	20	-	-
35/35/30(OBC/PE-PP/R1)	35	35	30	-	-
30/30/40(OBC/PE-PP/R1)	30	30	40	-	-
40/40/20(OBC/PE-PP/R2)	40	40	-	20	-
35/35/30(OBC/PE-PP/R2)	35	35	-	30	-
30/30/40(OBC/PE-PP/R2)	30	30	-	40	-
40/40/20(OBC/PE-PP/R3)	40	40	-	-	20
35/35/30(OBC/PE-PP/R3)	35	35	-	-	30
30/30/40(OBC/PE-PP/R3)	30	30	-	-	40

Compatibility and polymer miscibility of the blends was evaluated using Dynamic Mechanical Analysis (DMA) and the morphology of the blends was analyzed using Transmission Electron Microscopy (TEM). DMA and TEM evaluations were performed following the same procedure as described in Chapter-2. There have been several reports describing the effectiveness of determining the polymer compatibility and

miscibility characteristics of polymer blends (binary and ternary) using dynamic mechanical analysis and morphological analysis using microscopic techniques.[5, 6, 14-17]

Results and Discussion

Viscoelastic properties measured using dynamic mechanical analysis (DMA) of the OBC/PP blends and OBC/PE-PP blends with different hydrocarbon resins are discussed in the first part of this chapter, followed by morphological evaluation (TEM) of the OBC/PE-PP blends and OBC/PE-PP blends with different hydrocarbon resins.

Dynamic mechanical analysis of the OBC/PP blends with aliphatic resin (Resin 1) at three different concentrations is shown in Figure 9.

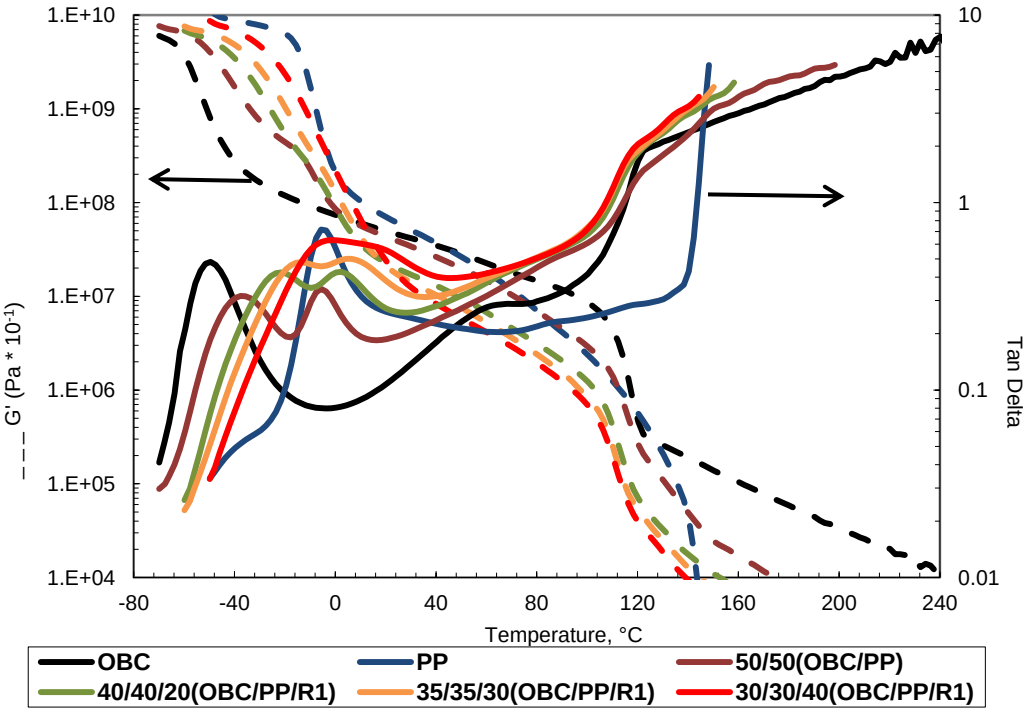

Figure 9. DMA of OBC/PP/Aliphatic unsaturated resin blends at different ratios

It can be seen from the above viscoelastic properties that both 20 wt% and 30 wt% additions of aliphatic unsaturated resin (R1) still show two glass transitions indicating immiscibility. However 40 wt% addition of aliphatic unsaturated resin shows a single, broad glass transition temperature. It should be noted that the first glass transition temperature and the second glass transition temperature significantly increased for the blends containing 20 wt% and 30 wt% aliphatic unsaturated resin (R1) indicating good miscibility of the resin in individual polymer phases. The glass transition temperature for the 40 wt% aliphatic unsaturated resin containing blend is close to that of PP polymer and shows a broad tan δ peak. Elastic modulus (G') decreases as the amount of unsaturated aliphatic resin in the blend increases. This is an indication of better miscibility as the aliphatic unsaturated resin concentration increases.

Figure 10 shows the viscoelastic characteristics of OBC/PP blends containing aliphatic-aromatic (5%) resin (R2) at different concentrations. This also follows the same trend as it has seen for the aliphatic unsaturated resin containing blends. Interestingly 40 wt% aliphatic-aromatic (5%) resin containing blends show a single glass transition, indicating miscibility similar to 40 wt% aliphatic resin blend. The lower elastic modulus of 40 wt% aliphatic-aromatic (5%) resin containing blends is also an indication of good miscibility of the different phases. Figure 11 shows the viscoelastic characteristics of aliphatic-aromatic (14%) resin containing OBC/PP blend.

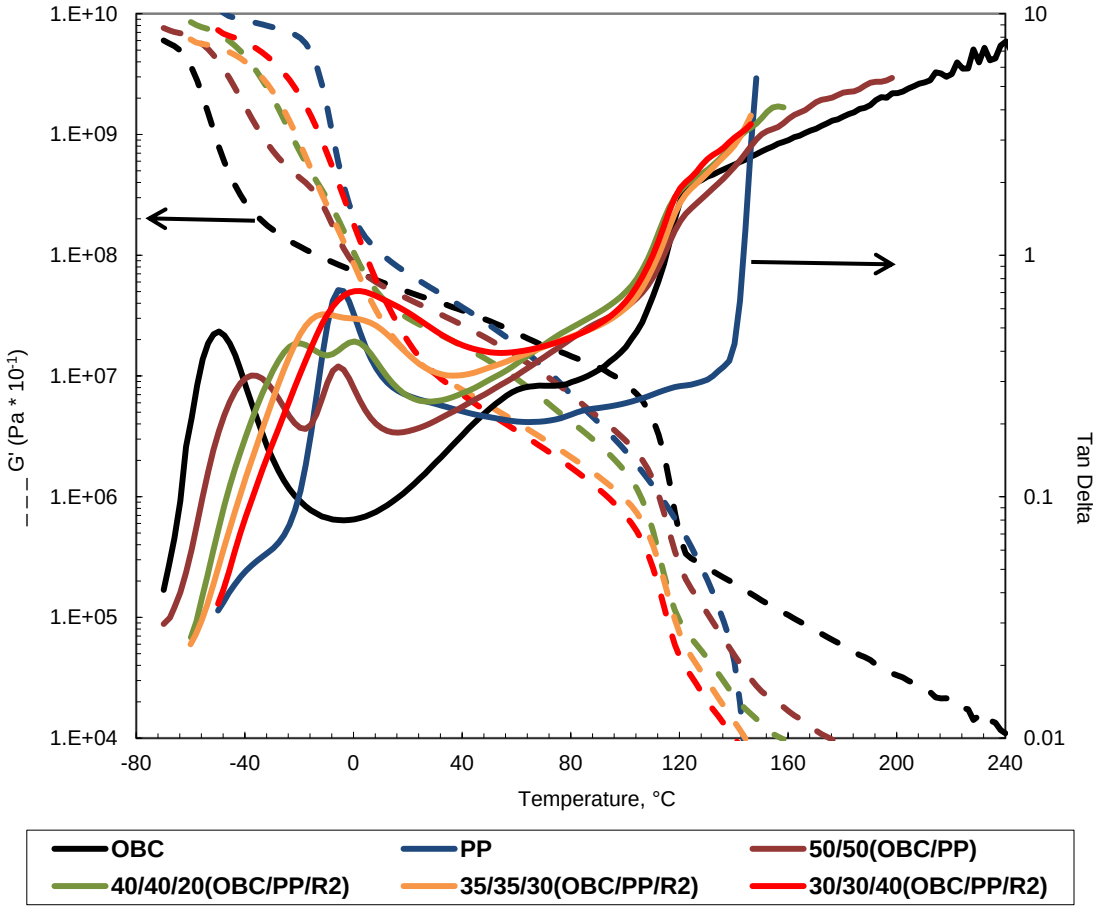

Figure 10. DMA of OBC/PP/Aliphatic-aromatic (5%) resin blends at different ratios

As can be seen from Figure 11, as the amount of resin increases, the total aromatic content in the formulation also increases, resulting in immiscibility even at 40 wt% addition levels. Also, as the amount of resin increases, T_g of the total formulation increases and the elastic modulus (G') of the formulation decreases. This is an indication of partial miscibility of the different phases, but it is not as good as with aliphatic unsaturated resin and aliphatic-aromatic (5%) resin containing blends.

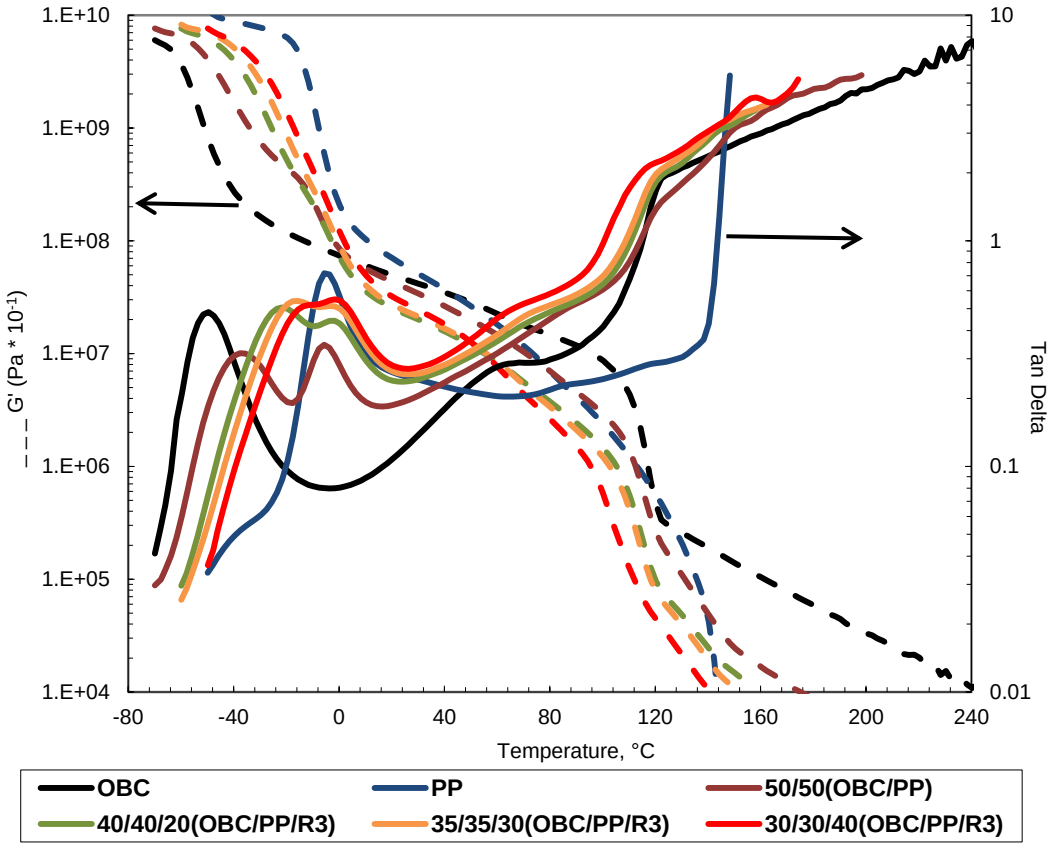

Figure 11. DMA of OBC/PP/Aliphatic-aromatic (14%) unsaturated resin blends at different ratios

Figure 12 shows the effect of aromatic content at 40 wt% addition levels for the unsaturated resin containing OBC/PP blends. As can be seen in Figure 12, 5% aromatic-aliphatic resin at 40 wt% addition level shows better miscibility characteristics (higher T_g, single tan δ curve, and lower elastic modulus) compared to aliphatic-aromatic (14%) resins (R3). We expected the aliphatic resin (R1) to show better miscibility due to the structural similarity in resin composition with ethylene-octene based OBC and polypropylene amorphous polymer blends.

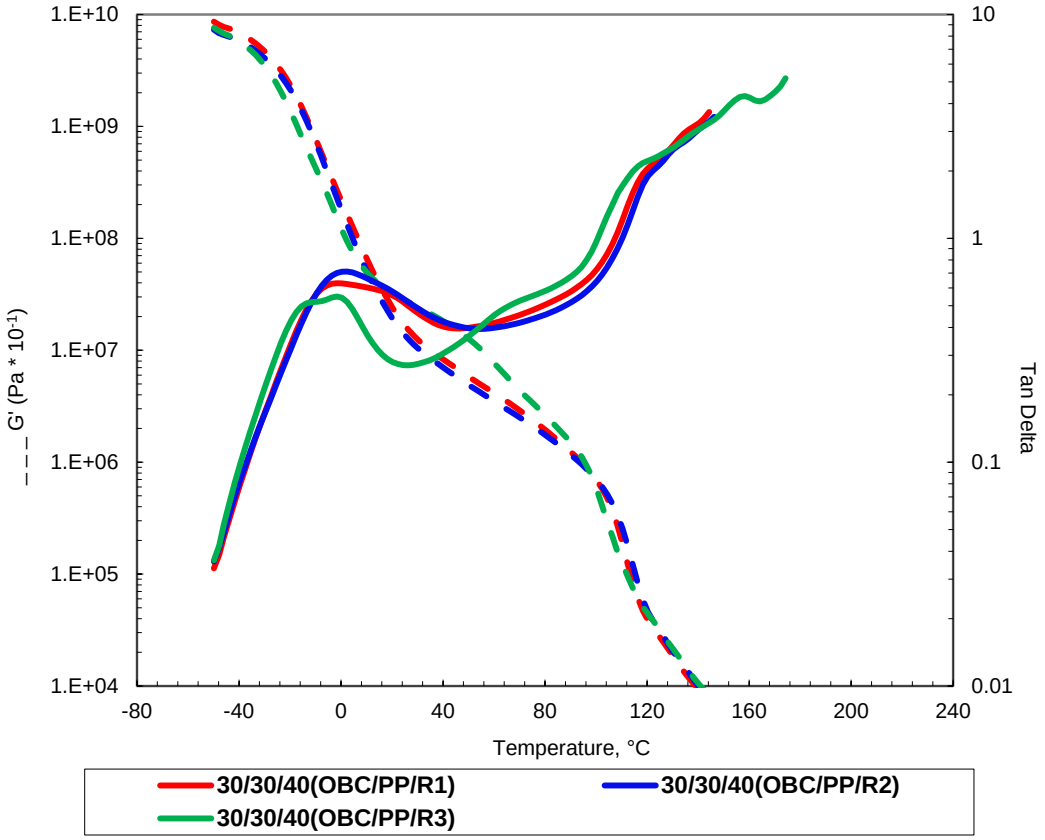

Figure 12. DMA of 40 wt% unsaturated resin containing OBC/PP blends with increasing resin aromatic content

Interestingly a small amount of aromatic content (5%) actually shows similar or slightly improved miscibility of OBC/PP blends compared to blends containing aliphatic unsaturated resin (R1). Figure 13 shows the ternary plot of OBC/PP blends with unsaturated hydrocarbon resins, binary blends of OBC with unsaturated hydrocarbon resins and binary blends of PP with unsaturated hydrocarbon resins. The bottom axis represents the amount of PP, and the circular dots represent the T_g of particular binary blends of PP with unsaturated hydrocarbon resins. The axis on the left is the amount of OBC. Axis on the right of the ternary plot represents the amount of hydrocarbon resin,

and the circular dots represent the T_g of particular binary blends of OBC with hydrocarbon resins. Ternary blend T_g is represented as circular dots in the middle of the ternary plot where the OBC, PP and amounts of each particular hydrocarbon resin intersects with respect to the corresponding blend ratios.

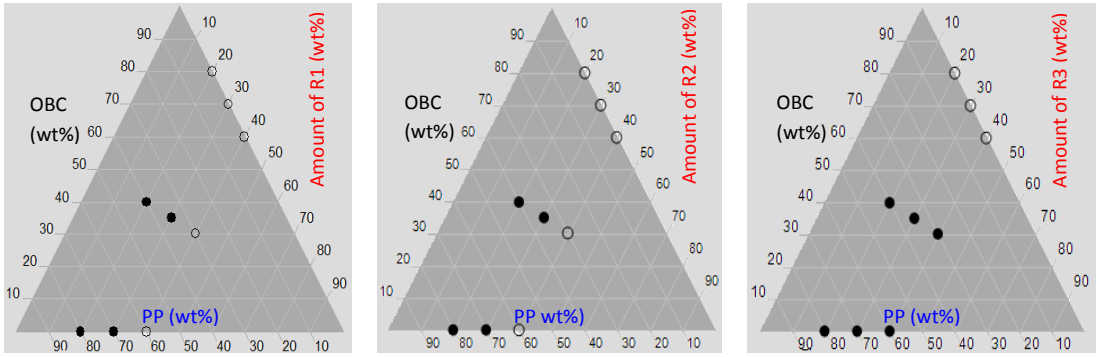

(a) (b) (c)

Figure 13. Ternary plot of glass transition temperatures for OBC/PP blends with resins. (a) Resin 1 (R1), (b) Resin 2 (R2), (c) Resin 3 (R3)

Blackened dots indicate blends with two T_g's and clear dots indicate blends with a single T_g. The amount of resin concentration was kept the same (20 wt%, 30 wt% and 40 wt%) for binary blends of polymers (OBC or PP) with hydrocarbon resins, (R1, R2 and R3), as for the ternary blends (two polymers with resin). As can be seen in Figure 13, binary blends of OBC polymer with any of the hydrocarbon resins shows a single T_g, and the aromatic content of resin has little effect on the compatibility. However, binary blends of PP with hydrocarbon resins show a completely different behavior such that as the aromatic content in the resin increases, the incompatibility also increases, resulting

in two T_g's at all concentrations of resin for the PP-R3 blends. Figure 14 below shows the effect of aliphatic hydrocarbon resin in OBC/PE-PP blends at three different ratios.

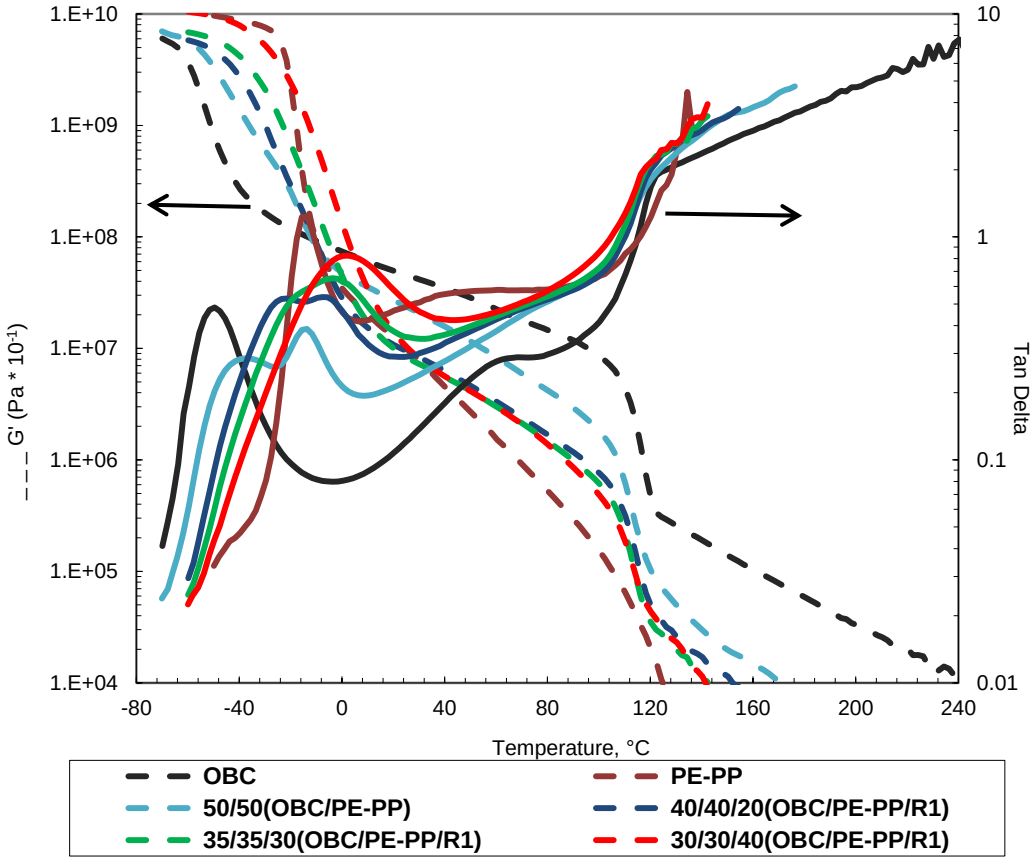

Figure 14. DMA of OBC/PE-PP/Aliphatic unsaturated resin blends at different ratios

As can be seen from Figure 14, 30 wt% and 40 wt% addition of aliphatic hydrocarbon resin to the OBC/PE-PP blends show a single glass transition temperatures and higher glass transition temperatures than that of the parent polymers. It is interesting to note that the storage modulus (G', at room temperature) of the 20 wt%, 30 wt% and 40 wt% aliphatic hydrocarbon resin containing OBC/PE-PP blends show a similar trend and is in between the individual polymer values and lower than the 50/50

OBC/PE-PP blend without any resin. This behavior is different than that of the OBC/PP blends containing aliphatic hydrocarbon resins (Figure 9), in which the blends containing resins showed lower modulus than that of the parent polymers. The G' values (at room temperature) in between the parent polymer show better miscibility between the interphase of the two polymer system, while the very low storage modulus (G', at room temperature) lower than the two parent polymers, and especially PP, shows that the resin is softening the PP phase more than that of the OBC/PP interphase. Figure 15 shows the viscoelastic properties of aliphatic-aromatic (5%) hydrocarbon resin containing OBC/PE-PP blend at different resin concentrations.

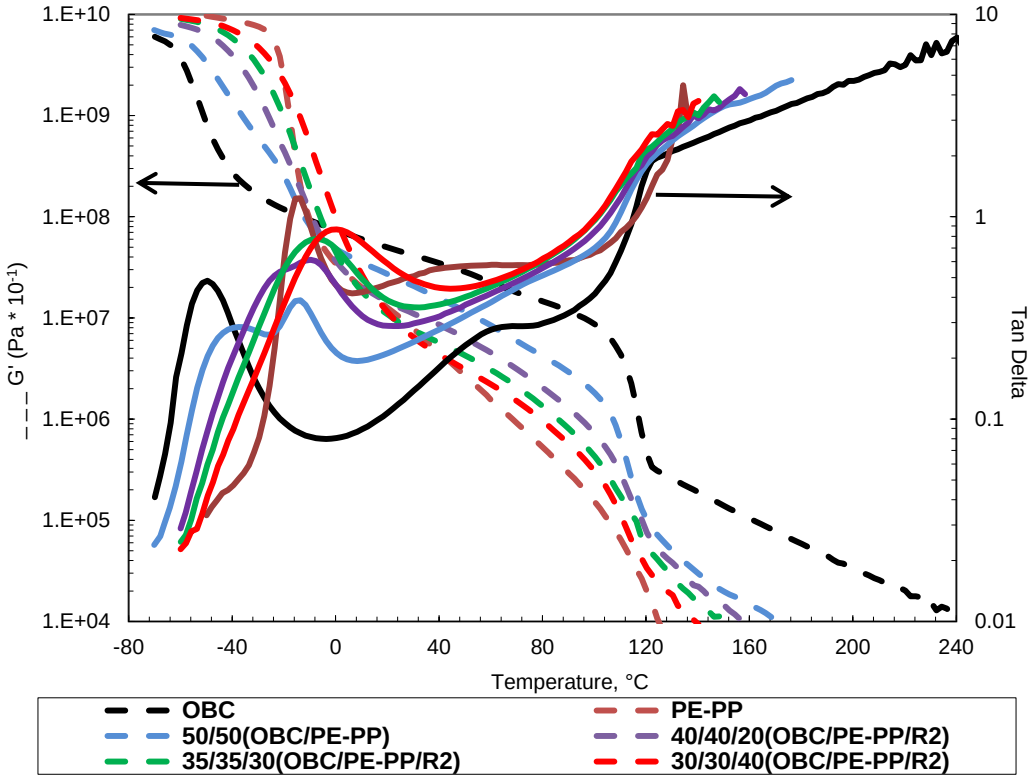

Figure 15. DMA of OBC/PE-PP/Aliphatic-aromatic (5%) unsaturated resin blends at different ratios

Interestingly aromatically modified aliphatic resins improve the miscibility characteristics of the OBC/PE-PP blends, even at low resin addition amount (20 wt%) as can be seen in Figure 15. As the resin amount increases, the miscibility also improves resulting in single glass transition at 30 wt% and 40 wt% resin addition. The elastic modulus also decreases as the aromatic resin amount increases and is in between both parent polymers and the 50/50 OBC/PE-PP blends. Figure 16 shows the highly aromatic (14%), aliphatic-aromatic unsaturated resin effect in OBC/PE-PP blends.

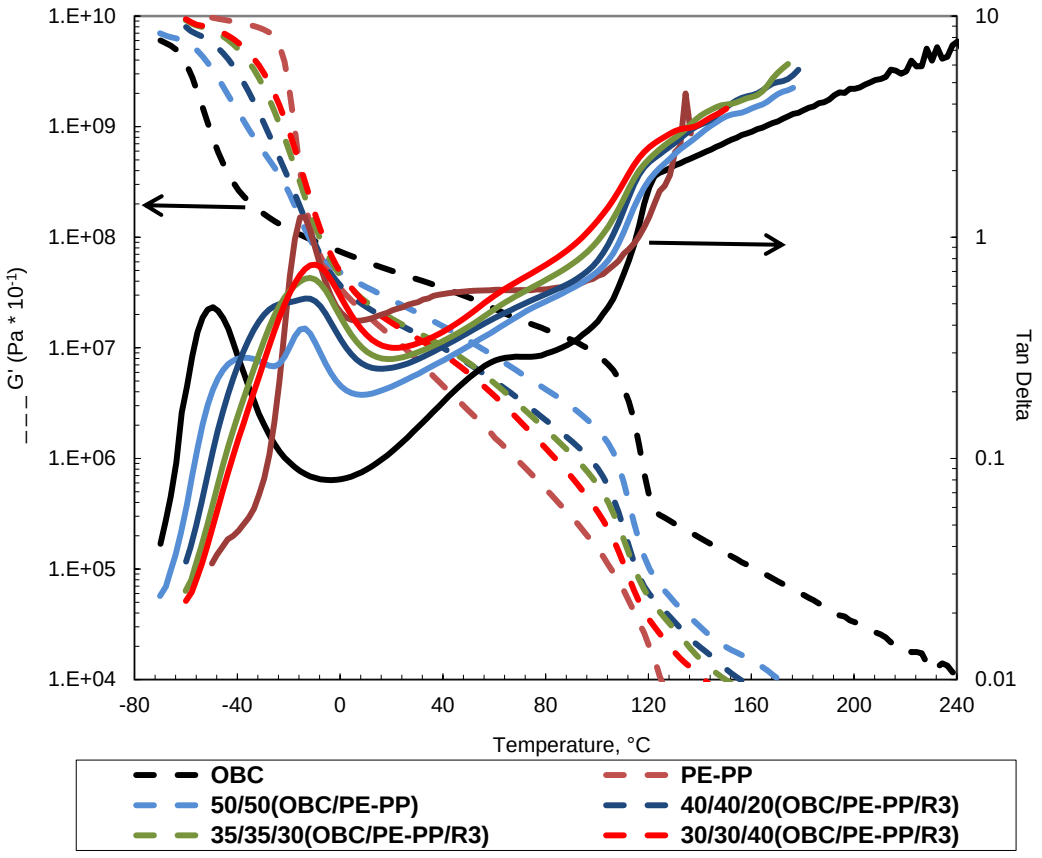

Figure 16. DMA of OBC/PE-PP/Aliphatic-aromatic (14%) unsaturated resin blends at different ratios

As mentioned earlier, higher aromatic content actually has definite influence in miscibility characteristics of OBC/PE-PP blends. 20 wt%, 30 wt% and 40 wt% resin addition amounts of 14% aromatic resin addition to OBC/PE-PP blends shows a single T_g, narrower tan δ curve, and lower elastic modulus characteristics, likely indicating improved miscibility. It is interesting to note that higher aromatic content resin addition to OBC/PP blends showed very poor miscibility characteristics. However in the case of OBC/PE-PP blends with higher aromatic content resin (14%), aromatic content seems to improve the miscibility behavior. Approximately 8% ethylene content in PE-PP polymer seems to improve the interfacial miscibility characteristics of OBC/PE-PP blend, when formulated with an aliphatic-aromatic resin. Figure 17 shows the influence of unsaturated resin aromatic content on OBC/PE-PP blend.

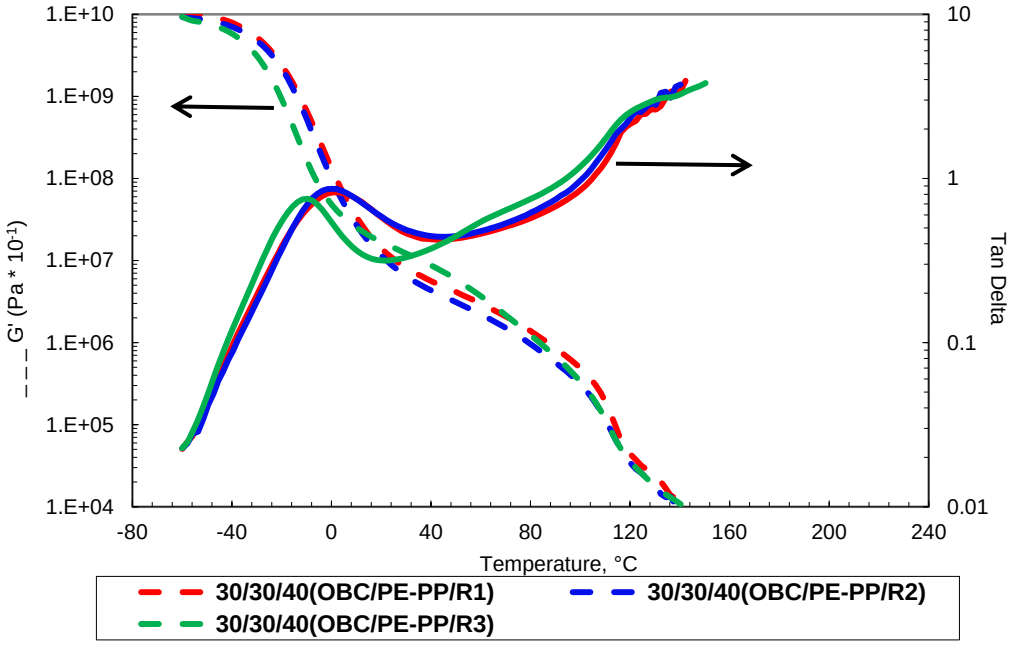

Figure 17. DMA of 40 wt% unsaturated resin containing OBC/PE-PP blends with increasing resin aromatic content

As can be seen (Figure 17), the higher aromatic content (14%) resin addition at 40 wt% level to OBC/PE-PP blends results in a single tan δ peak, indicating better miscibility between the blend components, compared to the lower aromatic content(5%) resin (R2) and aliphatic unsaturated resin (R1). Figure 18 shows the ternary plot of OBC/PE-PP blends with hydrocarbon resins, binary blends of OBC with unsaturated hydrocarbon resins and binary blends of PE-PP with hydrocarbon resins. Bottom axis represents the amount of PE-PP, and the circular dots represent the T_g of particular binary blends of PE-PP with hydrocarbon resins. The axis on the left corresponds to the amount of OBC. The axis on the right of the ternary plot represents the amount of unsaturated tackifier resin, and the circular dots represent the T_g of the particular binary blends of OBC with hydrocarbon resins. Ternary blend T_g is represented as circular dots in the middle of the ternary plot where the OBC, PE-PP and amounts of particular tackifier intersects with respect to the corresponding blend ratios.

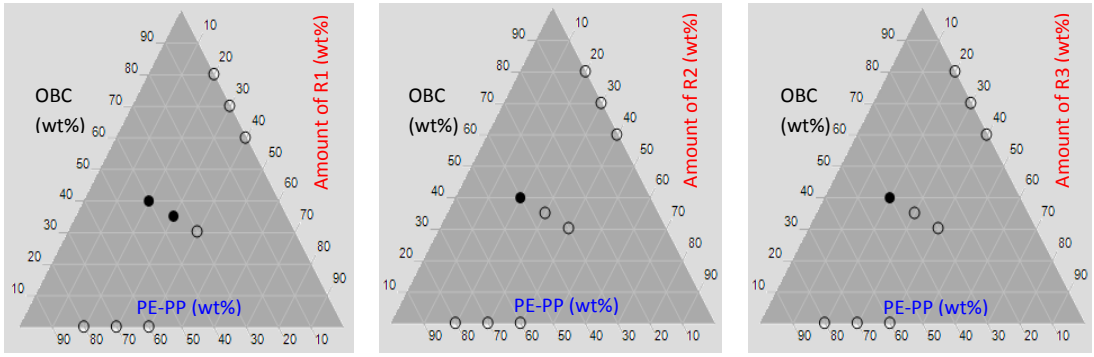

(a) (b) (c)

Figure 18. Ternary plot of glass transition temperatures for OBC/PE-PP blends with resins. (a) Resin 1 (R1), (b) Resin 2 (R2), (c) Resin 3 (R3)

Blackened dot indicates blends with two T_g's and the clear dot indicates blends with a single T_g. The amount of resin concentration was kept the same (20 wt%, 30 wt% and 40 wt%) for binary blends of polymers (OBC or PP with unsaturated hydrocarbon resins, R1, R2 and R3), as for the ternary blends (two polymers with resin). As can be seen in Figure 18, binary blends of OBC polymer with all three hydrocarbon resins shows a single T_g, and the aromatic content of the resin has little effect on the compatibility. Interestingly, binary blends of PE-PP with hydrocarbon resins also show a single T_g, and the aromatic content of the resin has little effect on the compatibility, which is a completely different behavior than that of the PP-resin blends, which showed two T_g's at higher polymer concentration levels (in the blends) and also with aromatic content of the resin. It should be noted that the polyethylene containing polymer shows better miscibility characteristics with hydrocarbon resins, irrespective of the aromatic content, which is evident from an OBC polymer stand point (which is an ethylene-octene polymer) and the PE-PP amorphous polyolefin stand point. The rigid backbone of PP with a bulky methyl group, compared to the more flexible linear polyethylene backbone, could help explain the differences we see in the miscibility behaviors for the blends.

Polymer miscibility characteristics can further by verified by observations through electron microscopy. In this study, Transmission Electron Microscopy (TEM) was employed to better understand the miscibility behavior of the OBC/PP and OBC/PE-PP blends with different hydrocarbon resins. Figure 19 shows the TEM micrographs of OBC/PP blends containing three different hydrocarbon resins.

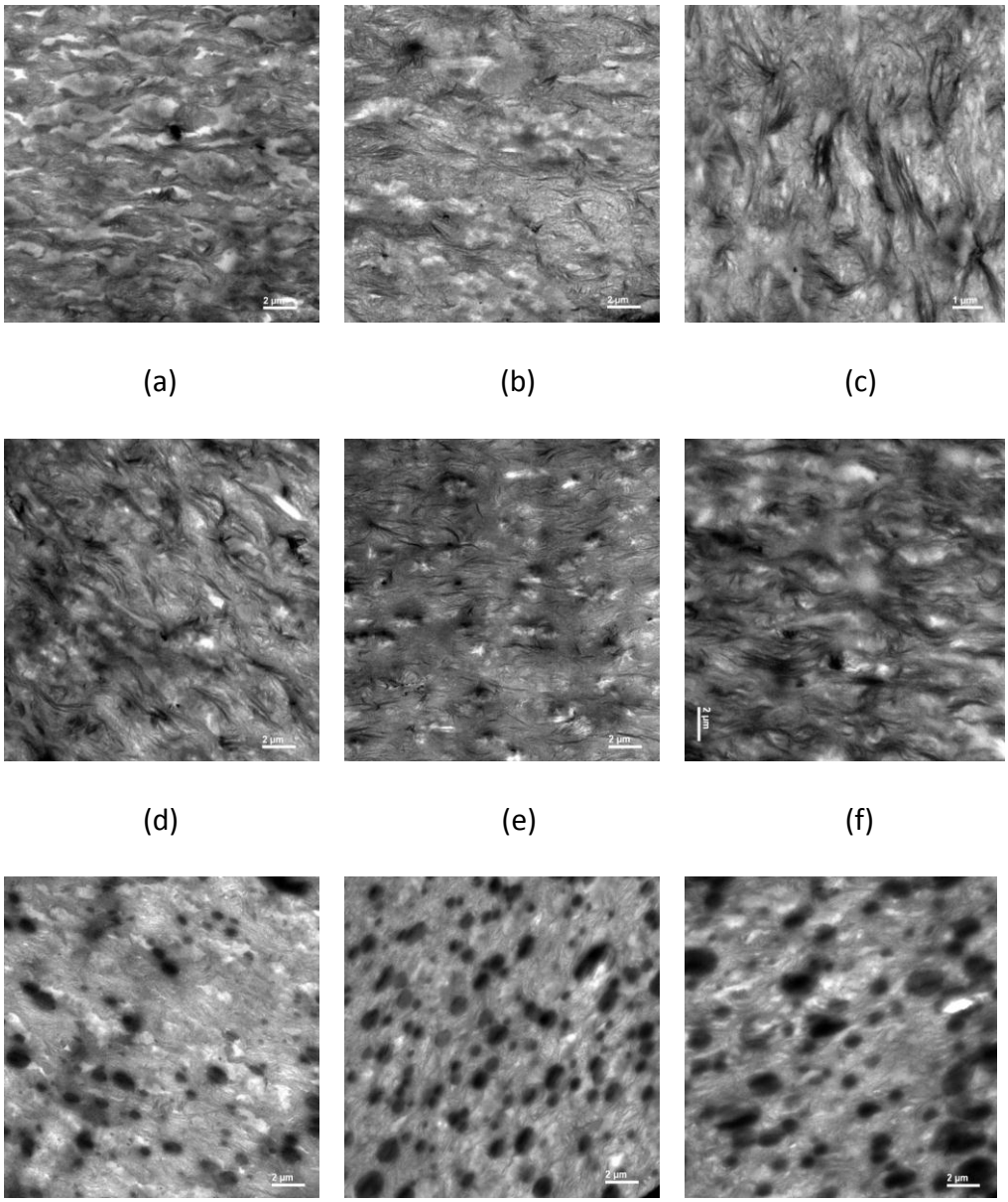

Figure 19. TEM micrographs of OBC/PP blend containing unsaturated resins. (a) 40/40/20(OBC/PP/R1), (b) 35/35/30(OBC/PP/R1), (c) 30/30/40(OBC/PP/R1), (d) 40/40/20(OBC/PP/R2), (e) 35/35/30(OBC/PP/R2), (f) 30/30/40(OBC/PP/R2), (g) 40/40/20(OBC/PP/R3), (h) 35/35/30(OBC/PP/R3), (i) 30/30/40(OBC/PP/R3)

The continuous phase and dispersed phase morphologies of the OBC/PP containing unsaturated resin blends are clear from the above TEM micrographs. TEM micrographs in rows represent the increasing amount of same unsaturated resin in the blend, while the TEM micrographs in columns represents the higher amount of aromatic content in ascending order at the same resin addition levels. The dark areas represent the OBC polymer phase containing resin, and the light dispersed phase is the PP with resin. Since it was difficult to selectively stain one of the phases due to the chemical nature of the blend components, the phase contrast is due to density differences. Improved miscibility of the 40 wt% aliphatic unsaturated resin (R1) containing OBC/PP blend can be correlated well to the single T_g observed from DMA (Figure 9), compared to the other two lower addition levels. Improved miscibility can be also seen with 30 wt% and 40 wt% addition of slightly aromatic (5%) aliphatic-aromatic resin (R2) containing OBC/PP blend, and can be correlated well to the single glass transition observed (Figure 10). However, high aromatic content (14%) unsaturated resin (R3) containing OBC/PP blend clearly shows the well dispersed dark aromatic resin phase along with light PP-resin phase. Slight immiscibility behavior of the OBC/PP blend containing highly aromatic (14%) aliphatic-aromatic unsaturated resin can also be correlated to the two different glass transition temperatures observed at all three addition levels (Figure 11).

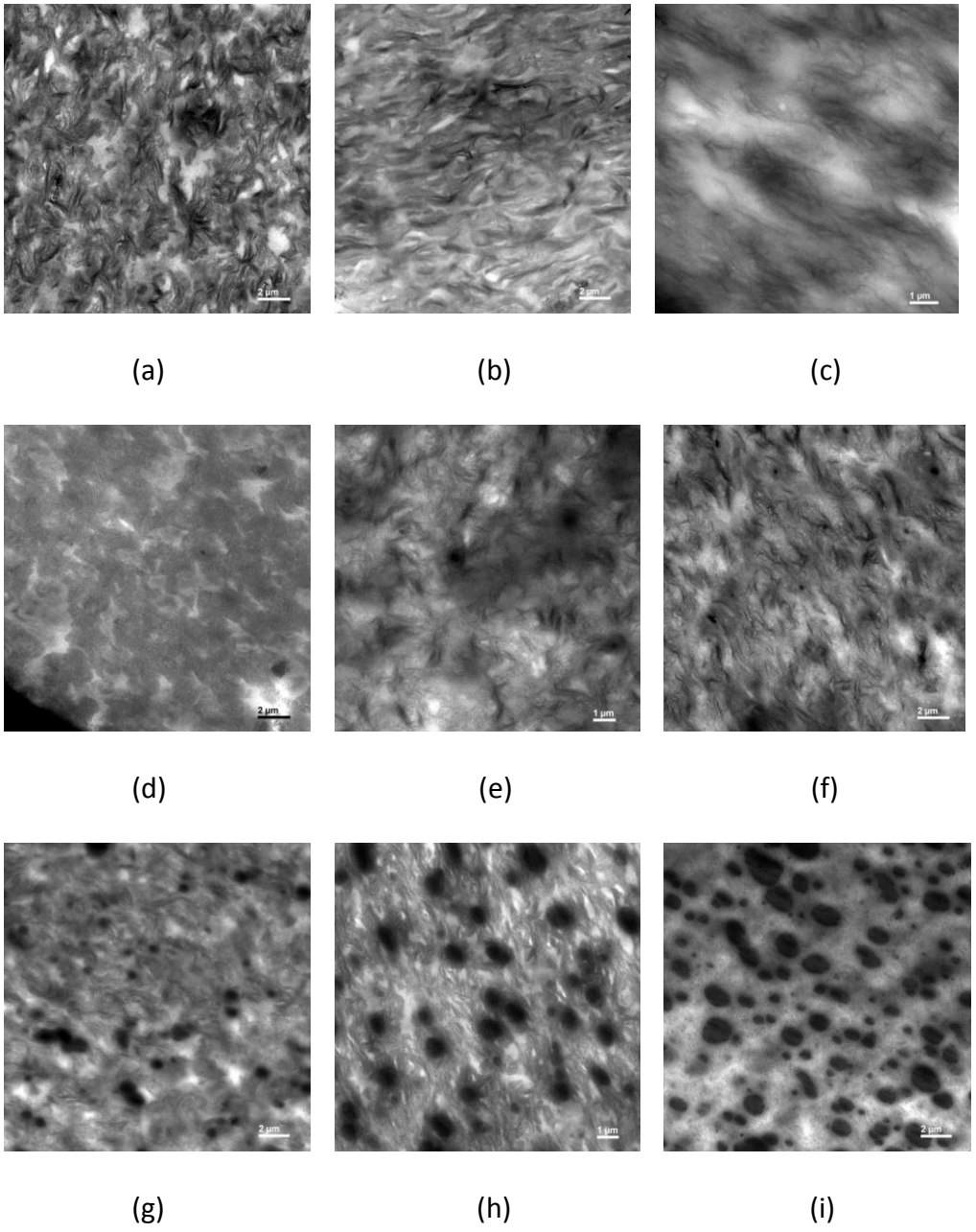

Figure 20. TEM micrographs of OBC/PE-PP blend containing unsaturated resins. (a) 40/40/20(OBC/PE-PP/R1), (b) 35/35/30(OBC/PE-PP/R1), (c) 30/30/40(OBC/PE-PP/R1), (d) 40/40/20(OBC/PE-PP/R2), (e) 35/35/30(OBC/PE-PP/R2), (f) 30/30/40(OBC/PE-PP/R2), (g) 40/40/20(OBC/PE-PP/R3), (h) 35/35/30(OBC/PE-PP/R3), (i) 30/30/40(OBC/PE-PP/R3)

Phase morphologies of OBC/PE-PP blends (Figure 20) with hydrocarbon resins are similar to that of OBC/PP blends with hydrocarbon resins, in which the OBC-resin matrix forms the continuous phase while the PE-PP–resin matrix forms the dispersed phase. The continuous and dispersed phase morphologies of the blends containing aliphatic unsaturated resin (R1) containing blends and slightly aromatic (5%) aliphatic-aromatic resin (R2) containing OBC/PE-PP blend is obvious in the case of 20 wt% addition levels. at 30 wt% and 40 wt% addition levels, even though there are some dark and light regions, it is not as obvious as for the 20 wt% addition levels in the aliphatic (R1) and slightly aromatic (R2) resin addition levels. It is interesting to note that at 30 wt% and 40 wt% addition levels of highly aromatic (14%) unsaturated resin (R3), containing OBC/PE-PP blend showed single tan δ peak, but the morphological analysis clearly shows ternary phase structures, which includes an OBC-resin continuous phase, light PE-PP-resin dispersed phase along with a resin dominated circular dark dispersed phase, as we seen for the OBC/PP blends containing highly aromatic (14%) unsaturated resin (R3). OBC/PP blends containing highly aromatic (14%) unsaturated resin (R3) DMA showed two tan δ peak which correlated well with the immiscibility characteristics observed in the morphological analysis. Even though we see a ternary phase morphology for OBC/PE-PP blends containing highly aromatic (14%) unsaturated resin (R3), the storage modulus, G' (Figure 16) of the blends, in between the parent polymers (lower than OBC and higher than PE-PP) indicates that the resin is in the OBC/PE-PP interphase, which improves the miscibility characteristics, resulting in a single tan δ peak. On the other hand OBC/PP blends containing highly aromatic (14%) unsaturated

resin (R3) showed lower modulus (G') than that of the parent polymers (Figure 11), indicating that the resin is softening both the parent polymer phases (especially OBC) more than that of the OBC/PP interphase, resulting in two tan δ peaks.

Mostofi *et al.*[17] and Hobbs *et al*.[18] reported a theoretical method to determine the phase morphology of ternary blend systems, especially the dispersed phase morphology. Both of the researchers used Harkins spreading coefficient concept, specifically used for ternary blends containing a continuous phase A and dispersed phases B and C.[17] The spreading coefficients λ_{BC} and λ_{CB} are defined as

$$\lambda_{BC} = \gamma_{AC} - \gamma_{AB} - \gamma_{BC} \qquad \& \qquad \lambda_{CB} = \gamma_{AB} - \gamma_{AC} - \gamma_{BC}$$

Where "γ_{ij}" is the interfacial tension between components 'i' and 'j' phases and is defined as

$$\gamma_{ij} = \gamma_i + \gamma_j - \left[\frac{4\gamma_i{}^d\gamma_j{}^d}{\gamma_i{}^d + \gamma_j{}^d}\right] - \left[\frac{4\gamma_i{}^p\gamma_j{}^p}{\gamma_i{}^p + \gamma_j{}^p}\right]$$

Where γ_i and γ_j are the surface tension of the components 'i' and 'j'. $\gamma_i{}^d$ and $\gamma_j{}^d$ are the dispersive portions, and $\gamma_i{}^p$ and $\gamma_j{}^p$ are the polar portions of the surface tension component 'i' and 'j' respectively. Negative spreading coefficient values, 'λ_{BC}' and 'λ_{CB}' will result in separate dispersed phases of minor components. If spreading coefficient 'λ_{BC}' is positive and spreading coefficient 'λ_{CB}' is negative, it will result in encapsulation of 'C' phase by 'B' phase.[17]

Table 7 shows the surface tension data obtained through contact angle measurements. Total surface tension is the sum of dispersive and polar portions. As the aromatic content of the hydrocarbon resins increases, the total surface tension also increases. Aliphatic-aromatic resin with high aromatic (14%) content show higher surface tension, not only in the dispersive portion, but also for the polar portion.

Table 7. Surface tension of OBC, PP, PE-PP and unsaturated hydrocarbon resins

Name	Surface Tension (mN/m)		
	Dispersive Portion (mN/m)	Polar Portion (mN/m)	Total surface tension (mN/m)
Resin 1 (R1)	46.9	0.02	46.92
Resin 2 (R2)	48.04	0.03	48.07
Resin 3 (R3)	49.84	0.59	50.43
OBC	18.36	0.11	18.47
PP	24.66	0.27	24.92
PE-PP	23.55	0.6	24.15

Polar portion of the surface tension for high aromatic content resin (R3) and PE-PP polymer are the same, while there is a significant difference in dispersive portions of the surface tension between the two. There is not much difference between the total surface tension of the PP and PE-PP polymers, but both of them are higher than that of the OBC polymer.

The spreading coefficients calculated for OBC/PP/unsaturated hydrocarbon resin blends and OBC/PE-PP/unsaturated hydrocarbon resin blends are given in Table 8. As we seen from the blend morphologies, OBC is considered as the continuous phase 'A'. PP polymer and PE-PP polymer were considered as the dispersed phase 'B'. Unsaturated hydrocarbon resins R1, R2 and R3 were considered as the dispersed phase 'C' for calculations.

Table 8. Spreading coefficients calculated for the OBC/PP/Resin and OBC/PE-PP/Resin blends

	OBC/PP	OBC/PE-PP
Resin 1 (R1)	λ_{BC} = 4.45	λ_{BC} = 3.28
	λ_{CB} = -18.68	λ_{CB} = -19.84
Resin 2 (R2)	λ_{BC} = 4.63	λ_{BC} = 3.44
	λ_{CB} = -20.03	λ_{CB} = -21.22
Resin 3 (R3)	λ_{BC} = 5.26	λ_{BC} = 4.46
	λ_{CB} = -22.50	λ_{CB} = -23.30

As can be seen from Table 8 that spreading coefficient 'λ_{BC}' is positive and spreading coefficient 'λ_{CB}' is negative, which will result in encapsulation of phase 'C' by phase 'B'. This means that in case of all the blends, the unsaturated hydrocarbon resin is encapsulated by the amorphous PP or amorphous PE-PP polymer in the dispersed phase, which depends on the blend composition.

Summary and Path Forward

- Ternary blends of OBC/PP with unsaturated aliphatic resins at higher resin addition levels showed compatibility behavior. Higher the aromatic content of the resin (especially R3) in OBC/PP blend, lower the compatibility.
- A ternary phase morphology was particularly observed for both OBC/PP and OBC/PE-PP blends with highly aromatic (14%) hydrocarbon resin, in which OBC forming the continuous phase, and PP, PE-PP and unsaturated hydrocarbon resins forming the dispersed phase with respective blend composition.
- Ternary blends of OBC/PE-PP with unsaturated hydrocarbon resins showed a completely different behavior than the OBC/PP/Resin ternary blends. Higher the aromatic content of the unsaturated hydrocarbon resin for OBC/PE-PP blends, higher the compatibility. This is mainly due to the better interfacial interaction between the OBC/PE-PP interphase provided by the aromatically modified unsaturated resin chemistry. This is further verified though the storage modulus, G' (Figure 16) of the blends, in between the parent polymers for OBC/PP/R3 blends (lower than OBC and higher than PE-PP), which indicates that the resin is in the OBC/PE-PP interphase that improves the miscibility, resulting in compatibility (single tan δ peak). On the other hand OBC/PP blends containing highly aromatic (14%) unsaturated resin (R3) showed lower modulus (G') than that of the parent polymers (Figure 11), indicating that the resin is softening both the parent polymer phases (especially OBC) more than that of the OBC/PP interphase, resulting in incompatibility (two tan δ peak).

- Harkins spreading coefficient concept was used to better understand the ternary blend dispersed phase morphology. Spreading coefficients indicate that the free unsaturated hydrocarbon resin is encapsulated by the amorphous PP or amorphous PE-PP polymer in the dispersed phase for the respective blend compositions.
- Aliphatic hydrocarbon resins seem to show better compatibility characteristics with OBC/PP blends. However, aromatically modified aliphatic unsaturated hydrocarbon resins show better compatibility characteristics with OBC/PE-PP blends. Overall it has been observed that OBC/PE-PP showed better miscibility characteristics with unsaturated hydrocarbon resins than that of the OBC/PP blends with unsaturated hydrocarbon resins.
- Since it has been observed that aromatic content or cyclic nature of the unsaturated hydrocarbon resin chemistry influences the compatibility behavior of the OBC/PP blends and OBC/PE-PP blends, it would be interesting to see the effect of saturated cycloaliphatic resins on the compatibility characteristics of OBC/PP and OBC/PE-PP blends. In the next chapter the effect of a saturated cycloaliphatic hydrocarbon resin and a linear aliphatic-cyclo aliphatic resin on OBC/PP blends and OBC/PE-PP blends will be discussed.

References

1. L. A. Utracki, *Polymer Alloys and Blends*, Hanser Gardner Publications Inc., Cincinnati (1989)

2. M. M. Coleman, J. F. Graf and P. C. Painter, *Specific Interactions and the Miscibility of Polymer Blends*, Technomic Publishing Company Inc., Lancaster (1991)
3. S. Datta and D. J. Lohse, *Polymeric Compatibilizers*, Hanser Gardner Publications Inc., Cincinnati (1996)
4. C. Koning et al., *Prog. Polym. Sci.*, 23, 707 (1998)
5. A. K. Kulshreshtha and A. K. Vasile (Ed.), *Handbook of Polymer Blends and Composites*, Rapra Technology Limited, Shawbury-UK (2003)
6. S. Krause, *Pure & Applied Chemistry*, 58 (12), 1553 (1986)
7. W. H. Sheout and H. H. Day, US Patent No. 3965 (1845)
8. R. G. Drew, GB Patent 312,610 (1930)
9. R. G. Drew, GB Patent 405,263 (1934)
10. J. B. Class and S. G. Chu, *J. Appl. Polym. Sci.*, 30, 805 (1985)
11. D. Satas (Ed.), *Handbook of pressure Sensitive Adhesive Technology (Third edition),* Satas & Associates, Warwick-RI (1999)
12. N. Nakajima et al., *J. Appl. Polym. Sci.,* 44, 1437 (1992)
13. P. M. Dunckley, *Adhesives Age*, 17 (Nov. 1993)
14. S. N. Yau and E. M. Woo, *Macromol. Rapid Commun.*, 17, 615 (1996)
15. S. Hamden et al., *Journal of Polymer Research*, 7 (4), 237 (2000)
16. L. M. Robeson (Ed.), *Polymer Blends*, Hanser Gardner Publications Inc., Cincinnati (2007)

17. N. Mostofi, H. Nazockdast and H. Mohammadigoushki, *J. Appl. Polym. Sci.,* 114, 3737 (2009)

18. S. Y. Hobbs, M. E. J. Dekkers and V. H. Watkins, *Polymer*, 29, 1598 (1988)

CHAPTER - 4. EFFECT OF SATURATED CYCLOALIPHATIC AND SATURATED LINEAR ALIPHATIC-CYCLOALIPHATIC HYDROCARBON RESINS ON BLENDS OF OLEFINIC BLOCK COPOLYMER AND LOW MOLECULAR WEIGHT PROPYLENE AND ETHYLENE-PROPYLENE AMORPHOUS POLYMERS

Abstract

A saturated cycloaliphatic hydrocarbon resin and a saturated linear aliphatic-cycloaliphatic hydrocarbon resin were selected for this study to understand the structural influence on the blend miscibility (OBC/PP and OBC/PE-PP). A 1:1 polymer blend ratio of OBC/PP and OBC/PE-PP was also selected for this study to better understand the influence of resin addition in three different levels 20 wt%, 30 wt% and 40 wt%. Dynamic mechanical analysis and transmission electron microscopy evaluations were also performed to determine the blend miscibility characteristics. Interestingly we did not observe much difference in miscibility characteristics between the two resin chemistries in both blend systems (OBC/PP and OBC/PE-PP). At lower resin addition levels (20 wt%) both blends (OBC/PP and OBC/PE-PP) showed immiscibility behavior irrespective of the resin chemistry, while at higher resin addition levels OBC/PP and OBC/PE-PP blends showed a single T_g, indicating miscibility with both resin chemistries. A continuous and a dispersed phase morphology were observed for both ternary blends using both resin chemistries, and Harkins spreading coefficient evaluations revealed that the free saturated aliphatic hydrocarbon resin is encapsulated by the amorphous PP or amorphous PE-PP polymer in the dispersed phase for the respective blend compositions. Overall it has been observed that OBC-PP and OBC/PE-PP blends showed

better miscibility characteristics with both saturated aliphatic hydrocarbon resins, irrespective of the difference in resin chemistries.

Introduction

The heterogeneous blend morphologies and limited miscibility behavior of olefinic block copolymer blends with amorphous polypropylene and polyethylene-propylene amorphous polymers containing unsaturated aliphatic and unsaturated aliphatic/aromatic resins were explained in the previous chapter. In this chapter the influence of a saturated cycloaliphatic resin and a saturated linear aliphatic-cycloaliphatic hydrocarbon resin on the dynamic mechanical properties and morphology of OBC/APO blends was studied. These hydrocarbon resins are of particular interest due to the fact that the aliphatic resins seem to show better miscibility because of the structural similarity in resin composition with ethylene-octene based OBC and polypropylene amorphous polymer blends, and also with ethylene-octene based OBC and polyethylene-propylene amorphous polymer blends. These saturated cycloaliphatic and linear aliphatic-cycloaliphatic hydrocarbon resins are hydrogenated, low molecular weight, high T_g amorphous materials of petroleum origin. One saturated cycloaliphatic hydrocarbon resin and one saturated linear aliphatic-cycloaliphatic hydrocarbon resin were selected for this study to understand the effect of structural influence on the blend miscibility characteristics, since both resins were aliphatic in character. An idealized structure of the saturated hydrocarbon resins is shown in Figure 21.

The influence of saturated hydrocarbon resins on the effect of morphology (phase modification) and viscoelastic properties have been investigated in this study.

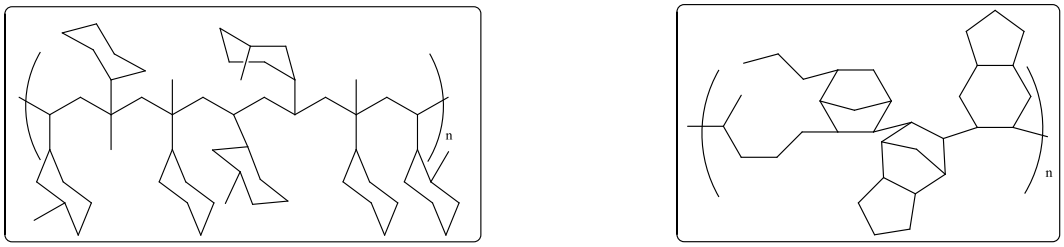

(a) (b)

Figure 21. Ideal structures of saturated hydrocarbon resins. (a) an ideal saturated cycloaliphatic resin structure, (b) an ideal saturated linear aliphatic -cycloaliphatic resin structure

Materials and Methods

A commercially available (INFUSE 9507®) 5 melt index (190°C, 2.16 Kg), 0.866 g/cm^3 density ethylene-octene based olefinic block copolymer (OBC) was obtained from Dow Chemical Company. Atactic propylene homopolymer amorphous polyolefin and ethylene-propylene amorphous polyolefin copolymers were obtained from Eastman Chemical Company. Properties of the amorphous polyolefins (atactic propylene homopolymer and ethylene-propylene copolymer) are given in Table 9. Properties of the saturated hydrocarbon resins selected for this study are given in Table 10.

Ring & Ball softening point, Molecular weight and surface tension evaluations were performed following the same procedure as described in Chapter 3.

Table 9. Properties of polymers

Name	Penetration Hardness (ASTM D5)	Viscosity (190°C) mPa.S (ASTM D3236)	T_g (°C)
PP (Propylene homopolymer)	18	2300	-10
PE-PP (Ethylene-propylene copolymer)	35	5700	-20

Table 10. Properties of the saturated hydrocarbon resins

Resin	Type	Ring & Ball Softening Point (^{0}C)	Molecular Weight Mn/Mw/Mz (Daltons)
Resin 4 (R4)	Cycloaliphatic	92	500/700/1100
Resin 5 (R5)	Linear aliphatic-cycloaliphatic	100	450/1000/2300

A 1:1 polymer blend ratio of OBC/PP and OBC/PE-PP was selected for this study to better understand the influence of resin addition in three different levels (20 wt%, 30 wt% and 40 wt%).

Blends were prepared using a Plasticorder Brabender at 150°C using roller blades, and blended for 20-45 minutes until the torque became constant. OBC/PP/Resin Formulations evaluated are given in Table 11 and OBC/PE-PP/Resin Formulations evaluated are given in Table 12.

Table 11. OBC-PP-Resin blend formulations in wt%

Formulation Description	OBC	PP	Resin 4 (R4)	Resin 5 (R5)
40/40/20(OBC/PP/R4)	40	40	20	-
35/35/30(OBC/PP/R4)	35	35	30	-
30/30/40(OBC/PP/R4)	30	30	40	-
40/40/20(OBC/PP/R5)	40	40	-	20
35/35/30(OBC/PP/R5)	35	35	-	30
30/30/40(OBC/PP/R5)	30	30	-	40

Table 12. OBC-(PE-PP)-Resin blend formulations in wt%

Formulation Description	OBC	PE-PP	Resin 4 (R4)	Resin 5 (R5)
40/40/20(OBC/PE-PP/R4)	40	40	20	-
35/35/30(OBC/PE-PP/R4)	35	35	30	-
30/30/40(OBC/PE-PP/R4)	30	30	40	-
40/40/20(OBC/PE-PP/R5)	40	40	-	20
35/35/30(OBC/PE-PP/R5)	35	35	-	30
30/30/40(OBC/PE-PP/R5)	30	30	-	40

Compatibility and polymer miscibility of the blends was evaluated using Dynamic Mechanical Analysis (DMA) and the morphology of the blends was analyzed using Transmission Electron Microscopy (TEM). Both evaluations were performed following the same procedure as described in Chapter 2.

Results and Discussion

Viscoelastic properties measured using dynamic mechanical analysis (DMA) of the OBC/PP blends and OBC/PE-PP blends with two different saturated hydrocarbon resins are discussed first, followed by description of the morphological evaluation (TEM) of the OBC/PE-PP and OBC/PE-PP blends.

Dynamic mechanical analysis of the OBC/PP blends with cycloaliphatic resin (Resin 4) at three different concentrations is shown in Figure 22.

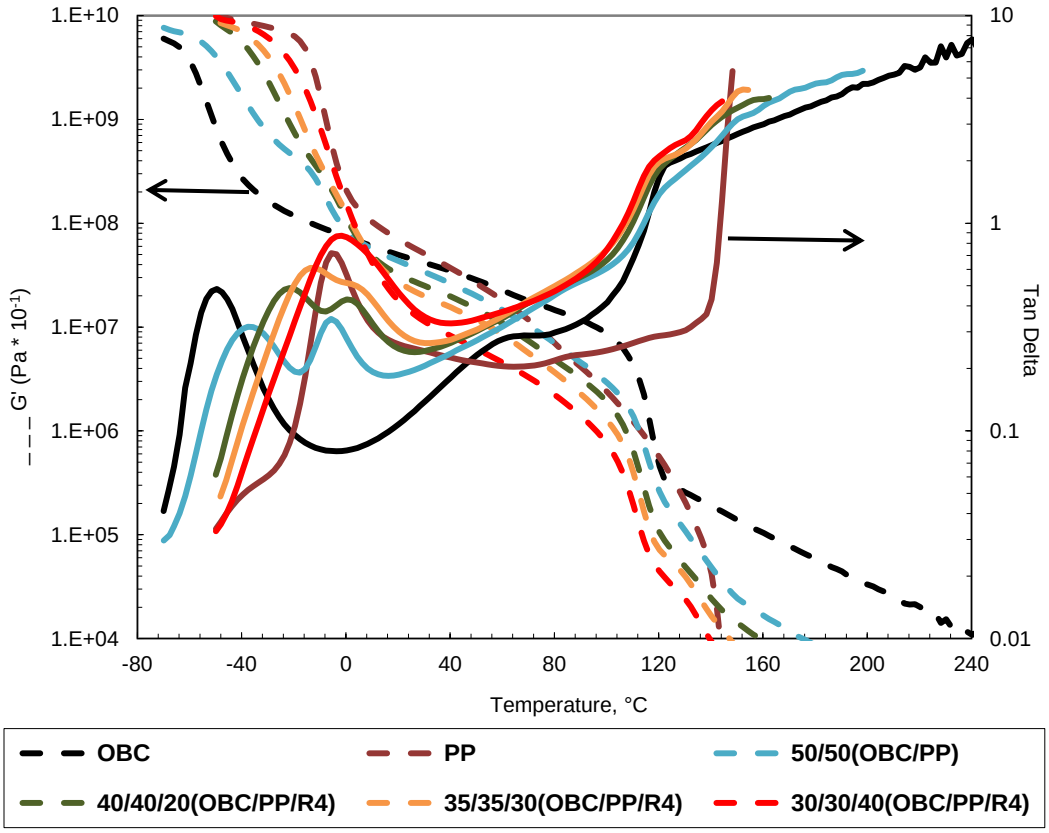

Figure 22. DMA of OBC/PP/Cycloaliphatic saturated hydrocarbon resin blends at different ratios

It can be seen from the above viscoelastic properties that both 20 wt% and 30 wt% additions of cycloaliphatic saturated resin (R4) still show two glass transitions indicating immiscibility. However 40 wt% addition of cycloaliphatic saturated resin shows a single, broad glass transition. It should be noted that the first glass transition temperature and the second glass transition temperature significantly increased for the blends containing 20 wt% and 30 wt% cycloaliphatic saturated resin (R4) indicating

some degree of miscibility, and the decrease in G' shows softening of the respective polymers by the resin addition. The glass transition temperature for the 40 wt% aliphatic saturated resin containing blend is close to that of PP polymer and shows a broad tan δ peak. Elastic modulus (G') decreases as the amount of saturated cycloaliphatic resin in the blend increases and is lower than that of the parent polymers. This may be an indication of the softening of the individual polymers. Figure 23 shows the viscoelastic characteristics of OBC/PP blend containing linear aliphatic – cycloaliphatic saturated resin (R5) at different concentrations.

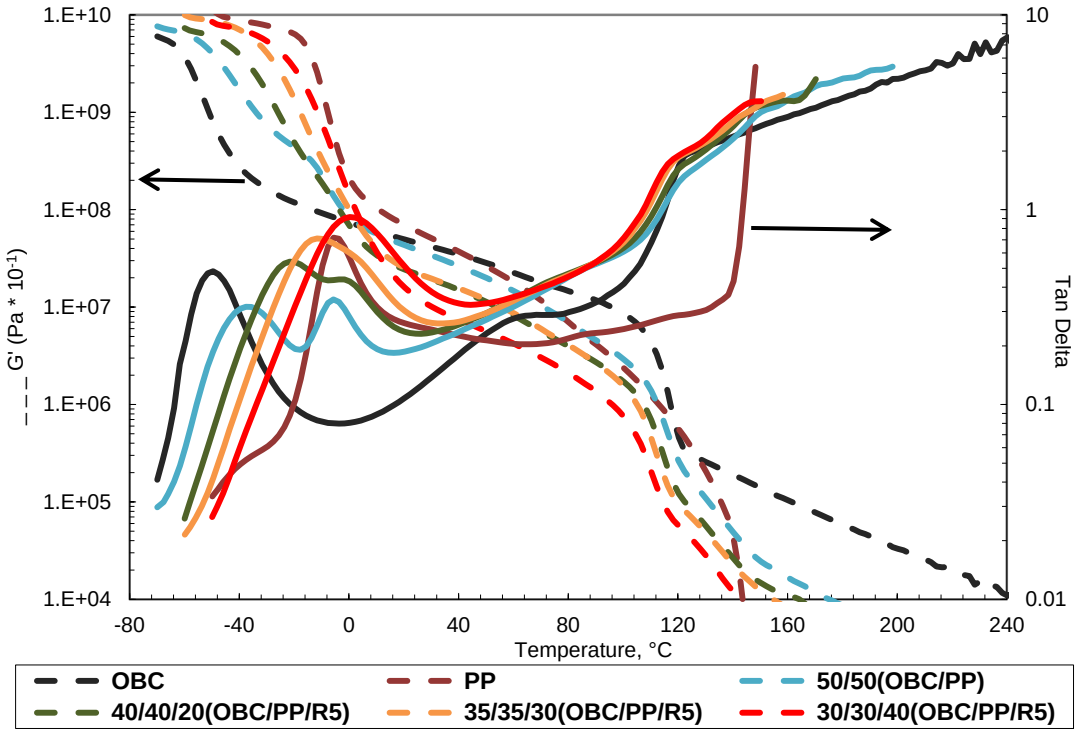

Figure 23. DMA of linear aliphatic-cycloaliphatic saturated hydrocarbon resin containing OBC/PP blends at different ratios

This follows the same trend as it has seen for the aliphatic saturated resin containing blends in previous work. Interestingly, blends containing 30 wt% and 40 wt% of linear aliphatic-cycloaliphatic resin show a single, broad glass transition temperature, but the modulus is lower than that of the parent polymers.

Figure 24 shows the effect of cycloaliphaticity at 40 wt% addition levels for the saturated resin containing OBC/PP blends. As can be seen in Figure 24, blends with cycloaliphatic and linear aliphatic-cycloaliphatic resin at 40 wt% addition level show similar viscoelastic behavior (single T_g, single narrow tan δ curve, and similar elastic modulus). There is not much difference in miscibility characteristics between the two resins in OBC/PP blends.

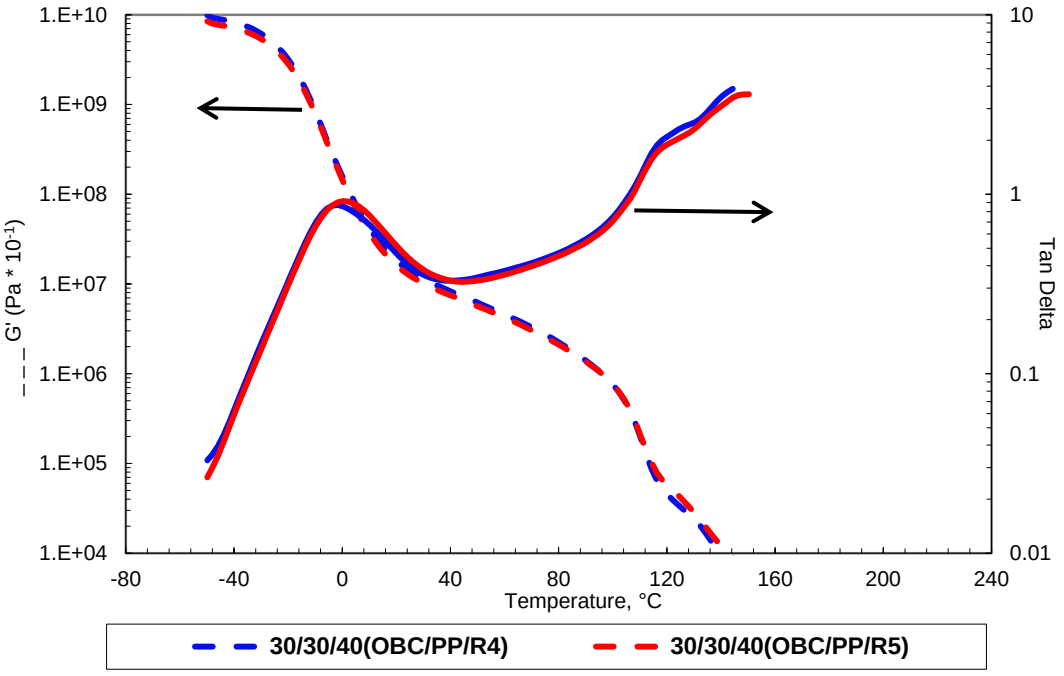

Figure 24. DMA of OBC/PP blends containing 40 wt% saturated hydrocarbon resin containing

Interestingly Resin 5 shows slightly higher T_g for OBC/PP blends compared to blends containing cycloaliphatic saturated resin (R4), and this is mainly due to the higher softening point of Resin 5. Figure 25 shows the ternary plot of OBC/PP blends with saturated hydrocarbon resins, binary blends of OBC with saturated hydrocarbon resins and binary blends of PP with saturated hydrocarbon resins. The bottom axis represents the amount of PP, and the circular dots represent the T_g of particular binary blends of PP with saturated hydrocarbon resins. The axis on the left represents the amount of OBC axis. The axis on the right of the ternary plot represents the amount of saturated tackifier resin, and the circular dots represent the T_g of particular binary blends of OBC with saturated hydrocarbon resins. The T_g of ternary blends is represented as circular dots in the middle of the ternary plot where the OBC, PP and amounts of particular tackifier intersects with respect to the corresponding blend ratios.

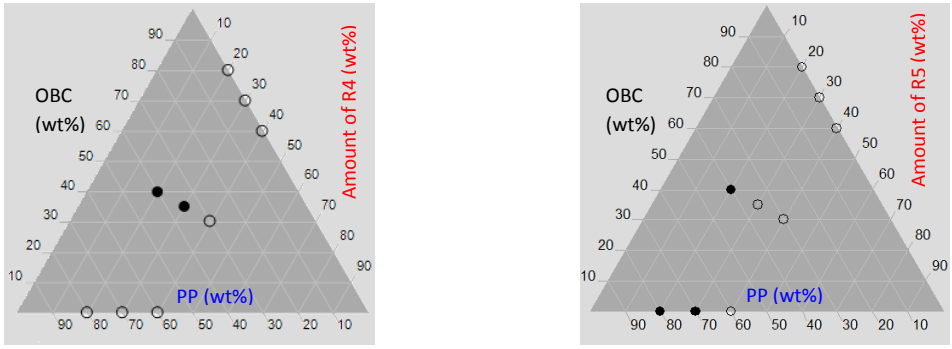

(a) (b)

Figure 25. Ternary plot of glass transition temperatures for OBC/PP blends with resins. (a) Resin 4 (R4) and (b) Resin 5 (R5)

Blackened dot indicates blends with two T_g and the clear dot indicates blends with single T_g. The resin concentration was kept the same (20 wt%, 30 wt% and 40 wt%) for binary blends (1 polymer with 1 resin) and ternary blends (2 polymers and 1 resin) of polymers (OBC and PP) with saturated hydrocarbon resins (R4 and R5). As can be seen in Figure 25, binary blends of OBC polymer with both saturated tackifier resins shows single T_g, and the cycloaliphaticity of resin has little effect on the compatibility. However, binary blends of PP with saturated hydrocarbon resins show a completely different behavior such that as the cycloaliphaticity in the resin increases, the compatibility also increases., resulting in a single T_g at all concentrations levels of resin addition for the PP-R4 blends, as indicated by the clear dots. Figure 26 below shows the effect of aliphatic saturated resin in OBC/PE-PP blends at three different ratios.

As can be seen from Figure 26, 30 wt% and 40 wt% addition of cycloaliphatic saturated resin in to OBC/PE-PP blends show single glass transition and higher glass transition temperatures than that of the parent polymers. It is interesting to note that the storage modulus (G', at room temperature) of the blends containing 20 wt%, 30 wt% and 40 wt% aliphatic saturated resin show similar trends. The storage modulus for these blends is intermediate between the individual polymer values without resin and lower than the 50/50 OBC/PE-PP polymer blend without any resin. This behavior is different than that of the OBC/PP blends containing cycloaliphatic saturated resins (Figure 22), in which the blends containing resins showed lower modulus than that of the parent polymers.

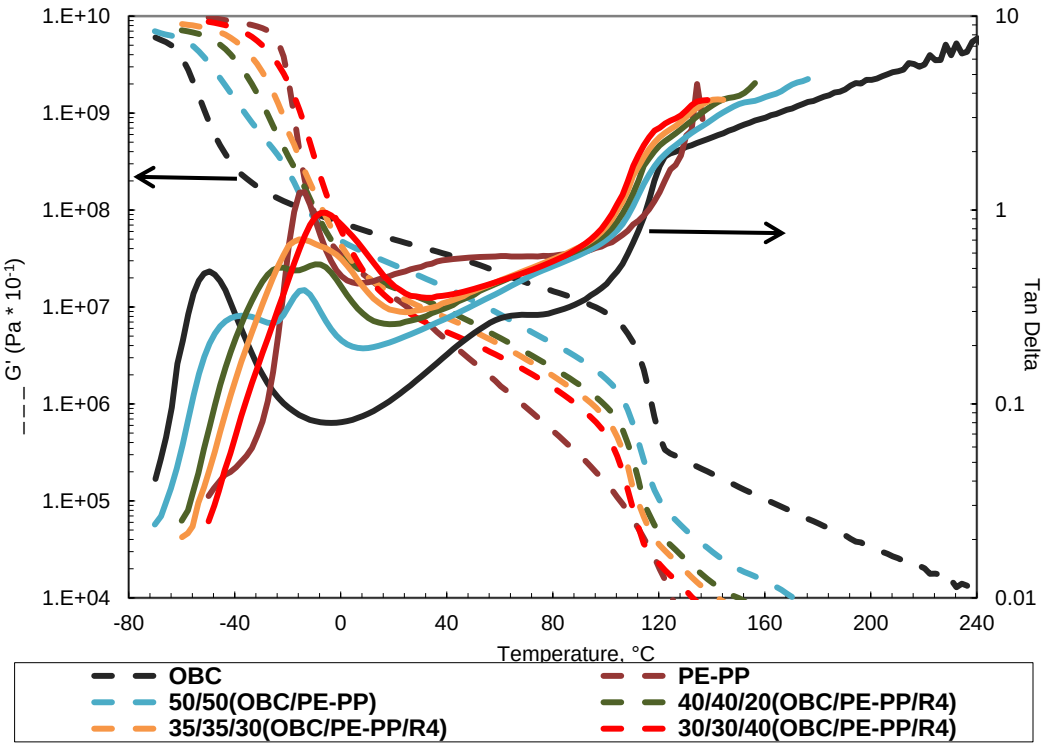

Figure 26. DMA of OBC/PE-PP/Cycloaliphatic saturated hydrocarbon resin blends at different ratios

Figure 27 shows the viscoelastic properties of linear aliphatic-cycloaliphatic saturated resin containing OBC/PE-PP blend at different resin concentrations. Interestingly linear aliphatic-cycloaliphatic modified saturated resins improve the miscibility characteristics of the OBC/PE-PP blends, even at low resin addition amount (20 wt%) as can be seen in Figure 27. As the resin amount increases, the miscibility characteristic also improves resulting in single glass transition at 30 wt% and 40 wt% resin addition. The elastic modulus also decreases as the resin concentration increases and the resulting storage modulus lies between both parent polymers and the 50/50 OBC/PE-PP blends.

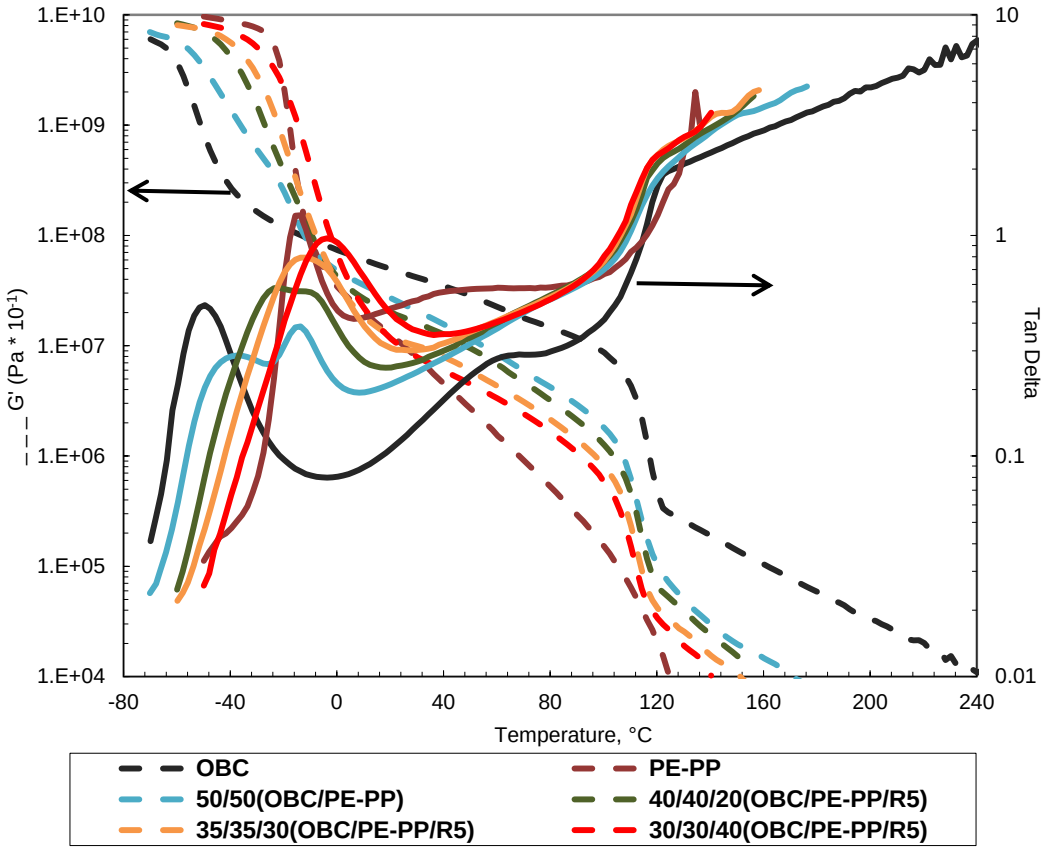

Figure 27. DMA of linear aliphatic-cycloaliphatic saturated hydrocarbon resin containing OBC/PE-PP blends at different ratios

As mentioned earlier, lower cycloaliphaticity (R5) of the resin actually has a definite influence in miscibility characteristics of OBC/PE-PP blends. OBC/PE-PP blends that contain 30 wt% and 40 wt% resin addition amounts of linear aliphatic-cycloaliphatic resin shows a single T_g, a narrower tan δ curve and a lower elastic modulus, indicating improved miscibility. PE-PP polymer seems to improve the interfacial miscibility characteristics of OBC/PE-PP blend, when formulated with a saturated resin. Figure 28 shows the influence of saturated resin aromatic content on OBC/PE-PP blend.

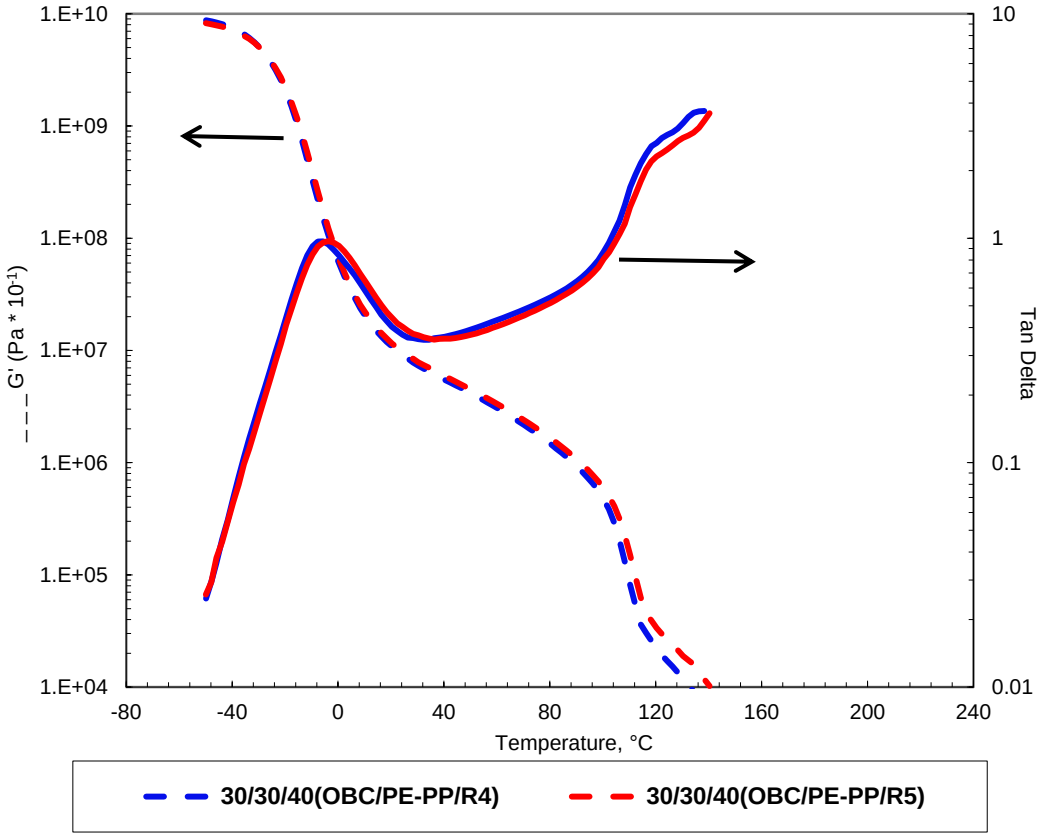

Figure 28. DMA of 40 wt% saturated resin containing OBC/PE-PP blends

As can be seen in Figure 28, the viscoelastic behavior of OBC/PE-PP blends with saturated hydrocarbon resins are very similar, indicating less influence on the resin chemistry (aliphatic and cycloaliphatic) at 40 wt% resin addition levels. Figure 29 shows the ternary plot of OBC/PE-PP blends with saturated hydrocarbon resins, binary blends of OBC with saturated hydrocarbon resins and binary blends of PE-PP with saturated hydrocarbon resins. The bottom axis represents the amount of PE-PP, and the circular dots represent the T_g of particular binary blends of PE-PP with saturated hydrocarbon resins. The axis on the left represents the amount of OBC in the blend. The axis on the right of the ternary plot represents the amount of saturated tackifier resin, and the

circular dots represent the T_g of particular binary blends of OBC with saturated hydrocarbon resins. The T_g of the ternary blend is represented by circular dots in the middle of the ternary plot where the OBC, PE-PP and amounts of particular tackifier intersects with respect to the corresponding blend ratios.

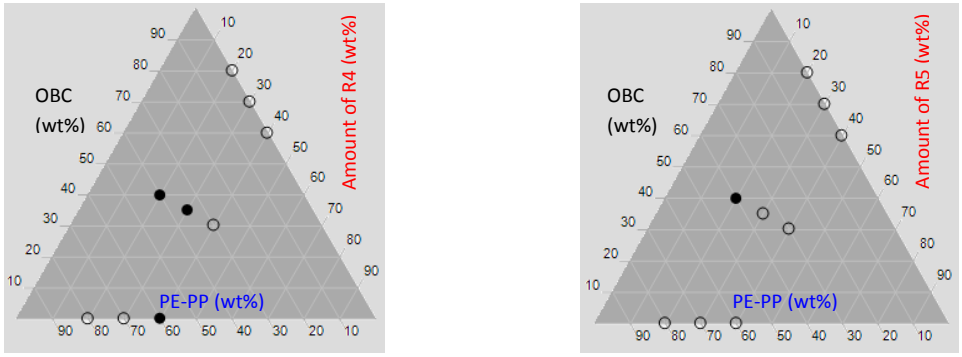

(a) (b)

Figure 29. Ternary plot of glass transition temperatures for OBC/PE-PP blends with resins. (a) Resin 4 (R4) and (b) Resin 5 (R5)

Blackened dots indicate blends with two T_g and the clear dot indicates blends with a single T_g. The amount of resin concentration was kept the same (20 wt%, 30 wt% and 40 wt%) for binary blends of polymers (OBC or PP with resin) and ternary blends (two polymers with resin). As can be seen in Figure 29, binary blends of OBC polymer with all three saturated tackifier resins shows single T_g, and the cycloaliphaticity of resin has little effect on the compatibility characteristics. Interestingly, binary blends of PE-PP with linear aliphatic-cycloaliphatic saturated hydrocarbon resins also show a single T_g, which is a completely different behavior than that of the PP-resin blends, which showed two T_g's at higher polymer concentration levels in the blends. The presence of propylene

in the copolymer creates a more rigid backbone with a bulky methyl group, compared to more flexible linear polyethylene backbone. This could be the reason for the differences observed in the miscibility of the blends.

Polymer miscibility characteristics can further by verified by observations using electron microscopy. In this study, Transmission Electron Microscopy (TEM) was employed to better understand the miscibility of the OBC/PP and OBC/PE-PP blends with different hydrocarbon resins. Figure 30 shows the TEM micrographs of OBC/PP blends containing three different saturated resin levels.

The continuous phase and dispersed phase morphologies of the OBC/PP containing saturated resin blends are clear from the above TEM micrographs (Figure 30). TEM micrographs in rows show the morphology of blends containing the same saturated resin at different levels in the blend. The TEM micrographs in columns show the change of morphology created with different resin structures. The dark areas are the OBC polymer phase containing resin, and the light areas are dispersed phase of the PP APO with resin. Since it was difficult to selectively stain one of the phases due to the chemical nature of the blend components, the phase contrast is due to the density differences. The improved miscibility of the 40 wt% aliphatic saturated resins containing OBC/PP blend can be correlated well to the single T_g observed from DMA (Figure 22 and Figure 23), compared to 20 wt% addition levels. Both resins (R4 and R5) being aliphatic in nature, it was very difficult to see any significant morphological differences between the blends through TEM.

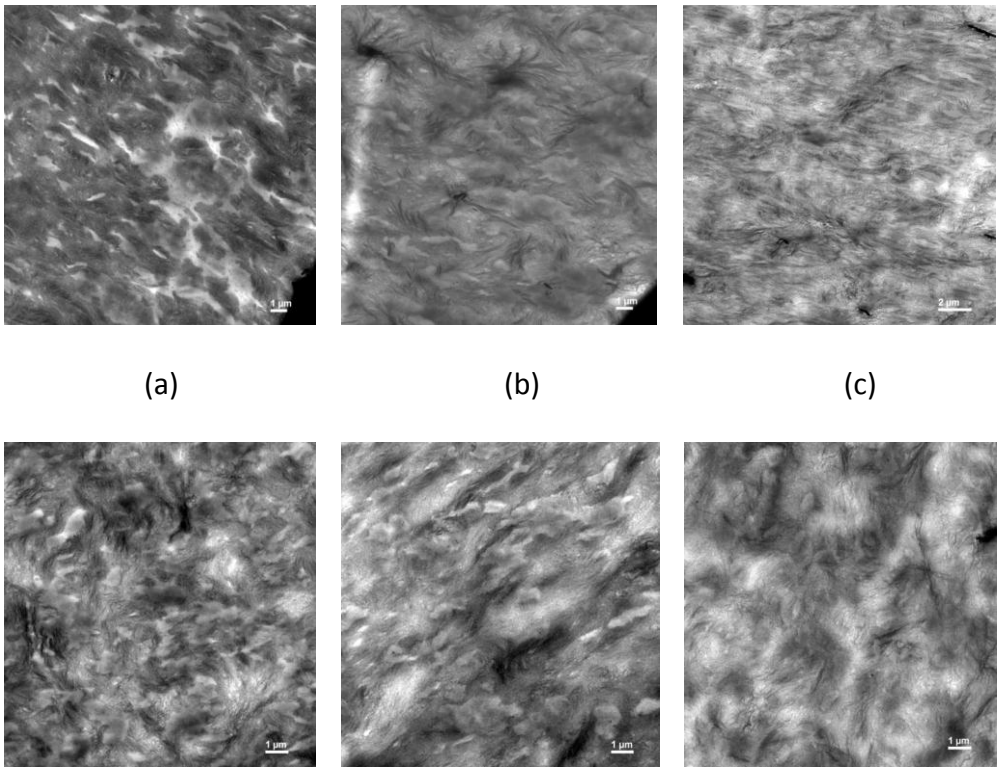

Figure 30. TEM micrographs of OBC/PP blend containing saturated resins. (a) 40/40/20(OBC/PP/R4), (b) 35/35/30(OBC/PP/R4), (c) 30/30/40(OBC/PP/R4), (d) 40/40/20(OBC/PP/R5), (e) 35/35/30(OBC/PP/R5), (f) 30/30/40(OBC/PP/R5)

Phase morphologies of OBC/PE-PP blends with saturated resins (Figure 31) are similar to that of OBC/PP blends with saturated resins, in which the OBC-resin matrix forms the continuous phase while the PE-PP–resin matrix forms the dispersed phase. The continuous and dispersed phase morphologies of the blends containing cycloaliphatic saturated resin (R4) containing blends and linear aliphatic-cycloaliphatic resin (R5) containing OBC/PE-PP blend is not that obvious as in the previous OBC-PP blends.

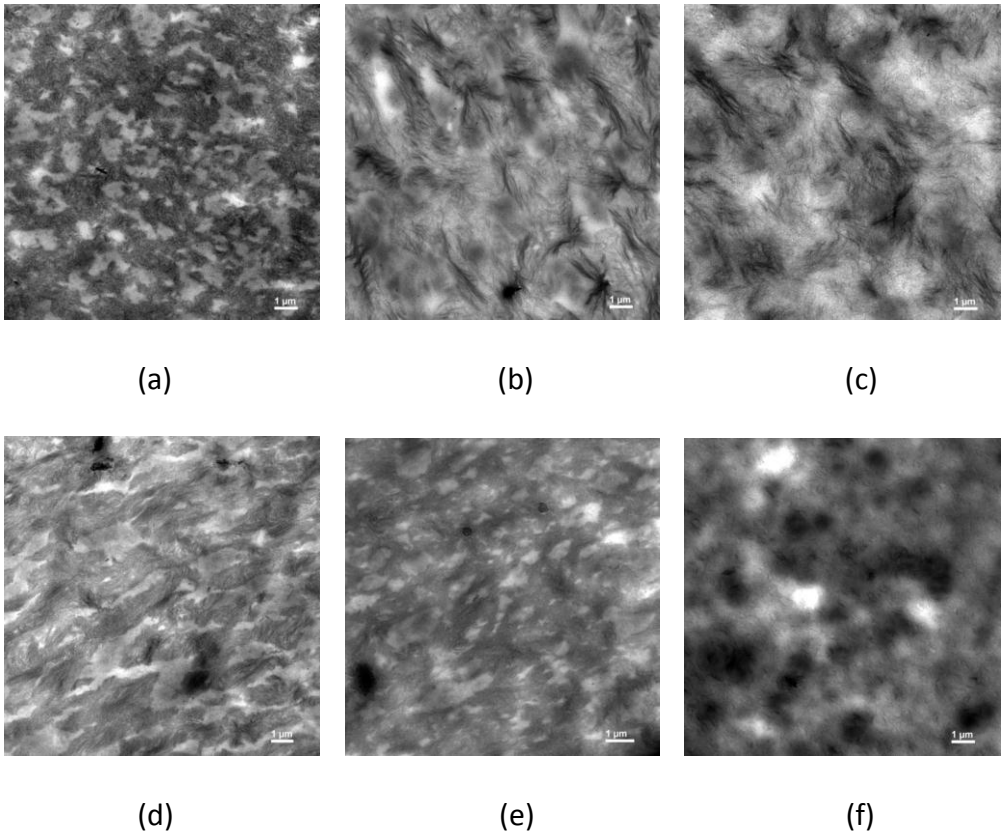

Figure 31. TEM micrographs of OBC/PE-PP blend containing saturated resins. (a) 40/40/20(OBC/PE-PP/R4), (b) 35/35/30(OBC/PE-PP/R4), (c) 30/30/40(OBC/PE-PP/R4), (d) 40/40/20(OBC/PE-PP/R5), (e) 35/35/30(OBC/PE-PP/R5), (f) 30/30/40(OBC/PE-PP/R5)

Mostofi *et al.*[6] and Hobbs *et al.*[7] reported a theoretical method to determine the phase morphology of ternary blend systems, especially the morphology of the dispersed phase. Both of the researchers used Harkins spreading coefficient concept, specifically used for ternary blends containing a continuous phase A and dispersed phases B and C, as explained in Chapter-3. Table 13 shows the surface tension data obtained through contact angle measurements.

Table 13. Surface tension of OBC, PP, PE-PP and saturated hydrocarbon resins

Name	Surface Tension (mN/m)		
	Dispersive Portion (mN/m)	Polar Portion (mN/m)	Total surface tension (mN/m)
Resin 4 (R4)	50.33	0.13	50.46
Resin 5 (R5)	38.96	0.02	38.98
OBC	18.36	0.11	18.47
PP	24.66	0.27	24.92
PE-PP	23.55	0.6	24.15

Total surface tension is the sum of dispersive and polar portions. As the cycloaliphatic nature of the saturated hydrocarbon resins increases, the total surface tension also increases. Cycloaliphatic resins show higher surface tension, not only in the dispersive portion, but also for the polar portion. The polar portion of the surface tension for cycloaliphatic resin (R4) and OBC polymer are the same, while there is a significant difference in dispersive portions of the surface tension between the two. There is not much difference between the total surface tension of the PP and PE-PP polymers, but both of them are higher than that of the OBC polymer.

The spreading coefficients calculated for OBC/PP/saturated hydrocarbon resin blends and OBC/PE-PP/saturated hydrocarbon resin blends are given in Table 14. As we see from the blend morphologies, OBC is considered the continuous phase ‘A’. PP

polymer and PE-PP polymer were considered the dispersed phase 'B'. Saturated hydrocarbon resins R4 and R5 were designated to be the dispersed phase 'C' for calculations.

Table 14. Spreading coefficients calculated for the OB/PP/Resin and OBC/PE-PP/Resin blends

	OBC/PP	OBC/PE-PP
Resin 4 (R4)	λ_{BC} = 5.08	λ_{BC} = 3.89
	λ_{CB} = -22.73	λ_{CB} = -23.91
Resin 5 (R5)	λ_{BC} = 3.07	λ_{BC} = 2.14
	λ_{CB} = -9.91	λ_{CB} = -10.83

As can be seen from Table 14, the spreading coefficient 'λ_{BC}' is positive and spreading coefficient 'λ_{CB}' is negative, which will result in encapsulation of phase 'C' by phase 'B'. This means that in case of all the blends, the saturated hydrocarbon resin is encapsulated by the amorphous PP or amorphous PE-PP polymer in the dispersed phase, depends on the blend composition.

Summary and Path Forward

- At lower resin addition levels (20 wt%) both blends (OBC/PP and OBC/PE-PP) are immiscible irrespective of the resin chemistry, while at higher resin addition

levels (30 wt% and 40 wt%) OBC/PP and OBC/PE-PP blends showed a single T_g, indicating improved miscibility with both resin chemistries.

- Continuous and dispersed phase morphologies were observed for both ternary blends using both resin chemistries, and Harkins spreading coefficient evaluations revealed that the free saturated, aliphatic, hydrocarbon resin is encapsulated by the amorphous PP or amorphous PE-PP polymer in the dispersed phase for the respective blend compositions.
- It has been observed that OBC-PP and OBC/PE-PP blends showed better miscibility characteristics with both saturated aliphatic hydrocarbon resins, irrespective of the difference in resin chemistries. Resin chemistry did not impact miscibility of the blend in either blend system (OBC/PP and OBC/PE-PP) at the higher resin addition levels.
- Since OBC/PE-PP blends showed slightly better miscibility characteristics with unsaturated hydrocarbon resin chemistry and saturated hydrocarbon resin chemistry, it has decided to evaluate this blend in a higher resin containing high T_g pressure-sensitive adhesive formulation, typically used for disposable diaper construction adhesive applications, due to the similarity in viscoelastic characteristics between the blends and the typical disposable diaper construction adhesive. This will be discussed in the next chapter.

References

1. A. K. Kulshreshtha and A. K. Vasile (Ed.), *Handbook of Polymer Blends and Composites*, Rapra Technology Limited, Shawbury-UK (2003)
2. S. Krause, *Pure & Applied Chemistry*, 58 (12), 1553 (1986)
3. S. N. Yau and E. M. Woo, *Macromol. Rapid Commun.*, 17, 615 (1996)
4. S. Hamden et al., *Journal of Polymer Research*, 7 (4), 237 (2000)
5. L. M. Robeson (Ed.), *Polymer Blends*, Hanser Gardner Publications Inc., Cincinnati (2007)
6. N. Mostofi, H. Nazockdast and H. Mohammadigoushki, *J. Appl. Polym. Sci.,* 114, 3737 (2009)
7. S. Y. Hobbs, M. E. J. Dekkers and V. H. Watkins, *Polymer*, 29, 1598 (1988)

CHAPTER - 5. PRESSURE-SENSITIVE ADHESIVES USING BLENDS OF OLEFINIC BLOCK COPOLYMER AND LOW MOLECULAR WEIGHT ETHYLENE-PROPYLENE AMORPHOUS POLYMERS CONTAINING SATURATED AND UNSATURATED HYDROCARBON RESINS

Abstract

Pressure-sensitive adhesives (PSAs) used in disposable diaper construction have been formulated using blends of olefinic block copolymer (OBC) and an atactic ethylene-propylene amorphous polyolefin (APO) polymer, with three different unsaturated hydrocarbon resins (with varying aromatic content), and also with two different saturated aliphatic hydrocarbon resin (with varying cycloaliphaticity). The viscoelastic properties of theses PSA formulations were studied using dynamic mechanical analysis (DMA). Viscosity profiles at five different temperatures were generated to better understand the application window for the resulting adhesive formulation. Adhesives used in disposable diaper construction were applied between a polyethylene backing and a nonwoven substrate with an air assisted spiral spray application technique on an Acumeter Spray Coater. After the adhesive was applied, peel adhesion testing on the samples was performed using an Instron Tensile Tester. It has been observed that the OBC/PE-PP based disposable diaper construction PSA has a lower application temperature along with wider tolerance for hydrocarbon resin chemistries, especially for the saturated aliphatic resins based PSA formulations.

Introduction

Since the advent and commercialization of Pampers® by P&G in the late 1950s, baby diapers, feminine hygiene care products and adult incontinent undergarments

have been an indispensable part of human life. Availability, cost, usefulness and affordability of the hygiene care products for the global human population has also created lots of challenges for the hygiene suppliers, especially in terms of cost, performance improvements, product design, and assembly processes.[1, 2] Diaper products are the largest volume of the disposable hygiene market.[2] Even though a baby diaper looks very simple in appearance, the components and assembly is rather complicated and can be seen in Figure 32.

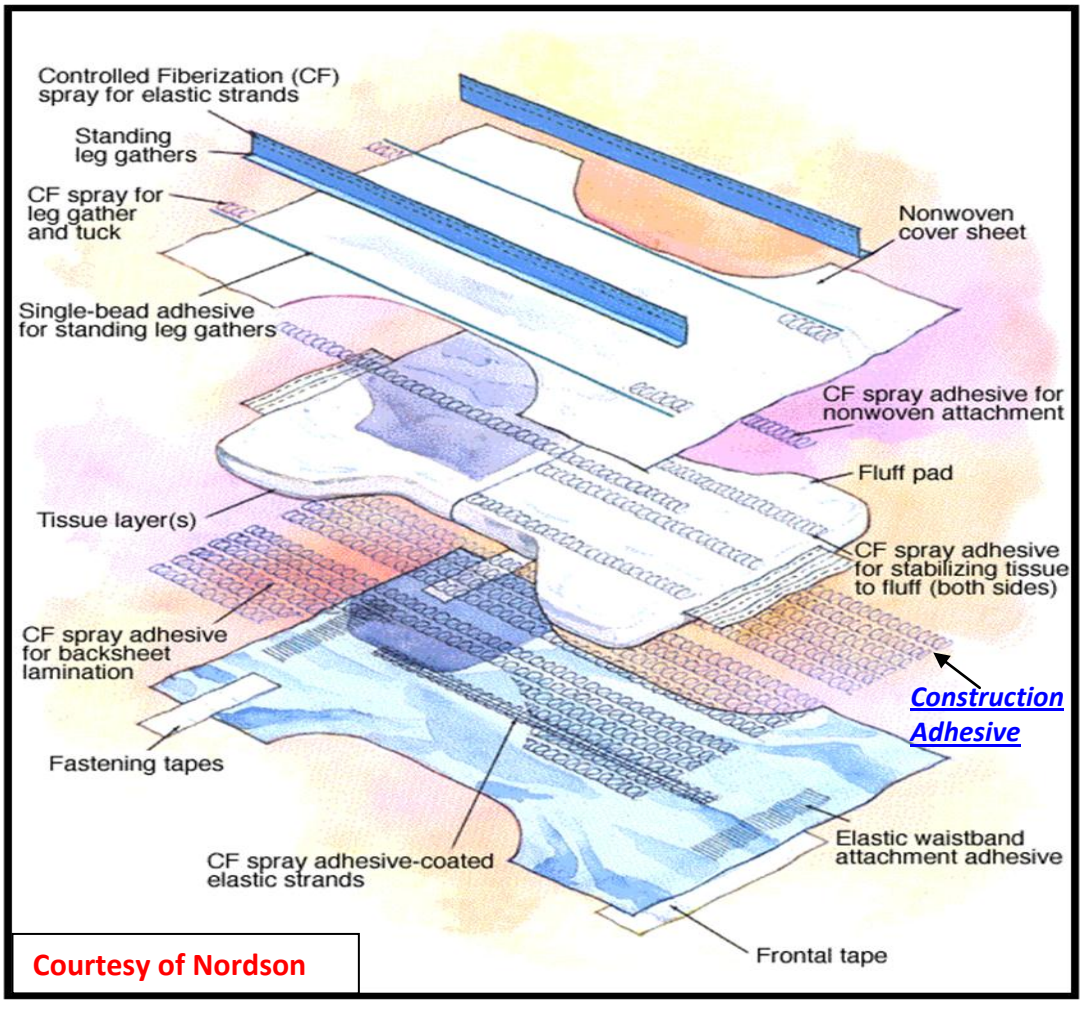

Figure 32. Different components of a disposable baby diaper

Hotmelt adhesives are a major component in the diaper assembly and are used to bond different parts of the diaper together. Two kinds of hotmelt adhesives are usually employed in a diaper assembly; a hotmelt pressure-sensitive construction adhesive used to bond the plastic and nonwoven fabric, and an elastic attachment adhesive that has higher elasticity and bonding strength to bond the legs and waist foam elastics with the plastic and nonwoven fabric.

Even though the early hotmelt adhesive assembly technologies were based on EVA-based hotmelt adhesives typically applied with slot-die coaters, the advent of styrenic block copolymer based hotmelt adhesive formulations[3] emerged as the prominent hotmelt adhesive of choice for the disposable hygiene articles since 1980s due to the versatility in product assembly and performance advantages.[2, 4-7] The next notable breakthrough in the pressure-sensitive adhesives (PSAs) for disposable hygiene article technology came through a newly developed hotmelt application technology in 1980s by Nordson known as hotmelt pressure-sensitive adhesive (PSA) air assisted spray technology.[8] As Raterman of Nordson reported,[8] this air assisted spray technology drastically enhanced the refinement of controlled fibrillation spray that resulted in more control over adhesive application amount, faster line speeds, use of thinner substrate materials (polyethylene and nonwoven fabric) resulting in superior economic advantages. Since then styrene block copolymer based pressure-sensitive adhesive systems with air assisted spray technology configurations (especially spiral spray patterns) has emerged as the work horse adhesive system and application method of choice for disposable hygiene articles.

The raw material availability dynamics, cost, in conjunction with performance improvements has led to significant advancement in the design, shape, assembly and process of disposable hygiene products.[1] As Fornes[1] pointed out, pressure-sensitive adhesives used in the disposable hygiene articles are one of the major means to achieve the cost savings, and process and performance enhancements. Even though styrenic block copolymer (especially SBS and SIS) based pressure-sensitive adhesives are still the work horse pressure-sensitive adhesive formulations for disposable hygiene applications (especially diaper), in recent years polyolefin based pressure-sensitive adhesive technology has been getting a lot of attention due to cost and availability.[9]

Major focus areas for the current disposable hygiene industry include pressure-sensitive adhesive raw material sustainability, lower adhesive application temperatures with improved bond strength.[1] We think the blends containing the olefinic block copolymer (OBC), amorphous ethylene-propylene (PE-PP) copolymers, and an unsaturated or saturated hydrocarbon resin can be formulated into a disposable diaper construction pressure-sensitive adhesive. This may provide better low temperature application properties with improved bond strength compared to the standard SBS based disposable diaper construction adhesive. In this chapter, olefinic polymer blends of OBC/PE-PP containing three different unsaturated hydrocarbon resins with varying aromatic content and two different saturated aliphatic hydrocarbon resins with varying cycloaliphaticity will be evaluated in a typical disposable nonwoven diaper construction adhesive.

Materials and Methods

A commercially available (INFUSE 9507®) 5 melt index (190°C, 2.16 Kg), 0.866 g/cm^3 density ethylene-octene based olefinic block copolymer (OBC) was obtained from Dow Chemical Company. Atactic ethylene-propylene amorphous polyolefin copolymer was obtained from Eastman Chemical Company. Properties of the amorphous polyolefin (atactic ethylene-propylene copolymer) are given in Table 15.

Table 15. Properties of polymers

Name	Penetration Hardness (ASTM D5)	Viscosity (190°C) mPa.S (ASTM D3236)	T_g (°C)
PE-PP (Ethylene-propylene copolymer)	35	5700	-20

Properties of the hydrocarbon resins selected for this study are given in Table 16. Ring & Ball softening point, % Aromatic content and molecular weight evaluations were performed following the same procedure mentioned in Chapter-3. A typical pressure-sensitive adhesive formulation for disposable diaper construction based on styrene-butadiene-styrene contains 20-25 wt% SBS polymer (20-40% styrene content), 55-60 wt% hydrocarbon resin, 20-25 wt% oil.[2]

Table 16. Properties of hydrocarbon resins

Resin	Type	Ring & Ball Softening Point (^{0}C)	% Aromatic content (NMR)	Molecular Weight Mn/Mw/Mz (Daltons)
Resin 1 (R1)	Aliphatic	95	0.5	800/1700/3500
Resin 2 (R2)	Aliphatic/Aromatic	95	5	850/2200/5500
Resin 3 (R3)	Aliphatic/Aromatic	95	14	800/1700/4000
Resin 4 (R4)	Cycloaliphatic	92	<0.5	500/700/1100
Resin 5 (R5)	Linear aliphatic-cycloaliphatic	100	<0.5	450/1000/2300

The higher resin content is required to obtain the necessary adhesive properties such as tack and peel. Typically 20-25wt% oil is added to control the viscosity of the total formulation so that it can be sprayed using air assisted hotmelt spraying techniques. An SBS-based PSA formulation for disposable diaper applications containing 20/60/20 Kraton® D1102 (SBS)/100°C softening point cycloaliphatic-aromatic hydrocarbon resin/naphthenic oil, was evaluated as a control. The control adhesive formulation was blended with a Plasticorder Brabender at 150°C using sigma blades. Polymer was initially masticated for 10 minutes with antioxidant before adding resin

and oil. Solid resins and oils were then added to the masticated polymer and blended for 20-45 minutes until the torque became constant.

Calsol® 5550 naphthenic oil was obtained from R.E Carroll industries, and antioxidant Irganox® 1010 was obtained from BASF. The OBC/PE-PP based disposable diaper construction PSA formulations, as shown in Table 17 were produced using mechanical agitation (Paddle type agitator controlled by a variable speed motor) in pint-sized cans with a heat block set at 177°C. Polymer and antioxidant were introduced into the can and heated up to 177°C under a nitrogen blanket. Resin followed by oil was then introduced into the can after the polymer was melted. This was agitated for 30 minutes until the mixture was completely homogenous. After thorough mixing, the adhesive was poured into a silicone lined cardboard box and allowed to cool. Disposable diaper construction PSA formulations evaluated are given in Table 17.

Viscoelastic properties of the pressure-sensitive adhesives were evaluated using Dynamic Mechanical Analysis (DMA). DMA evaluation was performed following the same procedure as described in Chapter-2.

Viscosity profiles were generated to determine the processability characteristics of the disposable diaper PSA. Viscosity measurements were carried out using a Brookfield viscometer (DV II, spindle #27) over a range of temperatures (130°C, 150°C, 170°C, 190°C and 210°C).

Table 17. Disposable diaper construction PSA formulations with OBC/PE-PP blends in wt%

Sample Name	Formulation Description	OBC	PE-PP	Resin	Calsol® 5550	Irganox® 1010
Disposable diaper construction PSAs with unsaturated hydrocarbon resins						
F1	With Resin R1	12.5	12.5	54 (R1)	20	1
F2	With Resin R2	12.5	12.5	54 (R2)	20	1
F3	With Resin R3	12.5	12.5	54 (R3)	20	1
Disposable diaper construction PSAs with saturated hydrocarbon resins						
F4	With Resin R4	12.5	12.5	54 (R4)	20	1
F5	With Resin R5	12.5	12.5	54 (R5)	20	1

Nonwoven adhesives formulations shown in Table 17 were evaluated for adhesive peel strength after the adhesive has been applied between a nonwoven fabric and PE backing (using Acumeter Spray Coater). Spiral spray adhesive patterns were created using an Acumeter Spray Coater, air assisted spraying equipment, which is shown in Figure 33.

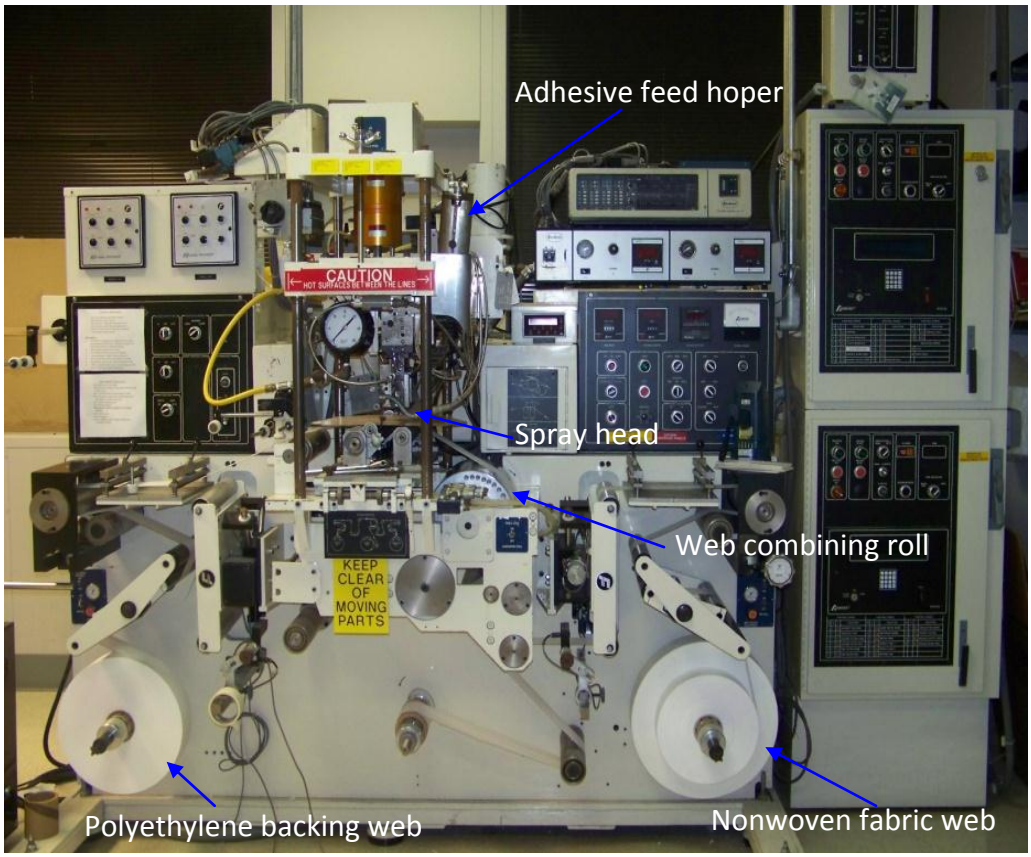

Figure 33. Acumeter Spray Coater hotmelt pressure-sensitive adhesive spraying equipment

The hot melt adhesive is melted in the 500mL feed hopper at a controlled temperature. The adhesive is then pumped with a gear pump through a nozzle, which is designed to use direct spray air to create a high-frequency pattern of hot melt adhesive. The spray air draws the adhesive into a fine fiber. This directed air causes the monofilament to spiral and cool as it is dispensed, delivering a highly consistent helical pattern as shown in Figure 34.

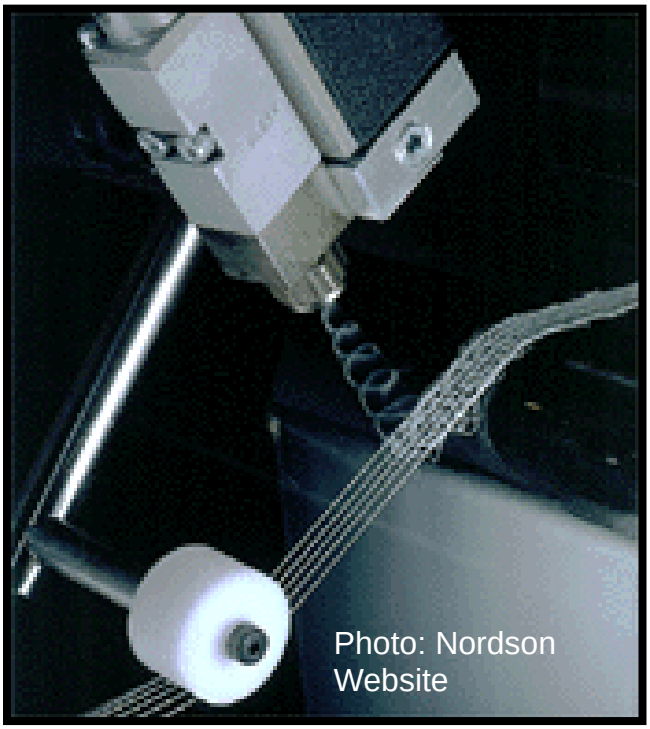

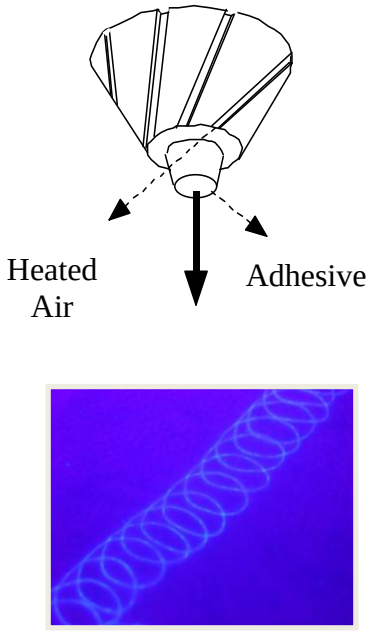

(a) (b)

Figure 34. (a) Disposable diaper adhesive spraying for an elastic attachment adhesive (for illustration), (b) a typical air assisted spraying head configuration in Acumeter Spray Coater spraying equipment and the resulting spiral spray patterns of pressure-sensitive adhesive (under UV light)

The run speed (X) for the Acumeter Spray Coater was set at 350 ft/min (1.78 m/sec) to obtain a targeted coat weight (C) of 6 gsm (grams per square meter) and also to keep the open time of the adhesives constant. The nozzle temperature was controlled between 149°C-163°C and the spray head temperature was controlled between 163°C-177°C. The width of the spiral patterns (W) was controlled to 0.5 inch (12.7 mm), and the number of spiral loops within an inch was controlled to 5-8 loops/inch (5-8 loops in 12.7 mm) as shown in Figure 35.

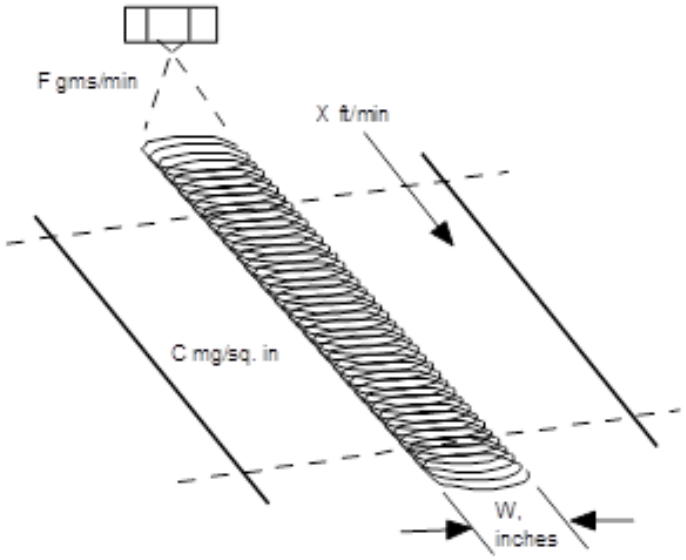

Figure 35. Disposable diaper construction adhesive spiral pattern measurements

After the adhesive was applied between the nonwoven fabric and PE back sheet, the peel adhesion testing on the samples was performed using a tensile tester.

Results and Discussion

The viscoelastic properties of disposable diaper construction PSAs based on OBCs and a comparative SBS-based control is given in Figure 36. As can be seen (Figure 36), the viscoelastic response for OBC/PE-PP based PSA is different than that of the typical SBS based control formulation. The PSA formulation (F1) containing unsaturated aliphatic resin (R1) and PSA formulation (F2) containing unsaturated slightly aromatic (5%) resin (R2) PSAs show a single broad T_g. However, the PSA formulation (F3) containing highly aromatic (14%) unsaturated resin (R3) PSA shows two T_g's, which is a clear indication of immiscibility. The first transition is around -20°C and a second broad transition around 42°C, which corresponds to the highly aromatic unsaturated resin (R3)

T_g. Both olefin based PSA formulations (F1 and F2) showed predominantly flow properties and less elastic characteristics which can be observed from storage modulus (G'). The storage modulus plateau (from room temperature to 55°C) representing the elastic characteristics of SBS based control over a wide application temperature range is very clear (Figure 36).

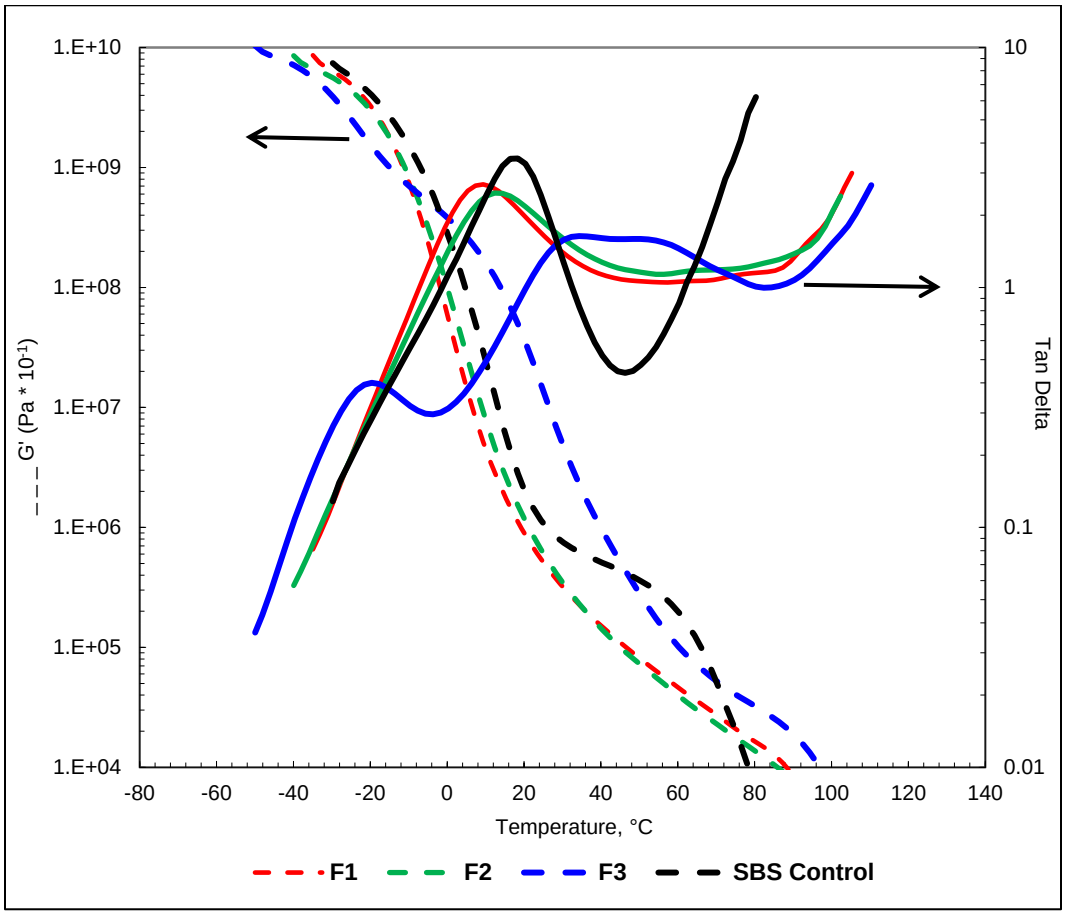

Figure 36. Disposable diaper construction PSAs formulations based on OBC and a comparative SBS based control

The shape of the Storage modulus plateau typically represents the strength of the adhesive over a measured temperature range. After the plateau, the adhesive will

start to flow. Figure 37 shows the viscoelastic properties of disposable diaper construction PSAs with saturated hydrocarbon resins and comparative SBS based control.

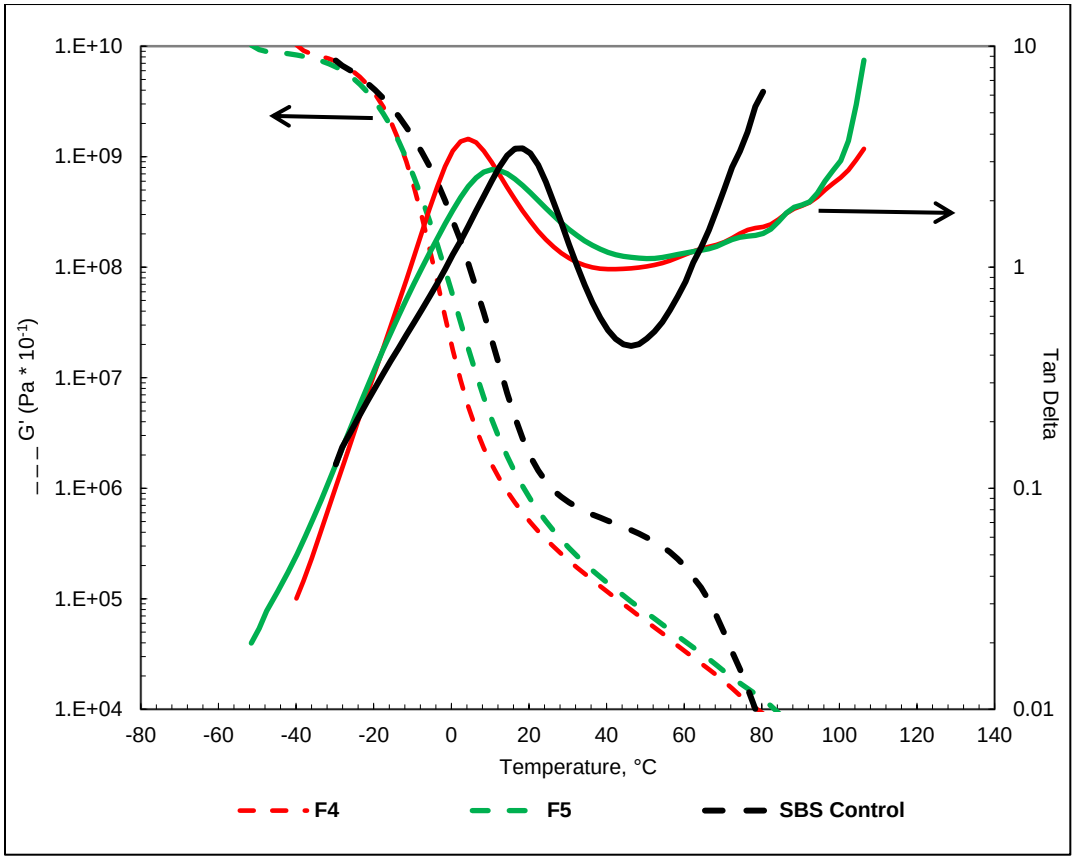

Figure 37. Disposable diaper construction PSAs with saturated hydrocarbon resins and comparative SBS based control

The PSA formulation (F4) containing cycloaliphatic resin (R4) shows a lower T_g, narrower tan δ and slightly lower modulus. The slightly lower T_g can be correlated to the 10°C lower softening point of the cycloaliphatic resin compared to both linear aliphatic-cycloaliphatic resin used in formulation F5, and the comparative SBS control. However, the elastic modulus plateau representing the strength of the adhesive bond

was still not as clear for the OBC/PE-PP with saturated aliphatic resin based PSA formulations, compared to the SBS based control. Figure 38 shows the viscosity profiles at five different temperatures for the disposable diaper PSA formulations.

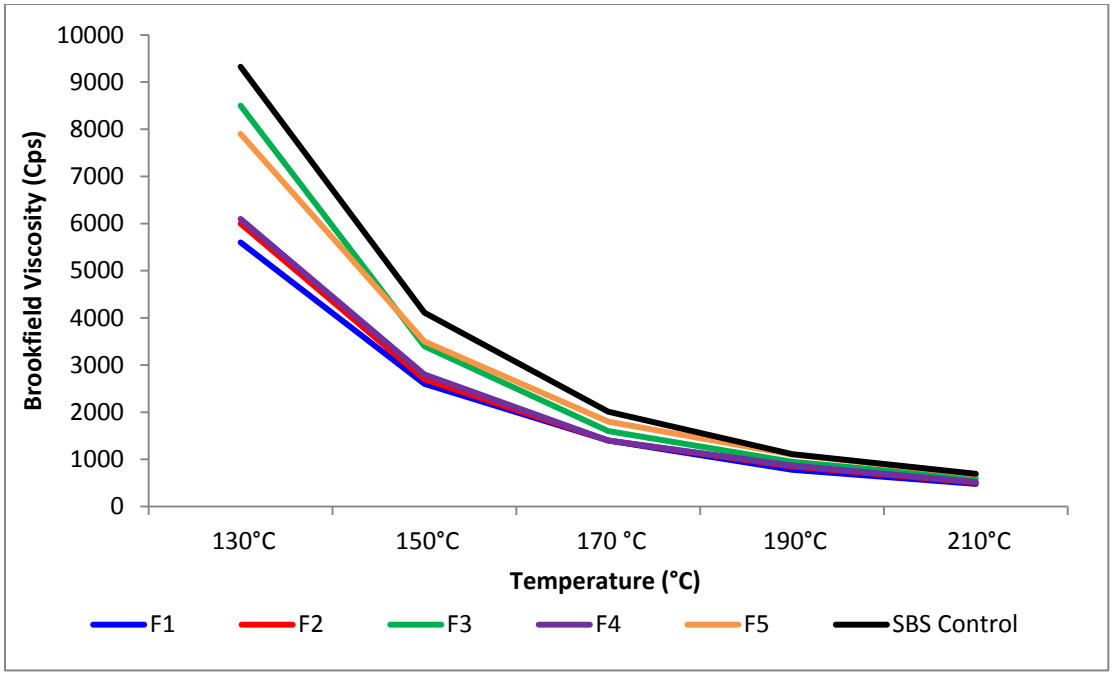

Figure 38. Viscosity profiles of disposable PSAs with hydrocarbon resins at five different temperatures

As can be seen (Figure 38), all OBC/PE-PP blends based disposable diaper formulation containing hydrocarbon resins show lower viscosity profiles at all five temperatures evaluated compared to the SBS based control adhesive. This is a clear indication that these adhesive formulations can be applied at lower application temperatures. The PSA formulation containing unsaturated aliphatic resin (R1), slightly aromatic unsaturated resin (R2) and cycloaliphatic saturated resin (R4) shows the lowest viscosity profiles, which are almost half the viscosity compared to the SBS based control,

and they are virtually the same from 150°C to 210°C. Better miscibility of the different adhesive formulations component can also be correlated well to the lower viscosity of the same blends. The immiscibility behavior of PSA formulation containing highly aromatic unsaturated resin (R3) may be correlated to the higher viscosity profiles, which are closer to the linear aliphatic-cyclo aliphatic saturated resin (R5) and also to the SBS based control. Since it has seen immiscibility behavior with PSA formulation (F3) containing highly aromatic (14%) unsaturated resin, we did not proceed with this formulation any further. We eliminated this particular formulation (F3) from spraying (using Acumeter Spray Coater). PSA formulations including, F1, F2, F4, F5 and the SBS control formulations were applied between a nonwoven fabric and PE backing using Acumeter Spray Coater to make a diaper construction like article, employing the same spraying conditions. It was able to get very good spiral spray patterns with all four OBC/PE-PP based adhesive formulations. After the adhesives were applied between the nonwoven fabric and PE back sheet, the peel adhesion testing on the samples was performed.

The peel adhesion results are shown in Figure 39. It can be seen in Figure 39 that a PSA formulation containing saturated cycloaliphatic resins (F4) gave the best adhesive peel strength followed by a formulation containing a saturated, linear aliphatic-cycloaliphatic resin (F5). Both of these formulations show similar adhesive performance compared to the SBS-based control formulation. Even though the PSA formulation containing unsaturated aliphatic resins (F1) showed higher peel strength, the standard deviation was very high, making this an inconsistent adhesive. The main reason for a

very high standard deviation can be due to the insufficient penetration of this particular adhesive when sprayed on to polyethylene backing, resulting in variation of bond strength between the PE and nonwoven fabric at different areas of the diaper construction article.

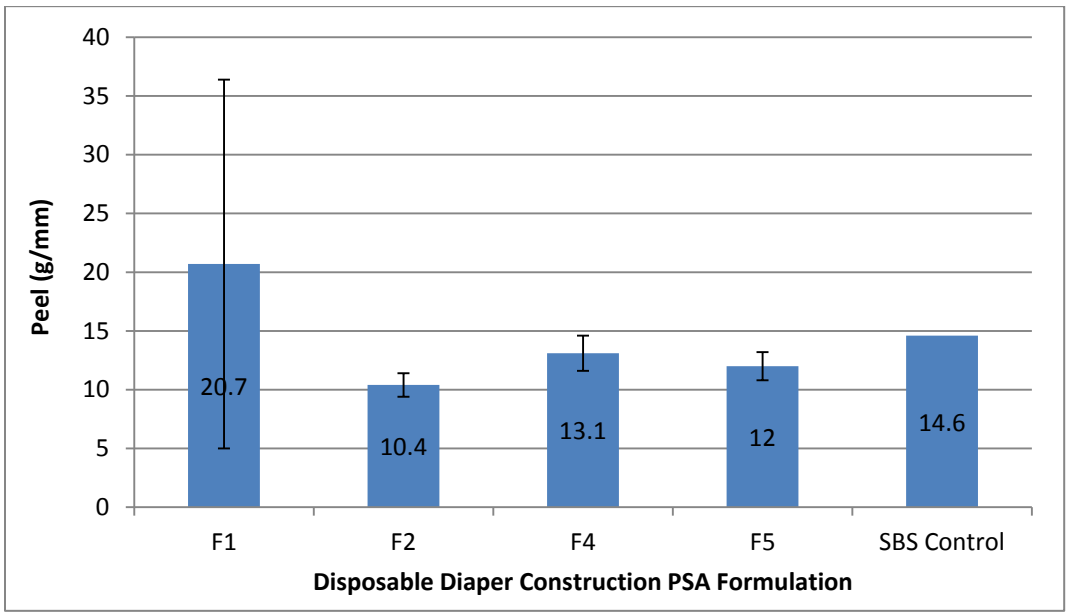

Figure 39. Adhesive peel of disposable diaper construction PSAs with hydrocarbon resins

The PSA formulation containing slightly aromatic unsaturated resin (F2) showed the lowest peel strength of all the formulations. The main advantages of the OBC/PE-PP based disposable diaper construction adhesive, compared to standard SBS based comparative formulation is that, the OBC/PE-PP based PSA formulations can be applied at lower applications temperature (from viscosity profiles), and these formulations also show a big formulation latitude with very good tolerance for different hydrocarbon resin

chemistries (especially saturated aliphatic and slightly aromatic-aliphatic unsaturated resins), with most of them giving good adhesive performance properties.

Summary and Path Forward

- Based on the learning from blend miscibility studies, it has successfully made disposable diaper construction pressure-sensitive adhesives with OBC/PE-PP blends, containing unsaturated hydrocarbon resins and saturated hydrocarbon resins.
- Viscoelastic performance of the OBC/PE-PP based adhesive formulations revealed that these formulations show predominantly flow characteristics than elastic performance as measured via Storage Modulus. The adhesive formulation (F3) containing highly aromatic (14%) unsaturated hydrocarbon resin showed some immiscibility.
- Disposable diaper construction adhesives based on OBC/PE-PP blends can be potentially applied at lower temperatures than that of the comparative SBS control formulation, since all the OBC/PE-PP based adhesives show lower viscosity profiles at a wide temperature range, irrespective of the resin chemistry.
- OBC/PE-PP blends based disposable diaper construction adhesives showed good sprayability characteristics, when applied using an air assisted spiral spray equipment, Acumeter Spray Coater.

- Peel adhesion evaluations of the disposable diaper construction article showed good adhesive peel properties, especially for the adhesive formulations containing saturated aliphatic hydrocarbon resin, which were comparable to the SBS based control.
- It can be concluded that OBC/PE-PP based PSA formulations can be applied at lower applications temperature (from viscosity profiles), and these formulations show a big formulation latitude with very good tolerance for different hydrocarbon resin chemistries (especially saturated aliphatic and slightly aromatic-aliphatic unsaturated resins), with most of them giving good adhesive performance properties, when compared to the evaluated comparative SBS based control.

References

1. M. Fornes, *Nonwovens Industry* (May 2009)
2. F. C. Jagisch and J. M. Tancrede, in: *Hand Book of Pressure-sensitive Adhesive Technology 3rd Ed.,* D. Satas (Ed.), pp. 346-398. Satas & Associates, Warwick-RI (1999)
3. J. T. Harlan Jr., US Patent No. 3,239,478 (1966)
4. D. A. Godfrey, US Patent No. 4,299,745 (1981)
5. P. P. Puletti, US Patent No. 4,419,494 (1983)
6. R. C. Schmidt Jr., S. K. Decowski Jr. and P. P. Puletti, US Patent No. 4,460,728 (1984)

7. R. C. Schmidt Jr. and P. P. Puletti, US Patent No. 4,526,577 (1985)

8. J. Raterman, *TAPPI Hotmelt symposium*, PP. 63-66 (1987)

9. C. Li Pi Shan et al., *30th International PSTC Technical Seminar Orlando-FL* (May 2007)

CHAPTER - 6. RHEOLOGICAL AND MORPHOLOGICAL EVALUATION OF NATURAL RUBBER LATEX-BASED PRESSURE-SENSITIVE ADHESIVES CONTAINING WATER-BASED ALIPHATIC HYDORCARBON TACKIFIER DISPERSION

Abstract

The effect of three water borne aliphatic hydrocarbon tackifier dispersions each with different softening points (70°C, 85°C and 95°C) were evaluated with natural rubber latex at two addition levels (25% and 50%) for pressure-sensitive adhesive (PSA) applications. No other additives were incorporated into the PSA formulations so that rheological effects of waterborne aliphatic hydrocarbon tackifier resin dispersions in Natural rubber-based PSAs could be clearly understood. Application of these water borne PSAs was evaluated, in terms of rheology, since flow parameters have very important influence in the convertibility (coating ability) of such adhesives. Morphological correlations with wet rheology for these water borne PSA formulations and starting materials revealed that the interaction between the latex particle and tackifier dispersion particle has a major influence in determining the viscosity characteristics at low to medium shear rate, where stirring, pumping and filtration processes occur. A shear thinning effect was also predominant in formulations with lower tackifier dispersion levels. The extent of shear thinning can be correlated well to morphology. Interestingly, all the PSA formulations tend to follow Newtonian behavior above a shear rate of 1000 s^{-1} and no shear thinning or shear thickening at higher shear rates was observed. The minimal change in viscosity at higher shear rates is a key parameter for high-speed coating techniques such as curtain coating and reverse

gravure, since any change in viscosity can affect coating uniformity and the wetting of the substrate surface during coating.

Introduction

Natural rubber-based pressure-sensitive type adhesives have been used for medical applications since 1845, when Day and his colleague improved adhesive plaster using India rubber, turpentine and pine gum.[1] Additional developments that followed concentrated on medical applications. In the 1880s, Robert Johnson, founder of Johnson & Johnson Company started the commercial manufacturing of natural rubber-based pressure-sensitive medical tapes.[2] 3M pioneered the industrial applications of natural rubber-based pressure-sensitive adhesives in the 1920s starting with masking tapes for automobile painting.[3, 4] In the early 1900s, most of the medical pressure-sensitive tapes based on natural rubber were calendered onto the substrate (thick films), while industrial pressure-sensitive adhesives from 3M were solvent coated onto the backing as thin films.[2, 4] Until the 1940s, solvent-borne Natural rubber-based pressure-sensitive adhesive technology dominated the market. Most of the early Natural rubber-based pressure-sensitive adhesives formulations contained natural rubber as the polymer, petroleum derived and/or rosin-based resin as a plasticizer or tackifier, and a solvent. In 1940 Eustis *et al.* of Kendall Company reported the use of natural rubber latex-based pressure-sensitive adhesive technology with very low volatile solvents compared to solvent-based pressure-sensitive adhesives.[5] Eustis used natural rubber latex as the polymer, rosin and/or hydrogenated rosin-based resin dispersion as a plasticizer and casein/gum arabic/karaya gum as the protective colloid to improve

adhesion of adhesive to the backing.[5] It is interesting to note that the natural rubber latex-based pressure-sensitive adhesive formulators still depend on some of the above mentioned key ingredients. According to an 2008 EPA report, 22% of the pressure-sensitive adhesive market is still based on natural rubber[2] and 3% of the total adhesives manufacturing segment remains based on Natural rubber.[6]

During World War II, the shortage of natural rubber created a need for synthetic polymers and emulsions. Styrene butadiene rubber, butyl rubber and acrylic rubber emulsions were the prominent technologies in the 1950s and 1960s as synthetic polymers for pressure-sensitive adhesives. Pressure-sensitive adhesive technologies using solvent-based, polyacrylate, synthetic polymers became more popular than the Natural rubber-based technologies especially in the medical market[2, 7, 8] because they caused less skin irritation and improved tack without additives. By the late 1970s, use of emulsion-based pressure-sensitive adhesive technologies surpassed solvent technologies due to more stringent health and environmental restrictions.[7, 8, 9] Natural rubber emulsion-based technologies dominated other emulsion technologies until the late 1970s.[9] Availability and economics combined with technical benefits of water-based acrylic PSAs popularized them in the early 1980s and this is still the dominant technology used in water-based PSAs today.[8]

Solvent and water-based pressure-sensitive adhesives are formulated with three major components, polymer, tackifying resins and other additives (plasticizers, stabilizers etc.). The polymer imparts strength and cohesive characteristics to the

pressure-sensitive adhesive. Tackifier resins are low molecular weight, high T_g amorphous materials of petroleum origin or naturally derived (pine chemicals). A good tackifier resin should have low molecular weight, sufficient compatibility with polymer type, and have a glass transition temperature (T_g) higher than the base polymer to effectively impart sufficient pressure-sensitive adhesive characteristics.[2, 10] In case of water-based, natural rubber PSAs, the tackifier resin is either dissolved in solvent and/or dispersed in water with the aid of surfactant. Since the late 1970s, the use of rosin-based tackifier resins dispersed into water without the use of solvent has been reported.[2, 9] Early tackifier dispersions were based on rosin resins dispersed in water with the aid of surfactants. The best known practice of dispersing the tackifier resin into water is the phase-inversion process, in which resin is first melted and then plasticized with surfactants/dispersing agents, and then the inversion process follows with addition of water under high shear mixing. The surfactant/emulsifier type and amount and the addition method before inversion can have significant effects in determining the quality and performance characteristics of a dispersion.[2, 11] Particle size and size distribution of the tackifier resin dispersion also affects the formulation coating performance and the final adhesive performance.[11-14]

In 1979, Oldack and Bloss [9] reported the compounding of natural rubber latex in water-based PSAs utilizing water-based resin dispersions. They evaluated the effect of water-based tackifier dispersions of polyterpene resin, hydrogenated rosin resin, and a hydrocarbon resin dispersion in natural rubber latex-based formulations on adhesive tack and shear.[9] Until the mid1980s, coating speeds of 300 m/min were achieved, but

recent developments in coating techniques allow running speeds up to 600 m/min.[8] One of the major challenges for water-based pressure-sensitive adhesives is the high-speed - high shear coating techniques that are currently employed. Since water-based tackifier dispersions are one of the major ingredients (25-50wt% of total formulation) in natural rubber-based water borne PSAs, the type, the amount and the interaction of the tackifier dispersion with latex is very critical in determining the coating ability, adhesive performance and economic viability.[11, 12] Gazeley reported the importance of choosing the right tackifier resin dispersion with respect to resin chemistry, resin dispersion concentration and the effect of surfactant in the total formulation. These factors were used to control the colloidal stability of the formulation, which in turn determined the coating characteristics.[11] De Hullu[12] also successfully demonstrated the importance of the amount and type of tackifier resin dispersion and the need for surfactant balance in the total PSA formulation for different coating techniques including Mayer rod and reverse gravure techniques.

The coating performance of water-based pressure-sensitive adhesives can be characterized through high shear rheology, which can be correlated to the resistance to flow at high shear rates imposed by most adhesive coating processes.[13, 14, 16] Control of formulation rheology is essential for good runnability and defect-free coating quality. Stirring, pumping and filtration operations create low to intermediate shear rates for typical water-based PSA formulations (Figure 40), but higher shear rates are created at the coating head. Gravure coaters apply a higher shear compared to Mayer rod or

Curtain coater techniques, but leveling, de-wetting and drying operations occur at shear rates less than 1 s^{-1}.

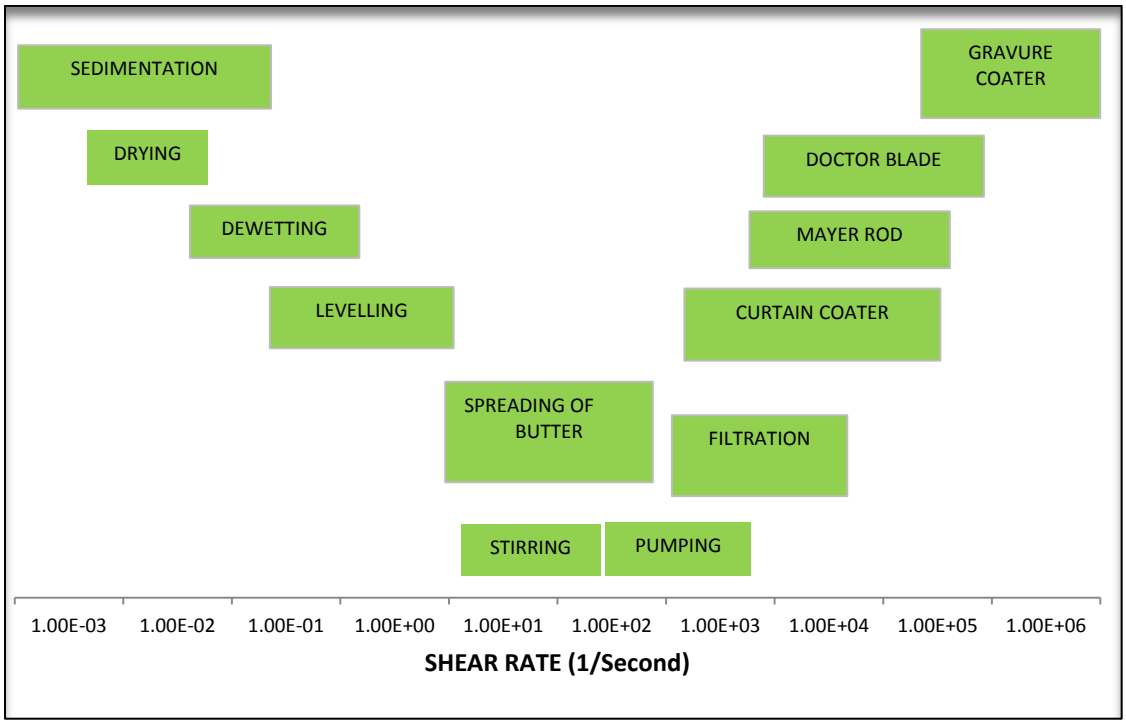

Figure 40. Viscosity and shear rate correlation with respect to different coating applications[13]

Rheology depends on the interaction between the latex and tackifier dispersion particles, the particle size and size distribution, and solids loading.[14, 15] The major challenge is to make an adhesive that will tolerate the high-speed - high shear coating technique combined with good final adhesive properties. In this study, the rheological and morphological characteristics of three different C5 aliphatic hydrocarbon tackifier resin dispersions in natural rubber latex-based water borne PSA formulations were evaluated.

Materials and Methods

Eastman Chemical Company produces C5 aliphatic hydrocarbon-based tackifier resin dispersions which have good compatibility with natural rubber latex even at 50 wt%. This is mainly due to the similarities in chemistries between the resin dispersion and polyisoperene-based natural rubber latex. Even though the selected tackifier dispersions are all of C5 aliphatic hydrocarbon based chemistry, the type and concentration of surfactant/dispersing agents for each of these three dispersions were different. Three dispersions were investigated here, that gave a 70°C, an 85°C and a 95°C ring and ball softening point, all obtained by incorporating C5 aliphatic hydrocarbon chemistry. The ring and ball softening point mentioned is not of the starting C5 aliphatic hydrocarbon resin, but of the dispersed resin, which includes resin and surfactant/dispersing agents. It should be noted that this study is mainly focused on the correlation of the rheological and morphological properties of the formulated PSA.

ASTM category 3 HARTEX 101 low ammonia natural rubber latex, 62% solids at pH 10 was obtained from Firestone Natural Rubber Company LLC. Resin dispersions were obtained from Eastman Chemical Company. Table 18 shows the basic properties of the C5 aliphatic hydrocarbon resin dispersions prepared from a low molecular weight, aliphatic, C5 hydrocarbon resin. 70°C softening point dispersion is dispersed with a long chain alkyl (C_{13}) anionic surfactant/dispersing agent (3 wt%), 85°C softening point dispersion is dispersed with a combination of long chain alkyl (C_{13}) and cycloaliphatic

surfactants/dispersing agents (5 wt%) and 95°C softening point dispersion is dispersed with a cycloaliphatic surfactant/dispersing agent (4 wt%).

Table 18. Properties of C5 aliphatic hydrocarbon dispersions

Designation	pH	% Solids
70°C softening point dispersion	4	50
85°C softening point dispersion	10	55
95°C softening point dispersion	10	55

Water-based pressure-sensitive adhesive formulations were formulated with HARTEX 101 natural rubber latex using resin dispersions at 25 wt% and 50 wt% addition levels based on a dry weight/solids basis. Blending of natural rubber (NR) latex and C5 aliphatic resin dispersions were carried out by mixing natural rubber latex and the C5 resin dispersion (at two different addition levels) at room temperature using a mechanical stirrer for 5 minutes at 100rpm. Formulations were then homogenized using a paint mixing roller for 30 minutes. The formulations evaluated are shown in Table 19.

Wet-rheological evaluations were performed using an AR 2000® constant stress rheometer (TA Instruments Inc. New Castle, DE) at 25°C with 40 mm parallel plates. A 0.5 mm gap set was used to obtain the shear rate range of 1 to 10000 s^{-1}.

Particle size analysis was performed using a Malvern Particle Analyzer-MS2000® Hydro instrument.

Table 19. PSA formulations

Formulation Description	75/25 (NR/70°C Dispersion)	75/25 (NR/85°C Dispersion)	75/25 (NR/95°C Dispersion)	50/50 (NR/70°C Dispersion)	50/50 (NR/85°C Dispersion)	50/50 (NR/95°C Dispersion)
HARTEX 101 – NR Latex	75	75	75	50	50	50
70°C softening point dispersion	25	-	–	50	-	–
85°C softening point dispersion	–	25	–	–	50	–
95°C softening point dispersion	–	–	25	–	–	50

Transmission electron micrographs were taken using a JEOL JSM 100CXII Microscopy. Using an applicator stick, a small amount of the viscous latex was

transferred to 20 drops of DI water. The resulting mixture was applied to a 400 mesh carbon-coated Formvar grid and the excess removed by wicking off with a filter paper. The grid was then stained with 1% phosphotungstic acid (pH adjusted to 7-8) for 90 seconds. Excess stain was then removed with a filter paper and the grid was allowed to dry. Transmission electron micrographs were then taken at an accelerating voltage of 80kV.

Results and Discussion

Pressure-sensitive adhesive formulations were divided into three parts based on the resin dispersion used (70°C dispersion, 85°C dispersion and 95°C dispersion). Wet rheology and morphology of the starting materials which include the HARTEX 101 natural rubber latex, the 70°C softening point dispersion, the 85°C softening point dispersion and the 95°C softening point dispersion will be discussed first. This will be followed by a description of the wet rheology and morphology of the pressure-sensitive adhesive formulations.

The wet rheological behavior of tackifier dispersions and Hartex 101 natural rubber latex (NR Latex) is given in Figure 41. The 85°C and 95°C dispersions show high initial viscosities at low to medium shear rates, while the 70°C dispersion and HARTEX 101 shows low initial viscosity. There are several factors that can influence the viscosity and rheological characteristics of dispersions. In general, pH, solids content, dispersing agents, particle form, particle size and size distribution are the major contributing factors.[16]

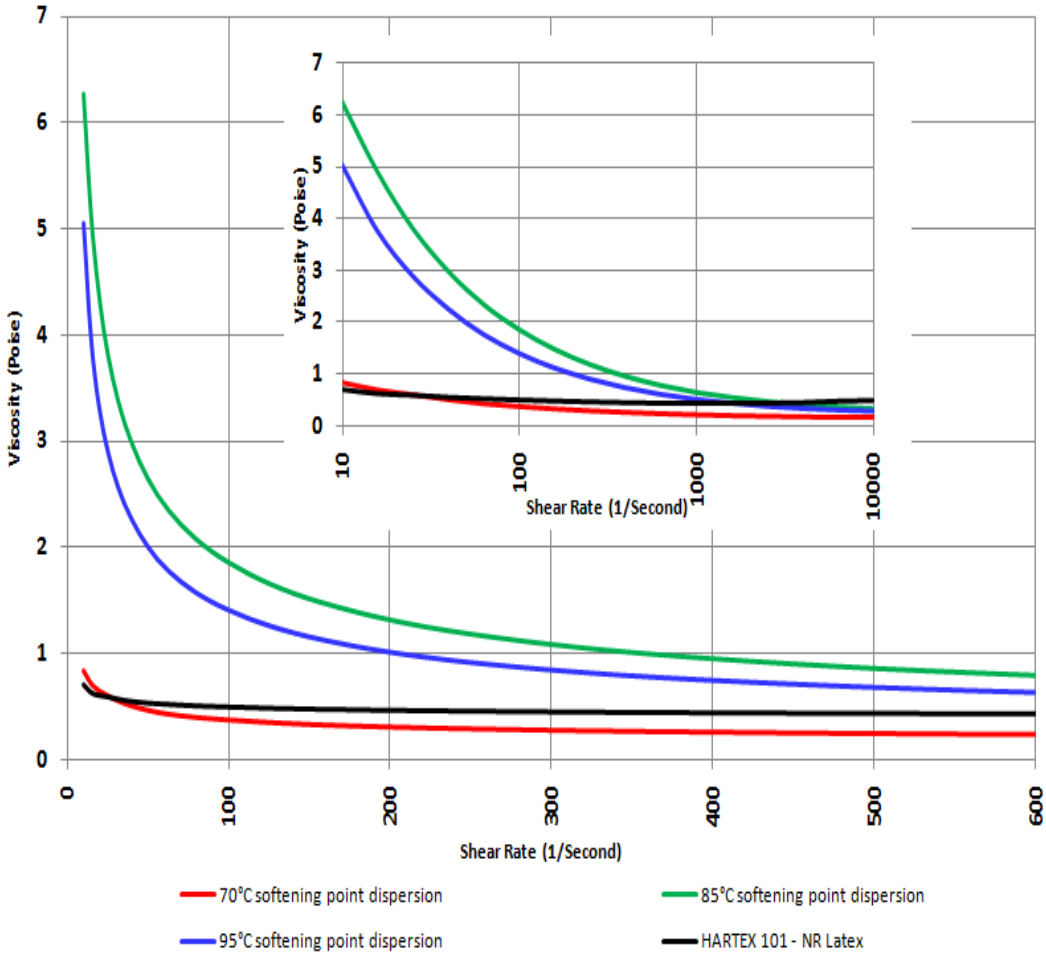

Figure 41. Rheological profiles of tackifier dispersions and HARTEX 101 - NR Latex

As can be observed from Table 18, both the 85°C and 95°C softening point dispersions have higher solids content (55%) and higher pH (10), while the 70°C softening point dispersion only has 50% solids and pH of 4. Even though the dependence of viscosity on pH is normally complex for dispersions, viscosity increases with increasing pH. Also, viscosity of dispersions tends to increase with higher solids content. This can be modeled by the Krieger-Dougherty equation.[20]

$$\frac{\eta}{\eta_0} = \left(1 - \frac{\Phi}{\Phi m}\right)^{-(\eta')\Phi m}$$

η and η_0 are the viscosities of the suspension and the medium respectively, Φ and Φ_m are the solid volume fraction in the suspension and maximum packing fraction respectively; (η') is the intrinsic viscosity. It can be inferred that particle shape, particle size and size distribution also influence the packing, and thus the viscosity. However, all four starting materials show Newtonian viscosity behavior above 1000s^{-1}.

Figure 42 shows the particle size distribution for three tackifier dispersions and Hartex 101 natural rubber latex. The mean particle size of 70°C softening point dispersion is larger (0.275 µm) and the mean particle size distribution is broader compared to the 85°C and 95°C softening point dispersions (0.180 µm).

HARTEX 101 – NR Latex has a large mean average particle size (0.875 µm) and a bimodal particle size distribution. Suspensions with bimodal and broad particle size distributions tend to have lower viscosity compared to suspensions with smaller average particle size and narrower particle size distribution. Small particles may fill the space between the larger particles resulting in lower viscosity due to lubricating inter-particle movements (packing more efficiently). This correlates well with the rheological observation.

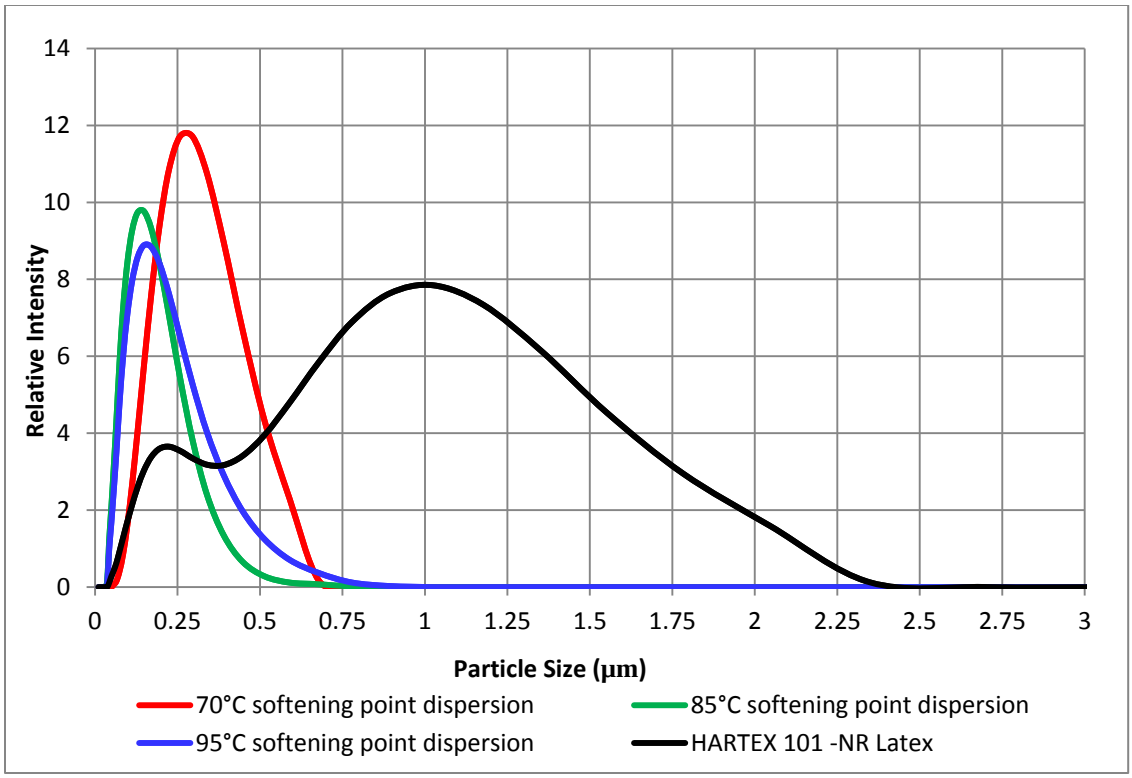

Figure 42. Particle size and size distribution of tackifier dispersions and HARTEX 101 – NR Latex

TEM micrographs in Figure 43 confirm that the particle size of the starting tackifier dispersions and Hartex 101 latex (Figure 42) are in the same range and this correlates well with the particle size analysis and the rheological evaluation. It is interesting to note that the 70°C and 95°C softening point dispersions seem to show similar morphology, while the 85°C softening point dispersion shows a completely different morphology with uniform, well aligned particles. This difference in particle morphology is due to the difference in type and concentration of surfactants/dispersing agents used in each of these dispersions.

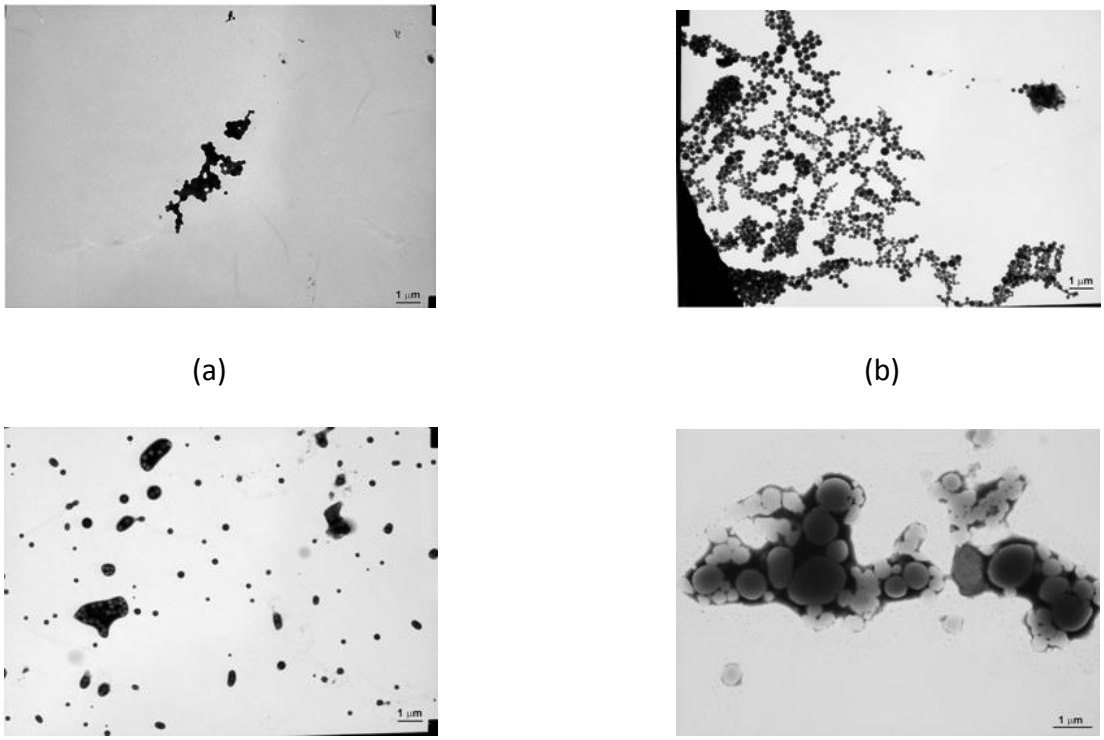

(a) (b)

(c) (d)

Figure 43. TEM micrographs of tackifier dispersions and HARTEX 101 – NR Latex. (a) 70°C softening point dispersion, (b) 85°C softening point dispersion, (c) 95°C softening point dispersion and (d) HARTEX 101 – NR Latex

Even though the 85°C and 95°C softening point dispersions have similar solids content and pH, the higher viscosity of the 85°C softening point dispersion is mainly due to the difference in particle interaction.

I. PSA formulations containing NR & 70°C softening point dispersion

Two different pressure-sensitive adhesive formulations containing the 70°C softening point dispersion were evaluated. Both 25% and 50% addition levels of 70°C

softening point dispersion in NR latex were studied. Figure 44 shows the effect of shear rate on viscosity.

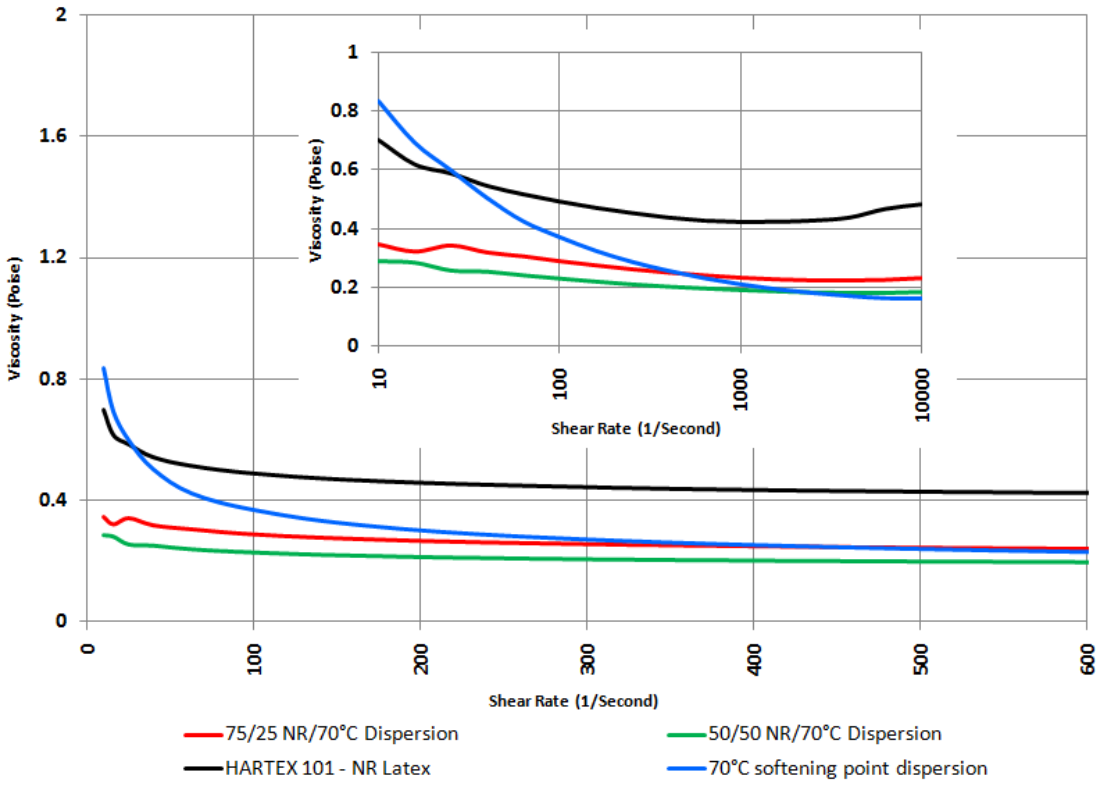

Figure 44. Rheological profiles of PSA formulations containing NR & 70°C softening point dispersion

The 75/25 NR/70°C softening point dispersion-based PSA formulation shows a slightly higher viscosity compared to the 50/50 NR/70°C softening point dispersion. Even though base polymer viscosity influences the overall viscosity of the system, the addition of tackifier resin dispersion reduces the viscosity. It is known that finer particles dispersed in a bimodal suspension behave like a lubricant/fluid (they pack together better) toward coarser particles and reduce the viscosity. This effect is very

dependent on the size ratio or concentration of the finer particle form, size and size distribution.[13, 14, 18] As can be seen from Figure 45, the particle size of the resin dispersion is smaller and has a narrower particle size distribution. This helps to reduce the viscosity of the blend.

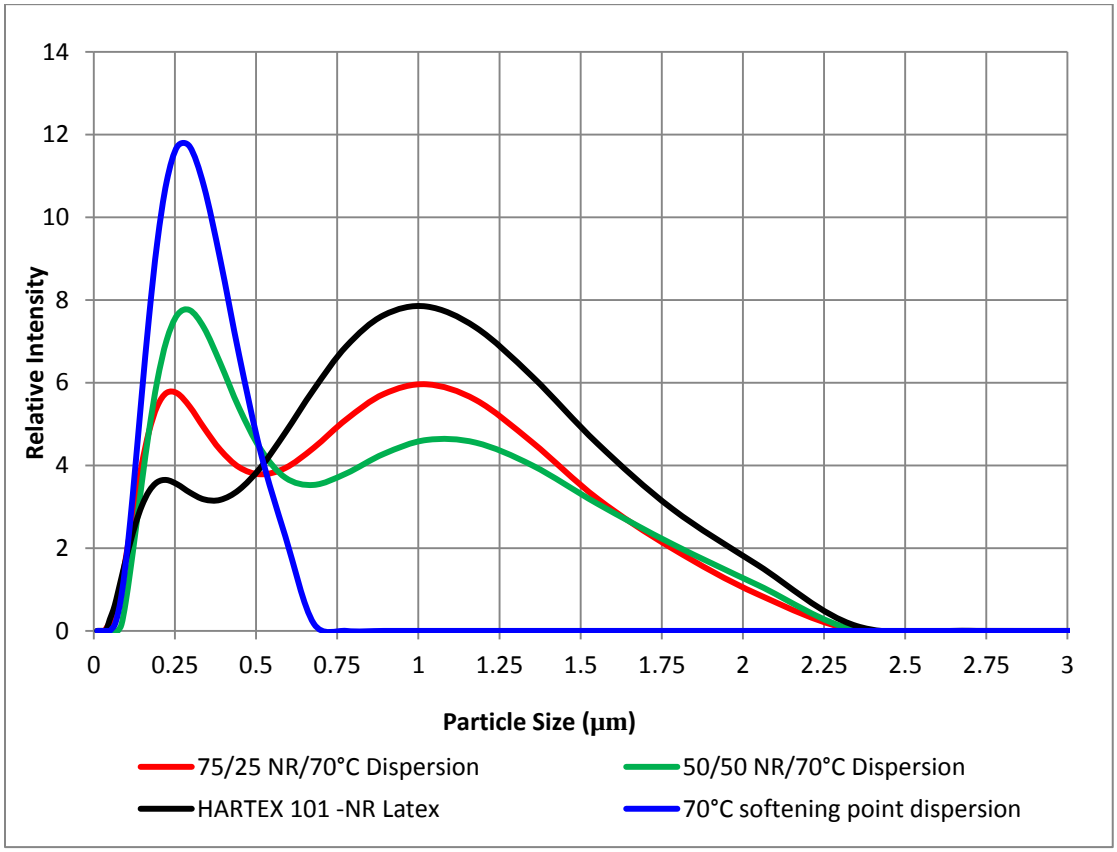

Figure 45. Particle size and size distribution of PSA formulations containing NR & 70°C softening point dispersion

It is clear that for the 50/50 NR/70°C softening point dispersion-based PSA formulation, the first (0.150 µm) and second peak (1 µm) correspond to the dispersion and natural rubber, respectively. In the 75/25 NR/70°C softening point dispersion-based PSA formulation, the second peak (1 µm) corresponds to natural rubber latex, while the

first peak (0.125 µm) is the slightly shifted smaller particle peak of natural rubber latex (0.115 µm), and is lower than the dispersion particle size (0.257 µm). This also explains the slightly higher viscosity of 75/25 NR/70°C softening point dispersion-based PSA formulation, in which the blend has a viscosity closer to natural rubber latex by itself. The bimodal particle distribution is also very clear in the TEM micrographs shown below in Figure 46. As can be seen, natural rubber latex particles are separated from the tackifier dispersion particles and there is no obvious interaction between the two.

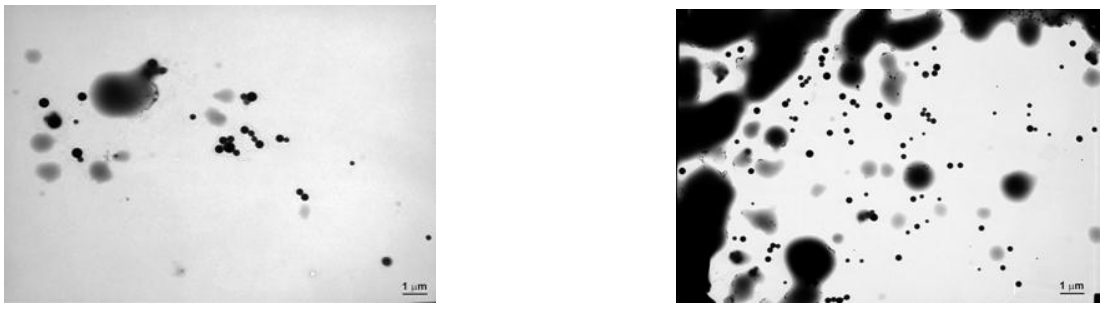

(a) (b)

Figure 46. TEM micrographs of PSA formulations containing NR & 70°C softening point dispersion. (a) 75/25 NR/70°C softening point dispersion-based PSA formulation, (b) 50/50 NR/70°C softening point dispersion-based PSA formulation

TEM also confirms that smaller tackifier resin particles can fit between the larger particles of natural rubber latex, and act as a lubricant for the same overall solids content, the distance between the particles, on average is increased, so the lubrication is improved to lower the total blend viscosity for 50/50 NR/70°C softening point dispersion-based PSA formulation.

This can, in turn, be translated into very good stability of both PSA formulations over a long shear rate range for any coating processes, since both formulations show almost Newtonian behavior above a shear rate of 500 s^{-1}, with no noticeable change in viscosity.

II. PSA formulations containing NR & 85°C softening point dispersion

The viscosity of the 85°C softening point dispersion is higher than that of the 70°C softening point dispersion mainly due to higher pH and higher solids content. Higher solids result in greater inter-particle interactions because the particles are closer together.[17, 19] Interestingly, the 75/25 NR/85°C dispersion-based-PSA formulation shows a higher initial viscosity, close to 85°C dispersion viscosity (Figure 47), compared to the lower initial viscosity of 50/50 NR/85°C dispersion-based PSA formulation, which is close to the viscosity of NR latex. This can be explained through the volume fraction dependence of viscosity. As Schaller explains[17], in a formulation with a bimodal distribution, if the interactions between the particles are higher at concentrations (0.25 volume fraction), the relative viscosity increase is very rapid, since volume fraction approaches a value in which particles are jammed together and are incapable of motion.[17] As the shear rate increases, the shear thinning effect of 75/25 NR/85°C dispersion-based PSA formulation is evident until 1000 s^{-1} and then it shows nearly Newtonian behavior.

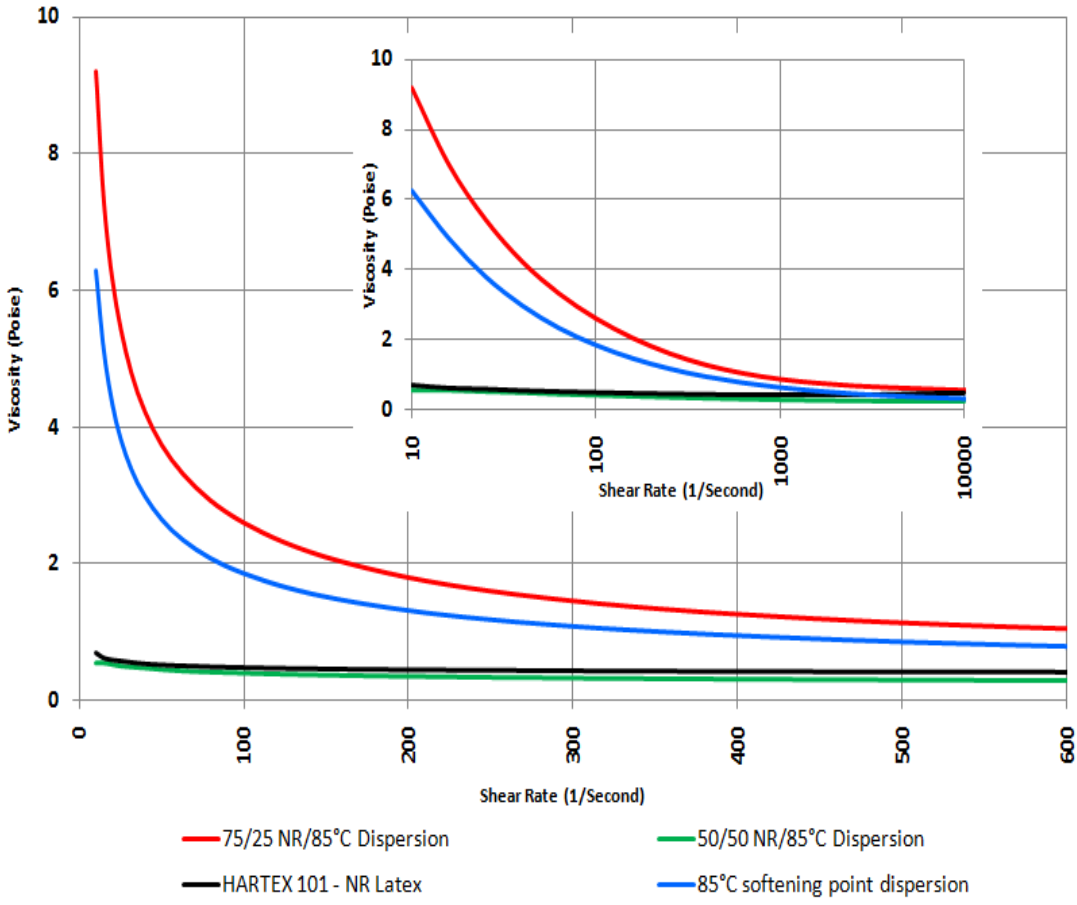

Figure 47. Rheological profiles of PSA formulations containing NR and 85°C softening point dispersion

The particle size distribution in Figure 48 shows the unexpectedly larger particle size distribution of the 75/25 NR/85°C dispersion-based PSA formulation as compared to the 50/50 NR/85°C dispersion-based PSA formulation. This can also be correlated well to the higher inter-particle interaction mentioned above at lower volume fractions. The particle size distribution of the 75/25 NR/85°C dispersion-based PSA formulation shows that the effective hydrodynamic volume of particles is significantly larger.

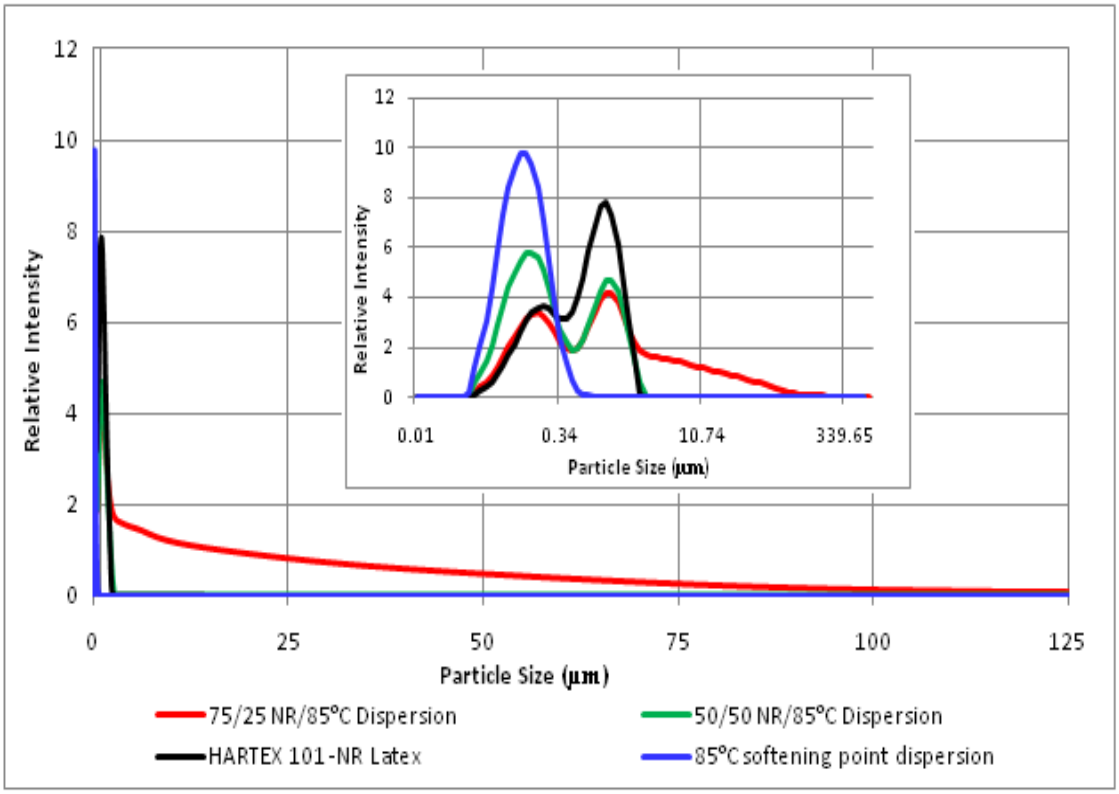

Figure 48. Particle size and size distribution of PSA formulations containing NR and 85°C softening point dispersion

Surface layers such as surfactants and dispersing agents can significantly increase the effective volume of emulsion particles at a particular volume fraction due to inter-particle interaction, resulting in higher hydrodynamic volume.[17, 19, 20] As mentioned earlier, the difference in surfactants/dispersing agents chemistries and volumes, has a dramatic effect on viscosity and softening points.

TEM micrographs (Figure 49) of the 75/25 NR/85°C dispersion-based PSA formulation correlate very well with the higher inter-particle interactions between NR latex particles and the 85°C softening point dispersion. Higher hydrodynamic volumes at lower volume fractions of 85°C softening point dispersion is evident for 75/25

NR/85°C dispersion-based PSA formulation. The 50/50 NR/85°C dispersion-based PSA formulation shows no interaction between the NR latex particles and the dispersion particles.

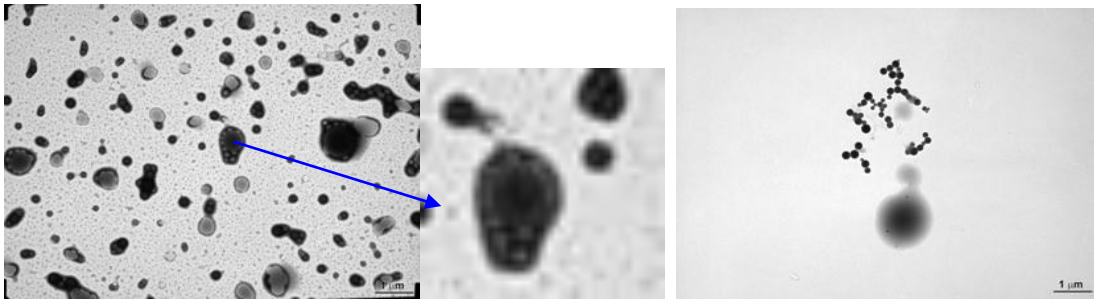

(a) (b)

Figure 49. TEM micrographs of PSA formulations containing NR and 85°C softening point dispersion. (a) 75/25 NR/85°C softening point dispersion-based PSA formulation, (b) 50/50 NR/85°C softening point dispersion-based PSA formulation

III. PSA formulations containing NR & 95°C softening point dispersion

Even though the initial viscosity (Figure 50)of the 95°C softening point dispersion is higher due to higher solids and pH, the 75/25 NR/95°C dispersion-based PSA formulation and the 50/50 NR/95°C dispersion-based PSA formulation show lower initial viscosity. In addition, the 75/25 NR/95°C dispersion-based PSA formulation shows slightly higher initial viscosity than the 50/50 NR/95°C dispersion-based PSA formulation. This correlates well with the particle size data (Figure 51). This can be traced back to the different type and amount of surfactant/dispersing agent employed in the 95°C dispersion.

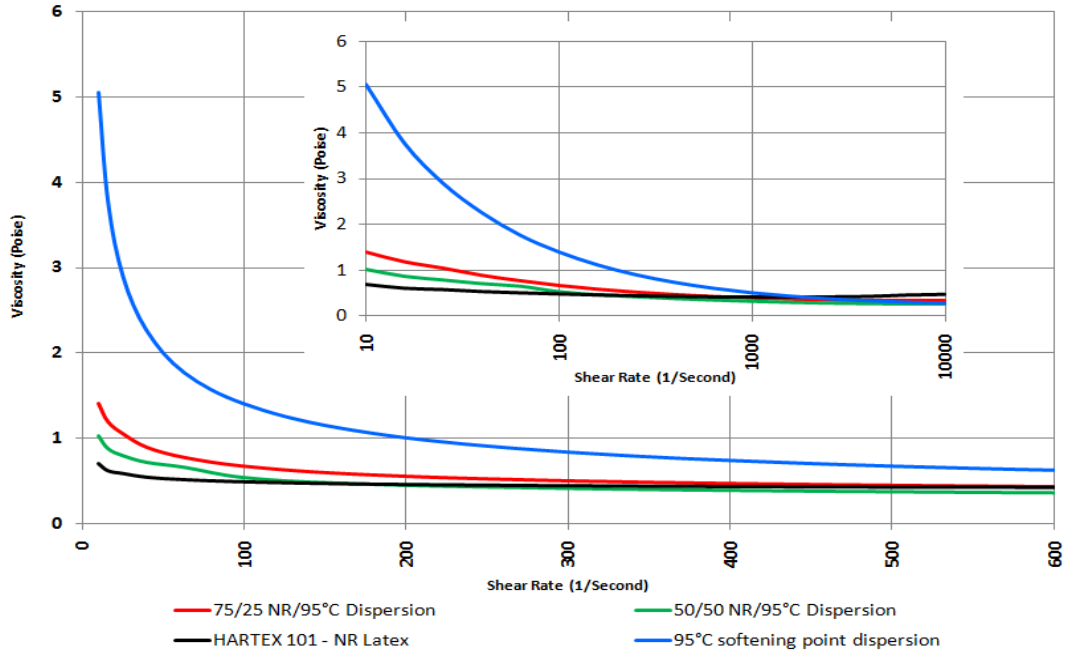

Figure 50. Rheological profiles of PSA formulations containing NR and 95°C softening point dispersion

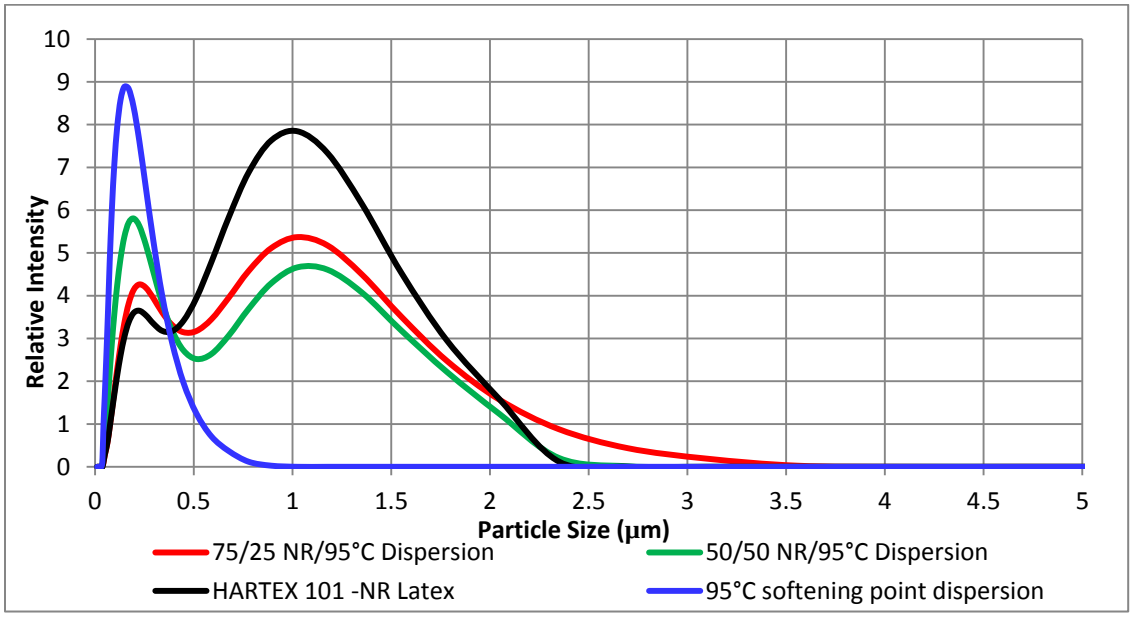

Figure 51. Particle size and size distribution of PSA formulations containing NR and 95°C softening point dispersion

TEM micrographs (Figure 52) of both 72/25 and 50/50 NR & 95°C dispersion-based PSA formulations show similar morphology. Neither of the NR & 95°C dispersion-based PSA formulations showed any significant interaction between 95°C softening point dispersion and natural rubber particles. The data can be correlated well to the rheology and particle size data. It can be seen that chemistry and the amount of surfactant/dispersing agents used in the tackifier dispersions has major influence in determining the Wet Rheology and morphology of the PSA formulations.

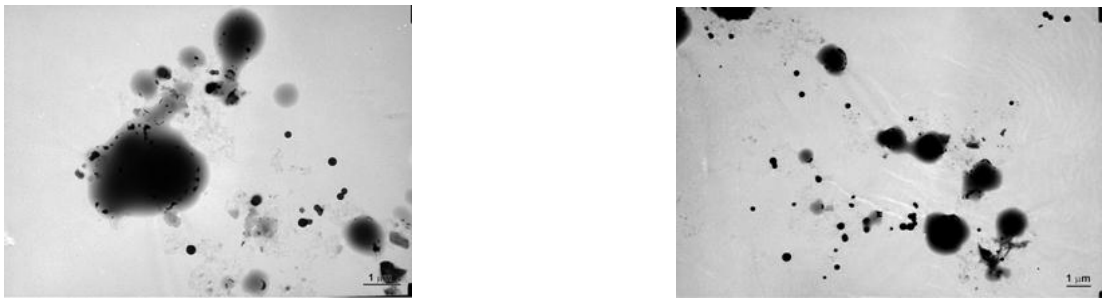

(a) (b)

Figure 52. TEM micrographs of PSA formulations containing NR and 95°C softening point dispersion. (a) 75/25 NR/95°C softening point dispersion-based PSA formulation, (b) 50/50 NR/95°C softening point dispersion-based PSA formulation

Higher particle interaction between the latex and tackifier dispersion, as seen with the 75/25 NR/85°C softening point dispersion containing PSA, can result in higher initial viscosity and shear thinning effects from low to medium shear rates. All of the evaluated PSA formulations show Newtonian behavior at high shear rates (above 1000 s^{-1}), where most of the coating processes occur.

Summary and Path Forward

- Aliphatic hydrocarbon tackifier dispersions with different solids content and softening points can be used as compatible tackifiers in natural rubber-based PSAs to obtain good rheological performance at medium to high shear rates.
- Higher solids and pH of the 85°C and 95°C softening point dispersions result in higher initial viscosity and shear thinning effects at low to moderate shear rates when compared to a 70°C softening point dispersion.
- Interestingly, a lower volume fraction (25%) of the 85°C softening point dispersion containing PSA formulation shows higher initial viscosity due to inter-particle interactions. Tackifier dispersion rheology and morphology are greatly affected by the type and amount of surfactant/dispersing agents employed. Particle size distribution data and morphological observation using TEM correlate well with the rheological observations.
- All of the higher volume fraction (50%) dispersion containing PSA formulations show nearly Newtonian behavior at medium to higher shear rates, where most adhesive coating processes occur.
- The percent solids and pH definitely influence the viscosity and shear thinning behavior, but the interaction between the natural rubber latex and tackifier dispersion particles is key in determining the viscosity at low to medium shear rates, where processes like filtration and pumping occur.
- It should be noted that all of the PSA formulations containing different softening point tackifier dispersions at different addition levels (25-50%) can easily be

processed through commonly used coating operations such as roll coating or curtain coating without the use of any other additives. Reverse gravure coating may require higher viscosity, which can be achieved easily through additional rheology modifiers.

References

1. W. H. Sheout and H. H. Day, US Patent No. 3965 (1845)
2. D. Satas (Ed.), *Handbook of Pressure Sensitive Adhesive Technology (Third edition),* Satas & Associates, Warwick, RI (1999)
3. R. G. Drew, GB Patent 312,610 (1930)
4. R. G. Drew, GB Patent 405,263 (1934)
5. W. Eustis and G.R. Orrill, US Patent 2,429,223 (1947)
6. *Natural Rubber Latex Adhesives*, Economics and Policy Analysis Branch and Economics, Exposure and Technology Division , Office of Pollution Prevention and Toxics, USEPA – Washington DC, May-7 2008
7. T. Sanderson, *Adhesives Age*, 31 (Dec. 1978)
8. W. Demarteau and J. M. Loutz, *Progress in Organic Coatings*, 27, 33 (1996)
9. C. Oldack and R. E. Bloss, *Adhesives Age*, 38 (Apr. 1979)
10. N. Nakajima et al., *J. Appl. Polym. Sci.* 44, 1437 (1992)
11. K. F. Gazeley, *1983 Proc. Industry Technical Conference*, *Pressure Sensitive Tape Council,* pp. 30-34 (Apr. 1983)

12. J. G. de Hullu, *3rd International PSTC Technical Seminar Orlando-FL*, pp. 137-140 (1998)

13. N. Willenbacher et al., *Adhesives and Sealants Industry Magazine,* 26 (Nov. 2003)

14. P. Rolfe, *Adhesives and Sealants industry Magazine*, 35 (Feb. 2010)

15. S. Florian and I. Novak, *J. Mater. Sci.*, 39, 649 (2004)

16. I. Benedek and L.J. Heymans, *Pressure Sensitive Adhesive Technology*, Marcel Dekker Inc., New York (1997)

17. E. J. Schaller, in: *Emulsion Polymerization & Emulsion Polymers*, P. A. Lovell and M.S El-Aasser (Ed.), pp. 437-466. John Wiley & Sons Ltd, New York (1997)

18. R. J. Farris, *Transactions of the Society of Rheology*, 12, 281 (1968)

19. B. P. Binks and S. O. Lumsdon, *Langmuir*, 17, 4540 (2001)

20. I. M. Krieger and T. Dougherty, *Transactions of the Society of Rheology*, 3, 137 (1959)

CHAPTER – 7. EVALUATION OF NATURAL RUBBER LATEX-BASED PRESSURE-SENSITIVE ADHESIVES CONTAINING ALIPHATIC HYDROCARBON TACKIFIER DISPERSIONS WITH DIFFERENT SOFTENING POINTS – ADHESIVE PROPERTIES AT DIFFERENT CONDITIONS

Abstract

Natural rubber latex-based water-borne pressure sensitive adhesives (PSAs) have been formulated with three aliphatic hydrocarbon water-based dispersions (varying softening points) at two different resin addition levels (25% and 50%). Time-temperature superposition analysis using WLF approximations for adhesive peel has revealed that the adhesives formulated with 50% resin addition level show good adhesive behavior. It has also been determined from time-temperature superposition analysis that peel force increases systematically with softening point and peel rate. Correlation of viscoelastic behavior with adhesive properties suggests that at least 50% resin addition level is needed to bring the natural rubber-based formulations into PSA criteria as defined by Dahlquist and others. Adhesive property evaluations performed on a high surface energy substrate (stainless steel) and low surface energy substrate (LDPE) suggested that optimum tack, peel and shear properties at room temperature were obtained for a formulation containing a higher softening point dispersion (95°C) at 50% resin addition level. Adhesive peel and tack tend to follow softening point trends as well. A 25% tackifier dispersion addition level did not provide any significant adhesion. Humid aging (50°C and 100% relative humidity) evaluations of the water-borne adhesives seem to correlate well with the room temperature adhesive property observations.

Introduction

From as early as 1845, natural rubber-based pressure sensitive adhesives have been formulated with natural or petroleum derived resins to improve tack and processing characteristics.[1-4] Most of the early work on natural rubber-based industrial pressure sensitive adhesives were solvent-based thin film systems pioneered by 3M. Availability of natural rubber as stabilized latex emulsions increased the use of emulsions-based pressure sensitive adhesive technologies and these systems began to dominate solvent-borne technologies by the 1970s. More stringent health and environmental restrictions also favored the natural rubber latex-based emulsion pressure sensitive adhesive technology until World War II, when availability became an issue.[5, 6, 7] Pressure sensitive adhesives with solvent-based or water-based, natural rubber latex have been formulated with other components, such as tackifying resins and additives (plasticizers, stabilizers etc.), since the first patent in 1845. Natural rubber imparts cohesive strength characteristics to the pressure sensitive adhesive, while tackifying resins impart adhesive characteristics such as tack and peel strength.[1-7]

Oldack and Bloss in 1979 reported[7] the compounding of natural latex in water-based PSAs utilizing water-based resin dispersions. They evaluated the effect of water-based tackifier dispersions of polyterpene resin, hydrogenated rosin resin and even a hydrocarbon resin dispersion in natural rubber latex-based formulation for adhesive tack and shear.[8] Although there is much reported literature on solvent-borne natural rubber pressure sensitive adhesives, there is limited literature regarding the natural rubber, latex-based pressure sensitive adhesive formulations. Recent acrylic-based

emulsion availability issues are prompting more and more formulators to go back to natural rubber latex-based PSAs from a performance, availability and economics stand point. Natural rubber-based PSAs can be used in a variety of applications such as masking tape, box sealing tape, protective film tape, and tape in medical applications. Given the wide range of applications involved, the PSAs formulated should withstand different environmental and physical conditions. Therefore, understanding the adhesive properties and mechanical behavior of a PSA in a variety of operating conditions and temperatures is very critical.[2]

Normally, pressure sensitive adhesive properties are characterized in three ways: peel, tack and shear strength (hold power). Evaluation of these properties is critical, since a PSA should adhere to different substrates with no more than finger pressure and should be removed from the substrate surface without leaving a residue. It has been demonstrated that PSA peel adhesion measurements provide more information on expected adhesive performance characteristics than tack or shear measurements. Peel is measured as the force required to remove a PSA. Interfacial and bulk properties of PSAs normally contribute to peel. Separating each element's contributions to the peel is very difficult. Therefore peel force, as reported, are normally the combined effect of these factors. Different models have been established to explain the peel of a PSA. The most commonly used models include a dash-pot model proposed by Voigt representing the viscous response to stress and a spring model suggested by Maxwell representing the elastic response to stress. Complex models using the Voigt-Maxwell concepts with

various configurations have also been established by other researchers to represent the true viscoelastic behavior of PSA peel.[9-11, 18]

The strength of the bond formed between an adhesive and substrate is characterized by measurement of peel strength, the force per unit width required to pull apart two strips of substrate held together by the adhesive as a function temperature and the rate at which the strips are separated. In practice, the range of temperatures and rates accessible by the existing measurement techniques is often limited. Also, because the test is destructive, a new sample must be used for each data point. This limits the number of data points which can be practically acquired. Time-temperature superposition is a technique which facilitates the analysis of peel strength data by allowing data acquired at different conditions to be plotted together on one plot of reduced force versus reduced rate. This allows the data to be fitted with a model function that can be used to extrapolate to conditions outside of the measurement range, as well as interpolate between measured points.[18-23] Time-temperature superposition is normally performed according to the WLF relationship.[10, 18, 24]

$$\log(a_T) = -\frac{C_1(T - Tg)}{C_2 + T - Tg}$$

Where C_1 and C_2 are empirically determined parameters, found to have the nearly universal values of 17.44 and 51.6 respectively,[10, 18, 24] 'a_T' is the WLF shift factor, '*T*' is the measurement temperature (K), and T_g is the glass transition temperature (K) of the sample. In the practical treatment of peel strength data, C_1 and C_2 are often treated

as adjustable parameters, with values chosen to optimize the superposition of points on the reduced plot.[10, 24]

Tack can be defined as the ability of the material to adhere instantaneously to a solid surface when brought into contact under very light pressure. Tack is the composite response of the PSA's bulk and surface properties. Tack is normally measured by the energy required to break the bond.[2, 9-11] Shear or hold power is the force required to pull the PSA from a parallel substrate and is normally reported as a function of holding time. Tack and peel represent the adhesive response of a PSA, while shear represents the cohesive characteristics of the PSA.[9-11] These properties are directly related to pressure sensitive adhesive response to stress, so tack, peel and shear can be correlated to the stress-strain response of a PSA as explained by Dahlquist in the late 1960s.[12] Many reports followed, correlating viscoelastic performance of PSAs obtained through rheological measurements to adhesive properties such as tack, peel and shear of a PSA.[12-16] Sheriff *et al.* and Class and Chu correlated the viscoelastic properties of natural rubber-based PSAs containing tackifier resin with adhesive properties, and reported that tackifier resin structure, molecular weight and concentration have significant influence in determining the viscoelastic characteristics of the PSA and thus, the adhesive properties.[14-16]

Unfortunately, most of the reported literature correlating the viscoelastic performance of natural rubber-based PSAs with adhesive properties was based on solvent-borne PSAs. In this study, a correlation of natural rubber-based, water-borne

PSA rheology with adhesive properties at different conditions and two different substrates are reported. Natural rubber water-borne PSAs are formulated with three different aliphatic hydrocarbon water-based tackifier dispersions having three different softening points. The effect of tackifier dispersion concentration and softening point on PSA rheology and adhesive properties are described. The effect of peel at different rates and at different temperatures has been iterated from time-temperature superposition experiments using WLF approximations.

Materials and Methods

ASTM category 3 HARTEX 101 low ammonia natural rubber latex, 62% solids at pH 10 was obtained from Firestone Natural Rubber Company LLC. A 70°C softening point dispersion, an 85°C softening point dispersion and a 95°C softening point dispersion were obtained from Eastman Chemical Company. Table 20 shows the basic properties of the C5 aliphatic hydrocarbon resin dispersions prepared from a low molecular weight, aliphatic, C5 hydrocarbon resin. The 70°C aliphatic hydrocarbon dispersion is dispersed with a long chain alkyl (C_{13}) anionic surfactant/dispersing agent, the 85°C aliphatic hydrocarbon dispersion is dispersed with a combination of long chain alkyl (C_{13}) and cycloaliphatic surfactants/dispersing agents and the 95°C aliphatic hydrocarbon dispersion is dispersed with a cycloaliphatic surfactant/dispersing agent.

Table 20. Properties of C5 aliphatic hydrocarbon dispersions

Designation	pH	% Solids
70°C softening point dispersion	4	50
85°C softening point dispersion	10	55
95°C softening point dispersion	10	55

Water-based pressure sensitive adhesive formulations were formulated with HARTEX 101 natural rubber latex using resin dispersions at 25 wt% and 50 wt% resin addition levels on a dry weight/solids basis. Blending of natural rubber, NR, latex and C5 aliphatic resin dispersions was carried out by mixing natural rubber latex and resin dispersion (at two different resin addition levels) by stirring at room temperature, using a mechanical stirrer for 5 minutes at 100rpm. Formulations were then homogenized using a paint mixing roller for 30 minutes. Formulations evaluated are given in Table 21.

The formulated samples in Table 21 were coated onto Mylar (2mil), using a knife-over-roll drawdown bar, and dried in an oven at 100˚C for 1 minute. The target coating thickness was 0.85-0.95 mils. The coated Mylar (2mil) was backed with silicone paper. PSA tapes were then cut into 1 inch strips for testing.

Tape samples were equilibrated in a constant temperature and humidity room (23˚C / 50% RH) overnight, prior to room temperature adhesive evaluations. After equilibration, the samples were evaluated for the properties shown in Table 22.

Table 21. PSA formulations

Formulation Description	75/25 (NR/70°C Dispersion)	75/25 (NR/85°C Dispersion)	75/25 (NR/95°C Dispersion)	50/50 (NR/70°C Dispersion)	50/50 (NR/85°C Dispersion)	50/50 (NR/95°C Dispersion)
HARTEX 101 – NR Latex	75	75	75	50	50	50
70°C softening point dispersion	25	-	–	50	-	–
85°C softening point dispersion	–	25	–	–	50	–
95°C softening point dispersion	–	–	25	–	–	50

Using PSTC-101 test method, the 180˚ peel strength test was performed on PSA samples on stainless steel substrate, at five different peel rates (4 in/min, 8 in/min, 12 in/min, 16 in/min and 20 in/min), and five different temperatures (5˚C, 15˚C, 25˚C, 35˚C and 45˚C for the time-temperature superposition evaluations.

Following the test methods described in Table 22, accelerated humid age evaluations of the coated adhesive samples were performed at room temperature after aging the coated adhesives samples in a constant temperature and humidity chamber (50˚C and 100% relative humidity) for a week.

Table 22. Adhesive property evaluation Pressure Sensitive Tape Council (PSTC) test methods[17]

Test	Substrate	Dwell time	PSTC test method[17]
180˚ Peel Strength	Stainless Steel and LDPE (low density polyethylene)	5 minutes	PSTC-101: International standard for peel adhesion of pressure-sensitive tape
Loop Tack	Stainless Steel and LDPE (low density polyethylene)	-	PSTC-16: Standard test method for loop tack
Hold Power 1”x 1” Contact Area 1000g weight	Stainless Steel and LDPE (low density polyethylene)	-	PSTC-107: International standard for shear adhesion of pressure-sensitive tape

Rheological analysis of the PSAs was performed using Dynamic Mechanical Analysis (DMA). A TA Instruments Ares RDA3® Rheometer was used in a parallel plate geometry. Dry adhesive was obtained by coating the formulations in Table 21 onto release paper (2 mil), using a knife-over-roll drawdown bar, and drying in an oven at 100˚C for 1 minute before applying to the platens in the DMA. The diameter of the plates was 8 mm and the gap was set at 2.33 mm. Frequency sweep experiments were performed between 0 and 400rad/s at 25°C. Temperature sweep experiment was performed between -80°C and 300°C with a heating rate of 6°C/min, by keeping the frequency at 10 Hz and the maximum strain at 5%.

Results and Discussion

Adhesive peel evaluation using time-temperature superposition experiments will be discussed first, followed by the viscoelastic characterization. Adhesive property evaluations such as peel, tack and hold power (shear) at two different conditions on two different substrates will be correlated as well.

The effect of peel at different peel rates has been evaluated using time-temperature superposition experiments and WLF approximations. PSA samples were adhered to stainless steel substrate. Next, the peel force at five different peel rates (1.69 mm/sec, 3.38 mm/sec, 5.08 mm/sec, 6.77 mm/sec and 8.46 mm/sec) at each of the five different temperatures (5˚C, 15˚C, 25˚C, 35˚C and 45˚C) was analyzed. Peel force '*P*' (gm/mm) was recorded at different peel rates (mm/sec). Time temperature superposition was performed using WLF approximations. Initially the peel force versus

peel rate data by temperature for each sample was generated. A time-temperature superposition plot of reduced peel force versus reduced rate was then achieved using WLF approximations. Reduced peel force value was calculated by multiplying by a factor equal to the reference temperature, T_{ref}, divided by the measurement temperature, T, both expressed in degrees Kelvin.

$$P_{reduced} = P\frac{T_{ref}}{T}$$

The next step was to transform the rate axis, log(r), into reduced rate, log (ra_T), where a_T is the shift factor according to the WLF relationship[10, 18]

$$\log(a_T) = -\frac{C_1(T - Tg)}{C_2 + T - Tg}$$

Where C_1 and C_2 are empirically determined parameters, found to have the nearly universal values of 17.44 and 51.6, respectively.[10, 18] Glass transition temperatures (T_g) for each of the PSA formulations was obtained from DMA analysis (Table 23). When superposition was achieved from the reduced plot, a linear fit to the log-log plot was obtained to enhance the quality of the fit. The fitted line from the shifted plot thus obtained was added to a linear model curve plot of peel force versus peel rate. Figures 53, 54, and 55 illustrate the reduced plots for 75/25 NR/Tackifier dispersion-based PSA and 50/50 NR/Tackifier dispersion-based PSA.

As can been seen from Figures 53, 54, and 55, at lower temperatures, higher peel force is required to peel the samples. The peel force was also higher at higher peel

rates. The reduced plot for 75/25 NR/Tackifier dispersion-based PSAs does not fit very well compared to the 50/50 NR/Tackifier dispersion-based PSAs when the universal C_1 (17.44) and C_2 (51.6) values are used (see Figure 53). This is mainly because the peel force for the formulations containing 25% tackifier dispersion are very low and considerable noise interferes with the proper shift. It was very difficult to obtain a better fit, even when changing the WLF universal parameter values (C_1 and C_2).

Interestingly, PSAs containing 50% tackifier dispersion fit very well with the standard WLF parameters and give a very good fit. It should be noted that the 50/50 NR/95°C dispersion-based PSA formulation shows the best fit of all the formulations. A linear model curve plot of (Figure 56) peel force versus peel rate was then generated using the fitted line. The effect of peel force at different peel rates for PSAs at room temperature is modeled from zero to a maximum peel rate of 100 in/min, which spans the range possible in practice. As can be seen from the model curve, formulations containing 25% tackifier dispersion show much lower peel force and the peel force plateaus after 20 in/min of peel rate. Interestingly, for PSAs containing 50% tackifier dispersion formulations, the peel force increases as the peel rate increases (up to 100 in/min). The PSAs containing 50% tackifier dispersions also show higher peel force as the softening point of tackifier dispersion increases. At equal concentrations of tackifier addition, higher softening point tackifier resins can improve the peel of the PSA, if it is within the viscoelastic criteria for PSAs.[18]

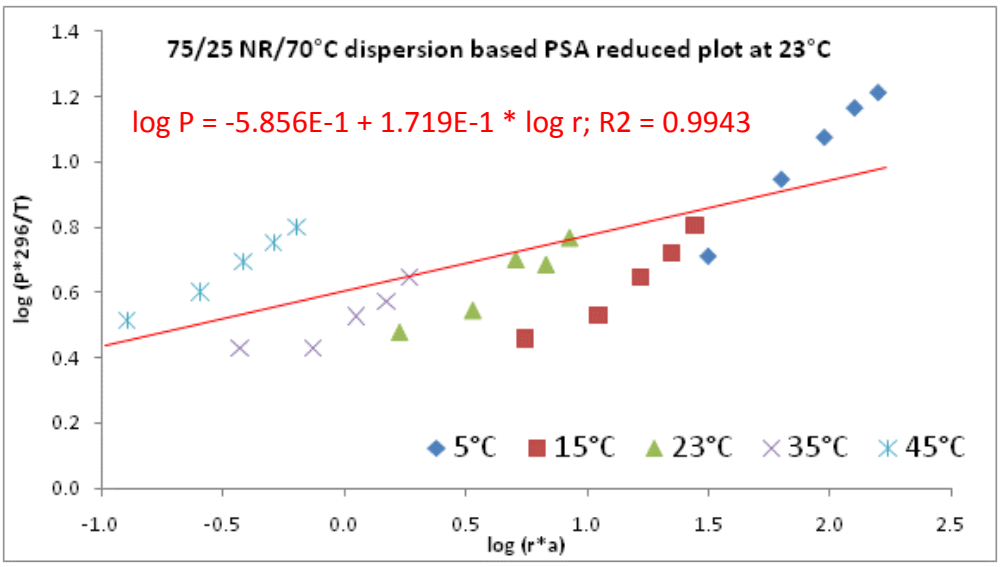

(a)

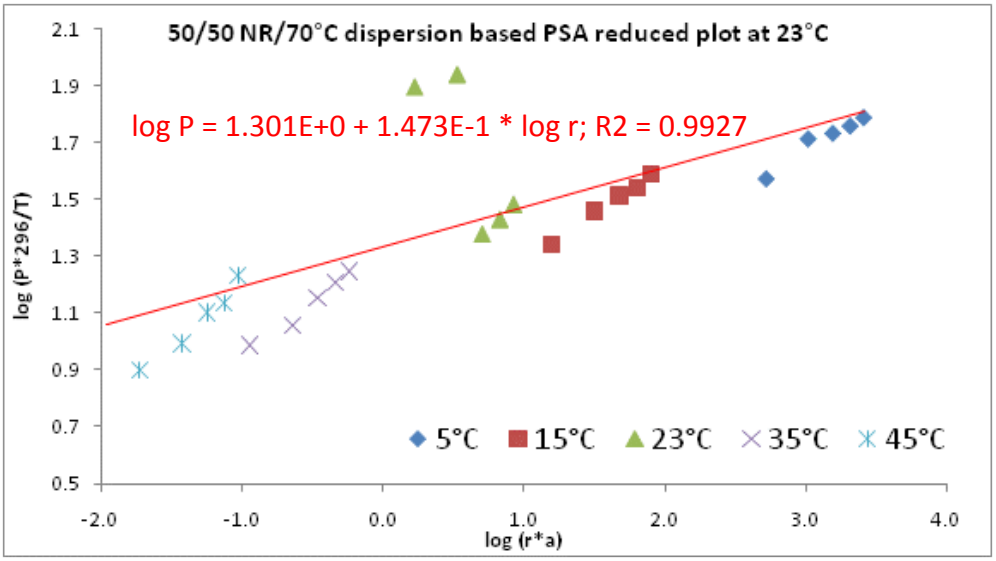

(b)

Figure 53. WLF reduced plots for (a) 75/25 NR/70°C dispersion-based PSA, (b) 50/50 NR/70°C dispersion-based PSA

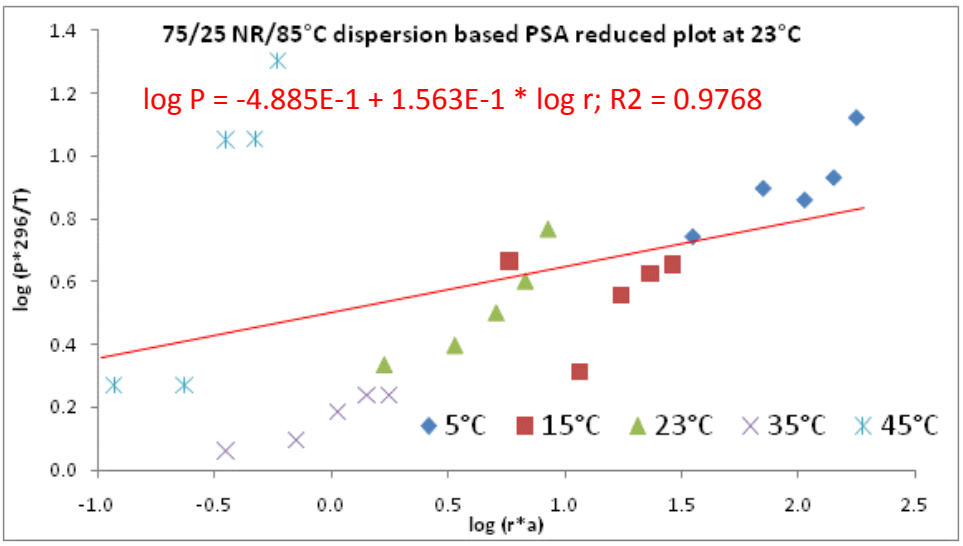

(a)

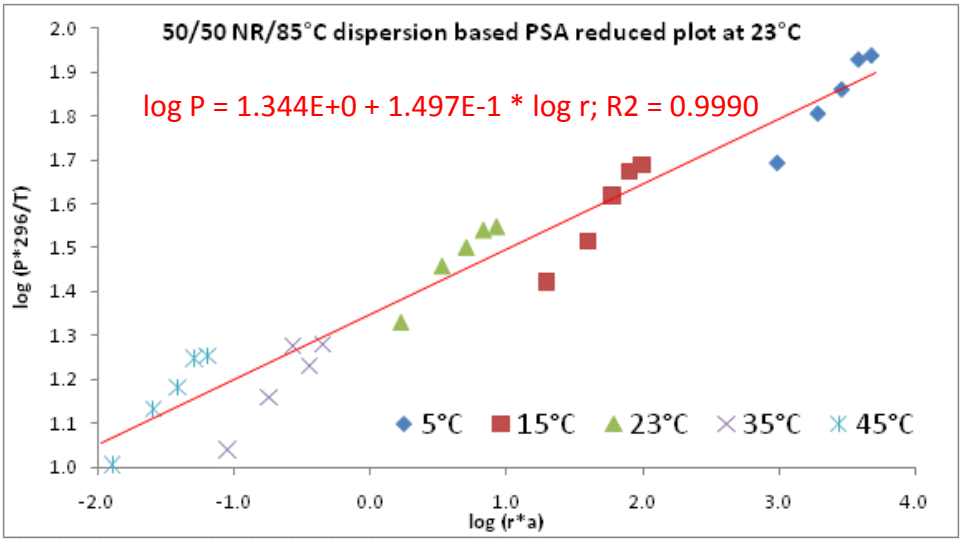

(b)

Figure 54. WLF reduced plots for (a) 75/25 NR/85°C dispersion-based PSA, (b) 50/50 NR/85°C dispersion-based PSA

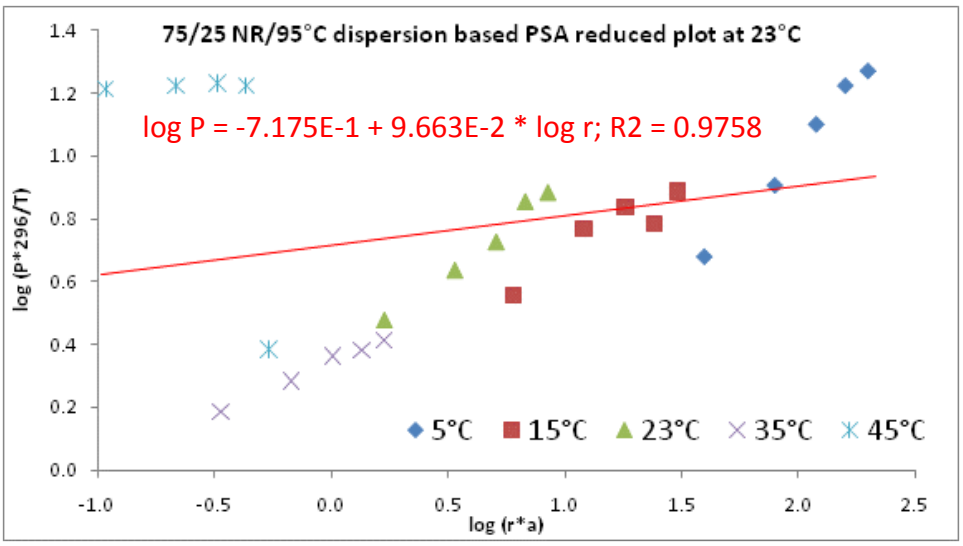

(a)

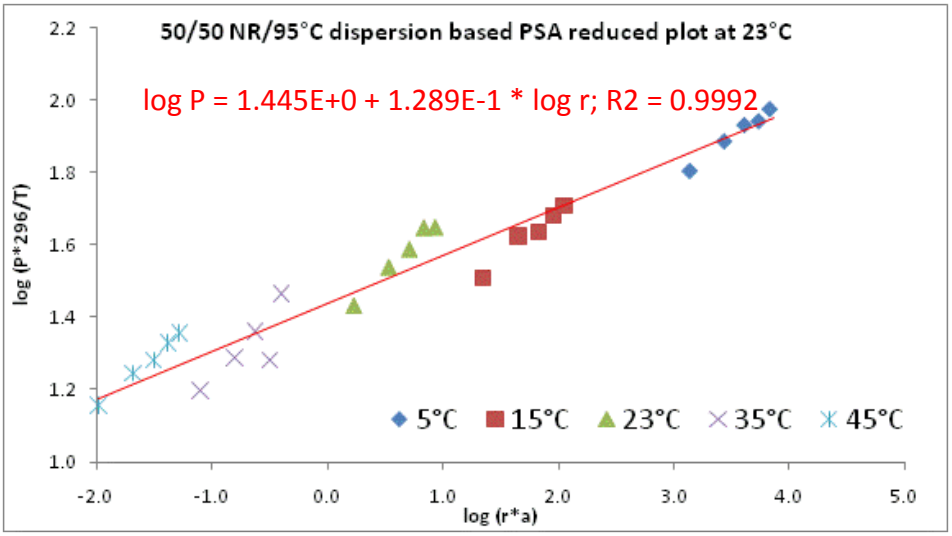

(b)

Figure 55. WLF reduced plots for (a) 75/25 NR/95°C dispersion-based PSA, (b) 50/50 NR/95°C dispersion-based PSA

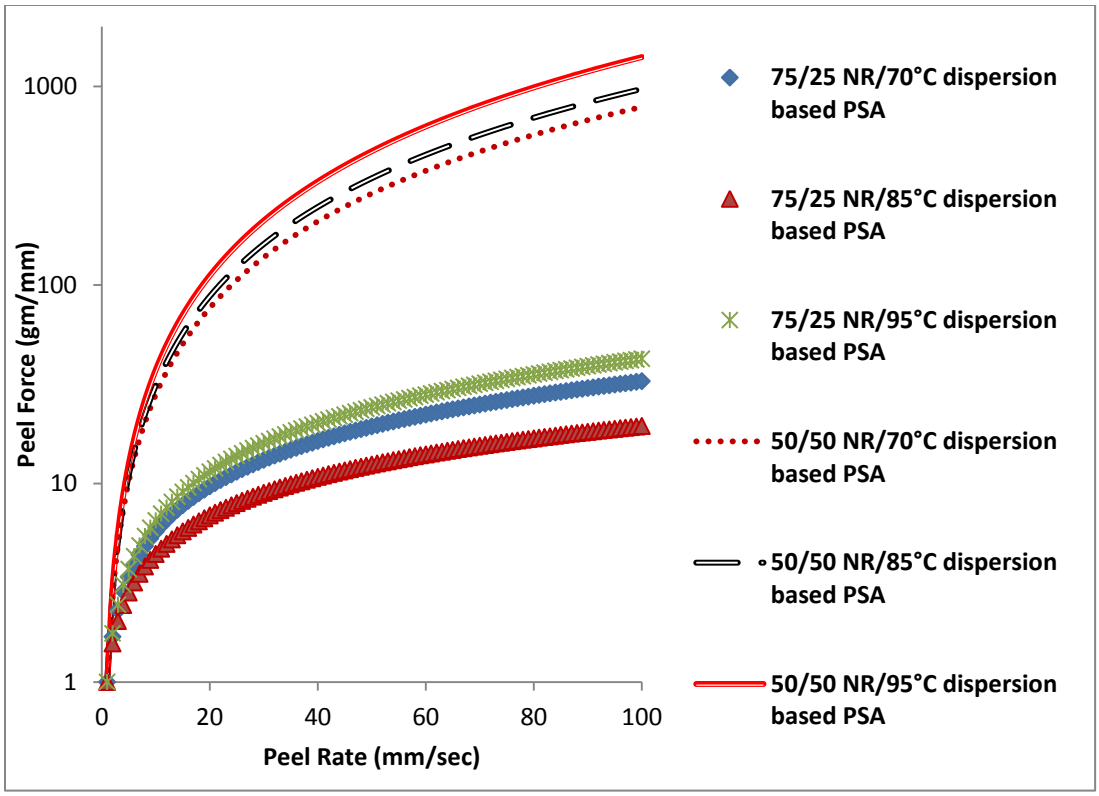

Figure 56. A linear model curve plot of peel force versus peel rate

Most of the reported water-borne, acrylic PSAs show cohesive to adhesive to slip-stick behaviors.[18-23] The performance of PSAs confirmed through time-temperature superposition experiments clearly demonstrates the superior adhesive peel performance of all the PSAs containing 50% tackifier dispersion at peel rates up to 100 mm/sec. The PSA containing 95°C softening point dispersion at 50% addition level performed best.

Viscoelastic behavior of PSAs has been obtained through dynamic mechanical analysis (DMA). A dry film adhesive response at constant temperature (25°C) was evaluated using dynamic oscillation tests on a DMA in a frequency sweep mode. In this evaluation, viscoelastic responses such as the elastic modulus (*G'*), viscous modulus (*G"*)

and the complex viscosity (η^*) are measured at different microscopic oscillations. Complex viscosity[25] (η^*) is calculated from the elastic and viscous modulus with respect to dynamic oscillations (Frequency 'ω') as shown below.

$$\eta^* = \left[\left(\frac{G''}{\omega}\right)^2 + \left(\frac{G'}{\omega}\right)^2\right]^{1/2}$$

Normally for viscoelastic materials, complex viscosity decreases with increasing frequency. The dynamic oscillation response of 75/25 NR/Tackifier resin dispersion formulations, is shown in Figure 57. As can be seen in Figure 5, the elastic and viscous modulus of natural rubber latex is high, resulting in higher complex viscosity compared to the formulated PSAs. PSAs with 70°C softening point dispersion show the lowest elastic and viscous modulus followed by the 95°C softening point dispersion containing PSA. Interestingly, the 85°C softening point dispersion containing PSA shows higher elastic and viscous modulus, which is very close to natural rubber. As Class and Chu observed, increasing softening point increases the modulus. The depression in modulus at lower frequencies for the PSA formulations as compared to base polymer (natural rubber) is typical for the compatible pressure sensitive adhesives blends.[15, 16] While this is true for most adhesive blends, the 85°C softening point dispersion containing PSA shows slightly higher modulus than the 95°C softening point dispersion containing PSA.

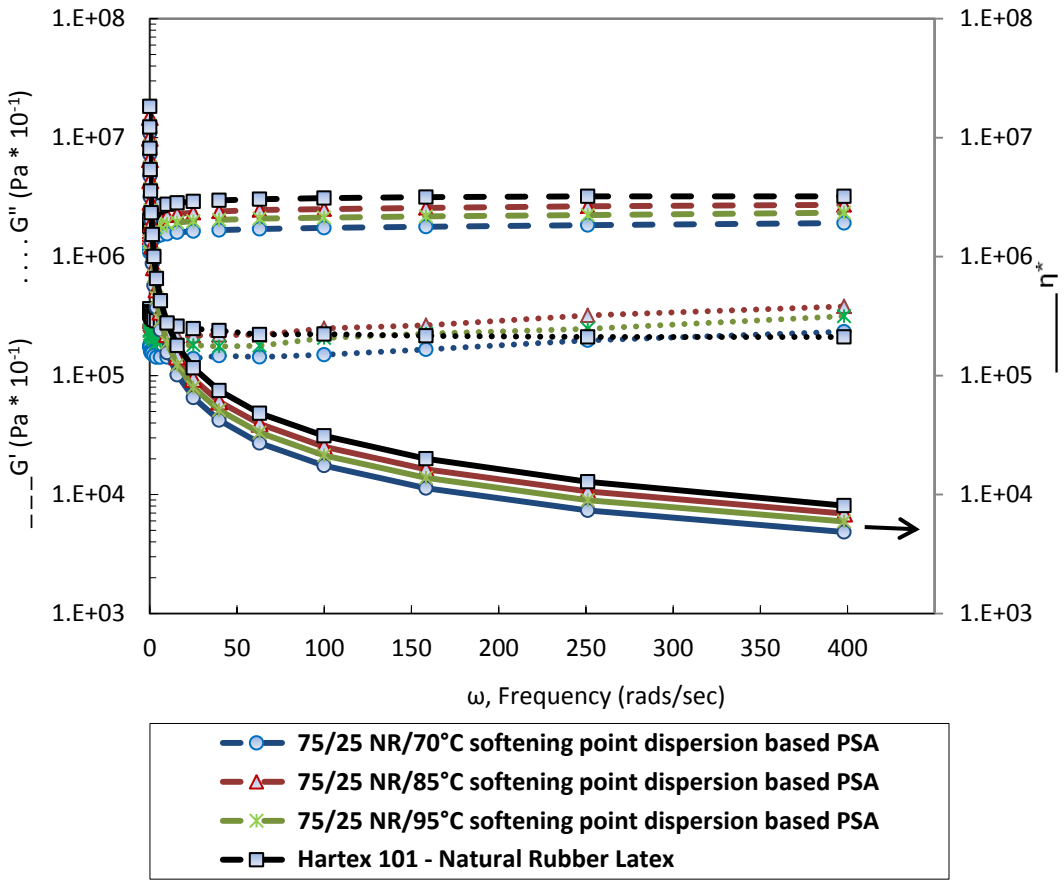

Figure 57. Dynamic Oscillation response of 75/25 NR/Tackifier resin dispersion PSAs

The same trend for the 85°C softening point dispersion containing PSA was observed for the 50/50 NR/85°C softening point dispersion containing PSA (Figure 58), even though the modulus differences are smaller. Interestingly, the 95°C softening point dispersion containing PSA shows lower modulus than the 70°C softening point dispersion containing PSA. It can be inferred that at 75/25 NR/Tackifier resin dispersion concentration, 70°C softening point dispersion containing PSA would be the softest, while at 50/50 concentrations, the 95°C softening point dispersion containing PSA would be the softest.

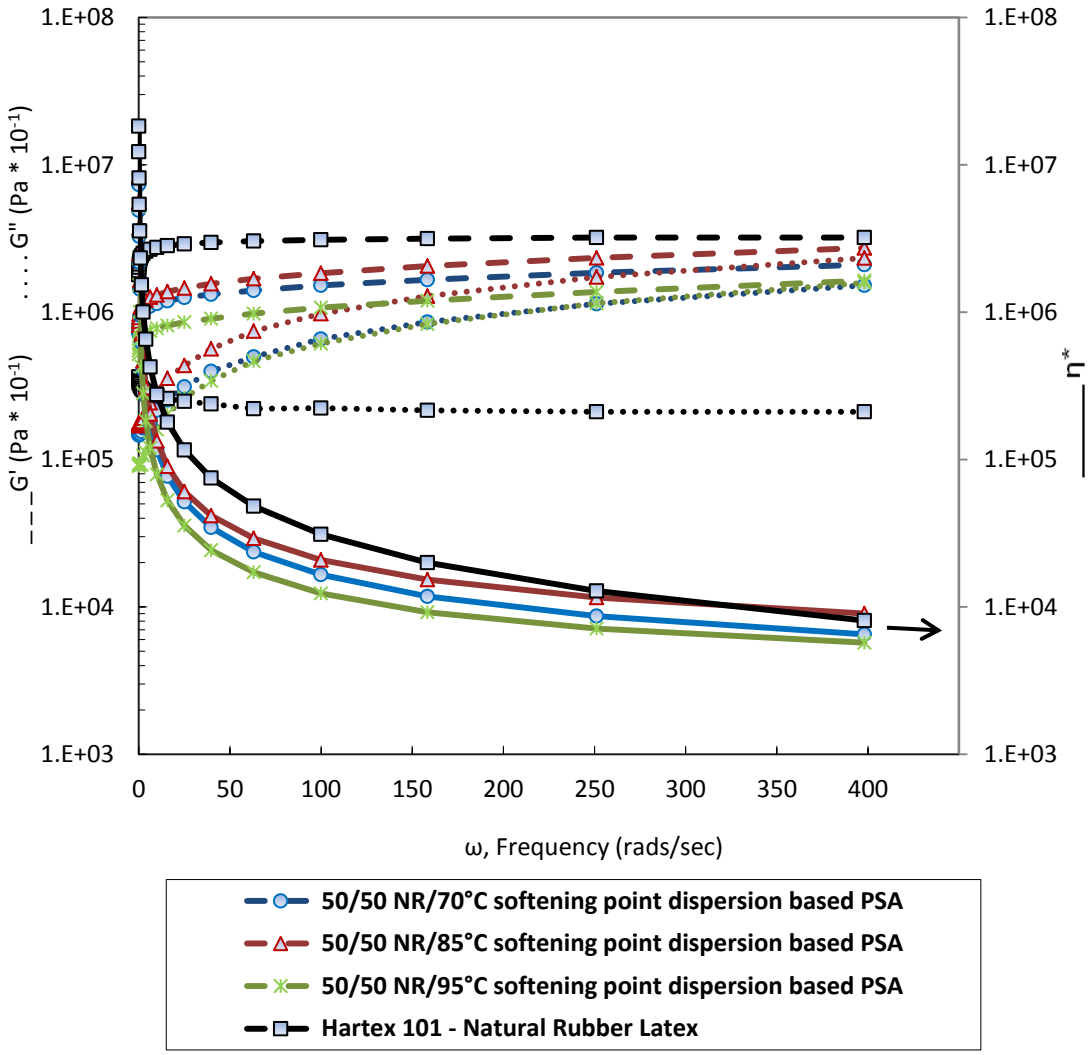

Figure 58. Dynamic Oscillation response of 50/50 NR/Tackifier resin dispersion PSAs

During bonding, the PSA is soft enough to flow and wet the substrate (lower modulus at low frequencies), and during peeling/de-bonding, the PSA is strong enough to withstand the stress (elevated modulus at higher frequencies). It can be seen that the elastic modulus increases slowly with frequency for all the formulations at 75/25 and 50/50 concentrations. The viscous modulus (G") stays almost constant for all the frequency ranges at 75/25 concentrations for all PSAs. At 50/50 concentration, the

viscous modulus is constant until a frequency of 10 rads/sec is reached, after which point it starts to increase as the frequency increases. Even though the viscous modulus of the 50/50 NR/95°C softening point dispersion containing PSA starts lower at low frequencies, at higher frequencies it overlaps with the 70°C softening point dispersion containing PSA. Physically, this correlates to being soft at low frequencies and strong at high, de-bonding frequencies.

It can be observed that 50% tackifier dispersion containing PSAs show lower elastic modulus than the 25% tackifier dispersion containing PSAs. As the amount of tackifier loading increases in a compatible PSA blend, the modulus decreases. Lower elastic modulus at lower frequencies within the PSA elastic modulus region (10^5-10^6 dynes/cm^2) has been explained by Dahlquist and Chu and can be correlated to good adhesive tack. Higher elastic modulus at higher frequencies can be correlated to peel strength.[16] The 50/50 NR/85°C softening point dispersion containing PSA is the stiffest and shows lower tack, but better cohesive properties. In this case, the 50/50 NR/95°C softening point dispersion containing PSA seems to show a good balance of wet-out, tack, peel and cohesive properties.

A temperature sweep at constant frequency was also performed on the dry film PSAs using dynamic mechanical analysis (DMA). Figure 59 shows the viscoelastic response for PSA containing 25% tackifier dispersions.

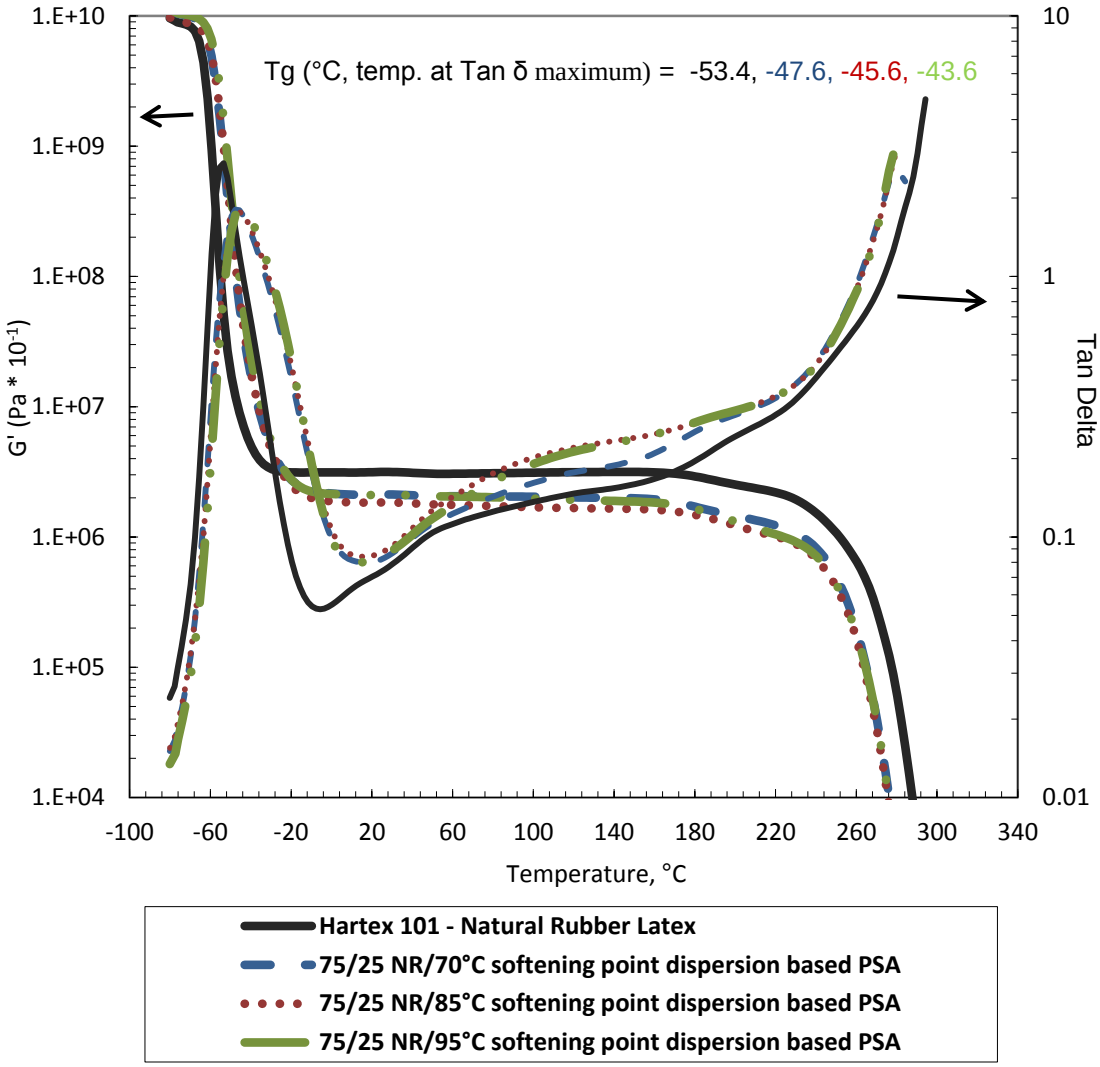

Figure 59. Viscoelastic response for NR and PSA containing 25% tackifier dispersions

Viscoelastic behaviors such as storage modulus and tan δ temperature can be seen in Figure 59. A narrow single tan δ reveals that all three aliphatic hydrocarbon tackifier dispersions are very compatible up to 50% addition levels with natural rubber latex (Figure 59 and Figure 60). T_g of the PSA blend systematically increases with softening points (Figure 59 and Table 23), and storage modulus of the blends systematically decreases with softening points, which is very typical of tackifier-modified

PSAs.[15, 16, 19] Earlier researchers such as Dahlquist, Satas, Chu and Glass reported that glass transition temperature (tan δ temperature) and storage modulus (G') at application temperature are the most important viscoelastic characteristics for PSA performance.[2, 12, 15, 16, 19]

Table 23. T_g of natural rubber and PSA formulations from DMA tan δ

Sample	**T_g (°C)**	**T_g (K)**
Natural rubber (Hartex 101) base latex	-53.4	219.7
75/25 NR/70°C dispersion-based PSA	-47.6	225.6
75/25 NR/85°C dispersion-based PSA	-45.6	227.6
75/25 NR/95°C dispersion-based PSA	-43.6	229.5
50/50 NR/70°C dispersion-based PSA	-15.6	257.6
50/50 NR/85°C dispersion-based PSA	-11.6	261.5
50/50 NR/95°C dispersion-based PSA	-9.6	263.6

In order for an adhesive to act as a good pressure sensitive adhesive, they defined that the PSA require a storage modulus (G') value of $2x10^5$ to $2x10^6$ dyne/cm^2 at room temperature, and a T_g about -15°C to 10°C. It can be seen (Figure 59) that PSA containing 25% tackifier dispersions, even with 95°C softening point dispersion, has too

low of a T_g and higher modulus to perform as a good pressure sensitive adhesive as defined by PSA criteria.[15, 16] This may be one of the reasons why PSA containing 25% tackifier dispersions shows poor peel performance. As Chu explains,[16] the T_g requirement for PSAs is mainly related to the de-bonding phenomenon of the adhesives, and thus it affects the peel adhesion, since peel is related to a high rate of deformation. The viscoelastic performance data correlates well with the time-temperature peel performance evaluation results for PSA containing 25% tackifier dispersions.

Figure 60 illustrates the viscoelastic response of the PSA containing 50% tackifier dispersions. The T_g of the PSA blends increases dramatically with softening point, and modulus of the blend decreases with increase in tackifier dispersion addition. The higher the softening point of tackifier resins, the higher the T_g of the blend. Interestingly, the entire PSA blend containing 50% tackifier dispersion seems to be in the PSA region as explained by Dahlquist and others.

The significant decrease in modulus for the PSA containing 50% tackifier dispersions compared to PSA containing 25% tackifier dispersions should be noted. The lower storage modulus value can be correlated to the time dependent wetting properties of the adhesive to the adherent.[16] Therefore, the PSA containing 50/50 NR/70°C dispersion and the PSA containing 50/50 NR/85°C dispersion may show better adhesive characteristics to low energy substrates than the PSA containing 50/50 NR/95°C dispersion. The higher tan δ value of the PSA containing 50% 95°C softening dispersion can also be correlated to higher tack. Lower tan δ minimum for the same

formulation can be correlated to better shear properties. A 50% tackifier dispersion addition level may be the maximum addition level to keep the PSA formulations in one phase. The small shoulder in the tan δ curve around -40°C (Figure 60) and the broadness of tan δ curve for the 50% tackifier dispersion addition levels are indications of reduction in compatibility compared to the 25**%** tackifier dispersion addition levels.

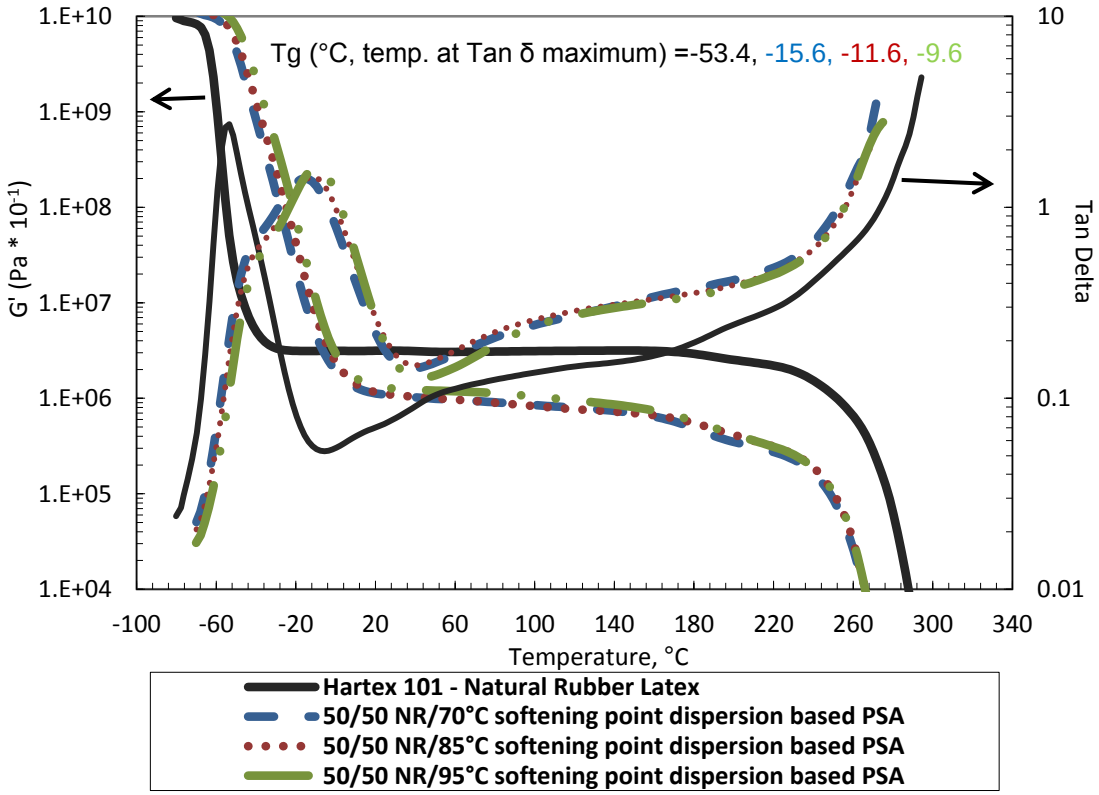

Figure 60. Viscoelastic response for NR and PSA containing 50% tackifier dispersions

Figure 61 illustrates the room temperature adhesive peel (180° peel), loop tack and shear (hold power) performance of PSAs containing both 25% and 50% tackifier dispersions on to a high surface energy substrate (stainless steel). As can be seen, the adhesive peel and tack for all 25% dispersion containing formulations to stainless steel is

very low, but the cohesive property hold power is very high. This correlates well with the viscoelastic behavior evaluation, such that the PSA containing 25% tackifier dispersions did not fall into the PSA criterion for T_g and modulus defined by Dahlquist and others. Peel performance of the PSA containing 25% tackifier dispersions also correlates well with the time-temperature superposition data. However, the hold power (shear) decreases as the softening point of the PSA containing 25% tackifier dispersions increases. This is mainly because higher softening tackifier dispersion at 25% addition level decreases the degree of elasticity, resulting in lower cohesive strength.

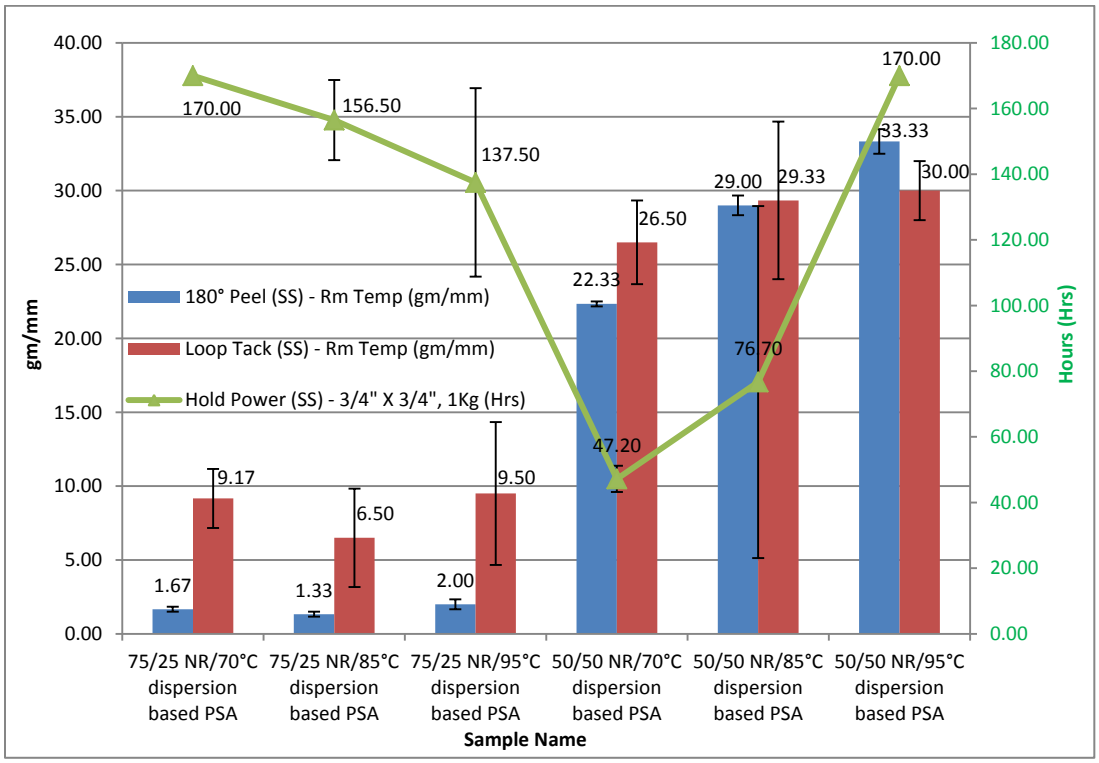

Figure 61. Room temperature adhesive peel (180° peel), loop tack and shear (hold power) performance of PSAs on stainless steel (SS) substrate

PSAs containing 50% tackifier dispersions show better adhesive properties compared to the PSAs containing 25% tackifier dispersions. For the PSAs containing 50% tackifier dispersions, adhesive properties such as peel and tack and the cohesive property hold power increase with increasing softening point of the tackifier dispersions. This also correlates well with the viscoelastic performance evaluations in such a way that the PSA containing 50% tackifier dispersions follow T_g and modulus criteria for PSAs defined by Dahlquist and others. The higher tack and shear properties for the PSA containing 50/50 NR/95°C softening point tackifier dispersion was predicted during the viscoelastic performance evaluation, and it correlates well with the PSA performance to stainless steel substrate. Higher tan δ values of an adhesive correspond to a higher loss modulus, which then corresponds to better adhesive properties. Lower tan δ minimum value corresponds to a higher elastic modulus, resulting in better cohesive strength (hold power). Figure 62 illustrates the room temperature PSA performance on the low surface energy substrate LDPE.

The adhesive properties, tack and peel are lower for all PSAs on LDPE compared to stainless steel substrate. The cohesive property hold power to LDPE for PSAs containing 25% tackifier dispersions is very high, while the adhesive peel and tack are significantly low. However, PSAs containing 50% tackifier dispersion show better adhesive peel and tack. Even though the adhesive peel for PSAs containing 50% tackifier dispersions gradually increases with softening point, the adhesive tack shows no correlation to softening point. At 50% addition level, the 85°C tackifier dispersion-based PSA shows the lowest tack and hold power. The difference is mainly due to the

difference in surface energy characteristics of the substrate, LDPE. It is interesting to note that the PSA containing 95°C tackifier dispersion at 50% resin addition level shows the best adhesive and cohesive characteristics on both stainless steel and LDPE substrates. This correlates well with the viscoelastic performance evaluations and the time-temperature superposition evaluations for the adhesive peel.

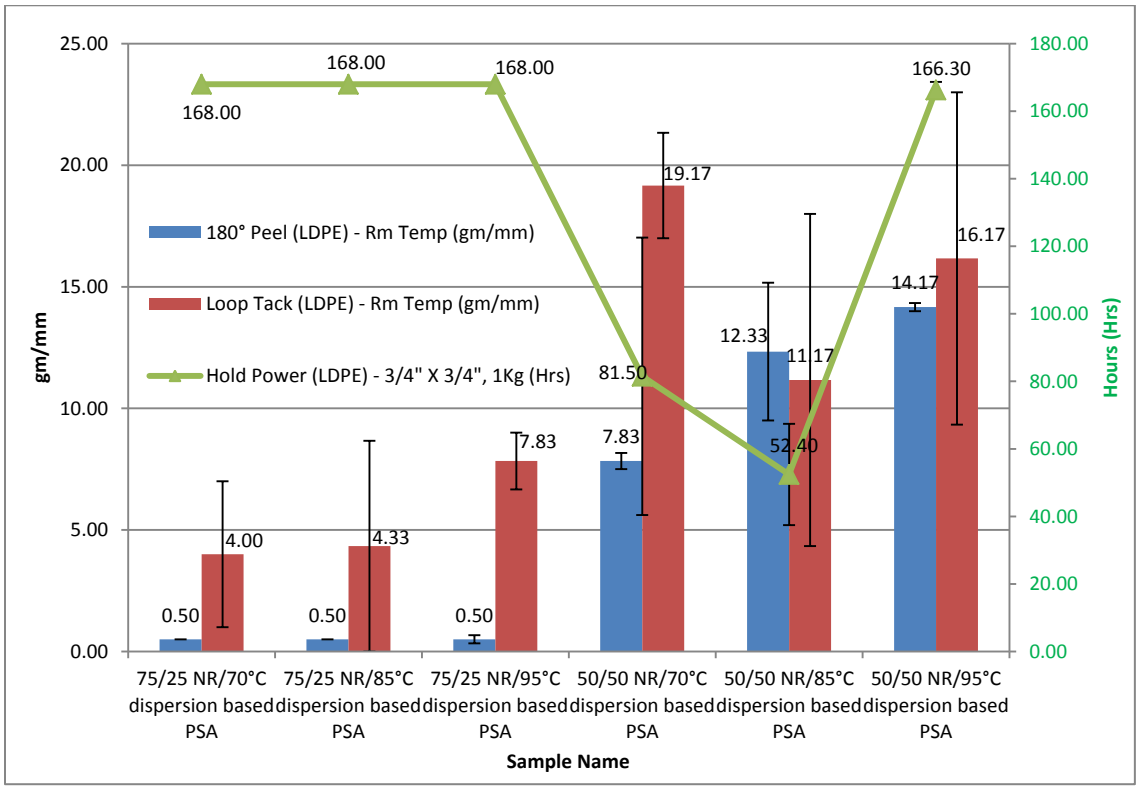

Figure 62. Room temperature adhesive peel (180° peel), loop tack and shear (hold power) performance of PSAs on low density polyethylene (LDPE) substrate

Figures 63 and 64 show the adhesive property evaluations of the PSAs after one week of accelerated humid aging (50°C and 100% relative humidity). The accelerated humid aging evaluations are normally performed to correlate the performance of the PSA with real world high temperature-high humidity conditions.

It can be seen that one week of accelerated aging (humid aging) conditions has increased the tack, peel and shear properties of the adhesive compared to the initial room temperature evaluations. This is typical for humid aged PSA samples. The PSAs containing 25% tackifier dispersion still show poor adhesive peel and tack, but good cohesive property (hold power), similar to the room temperature performance.

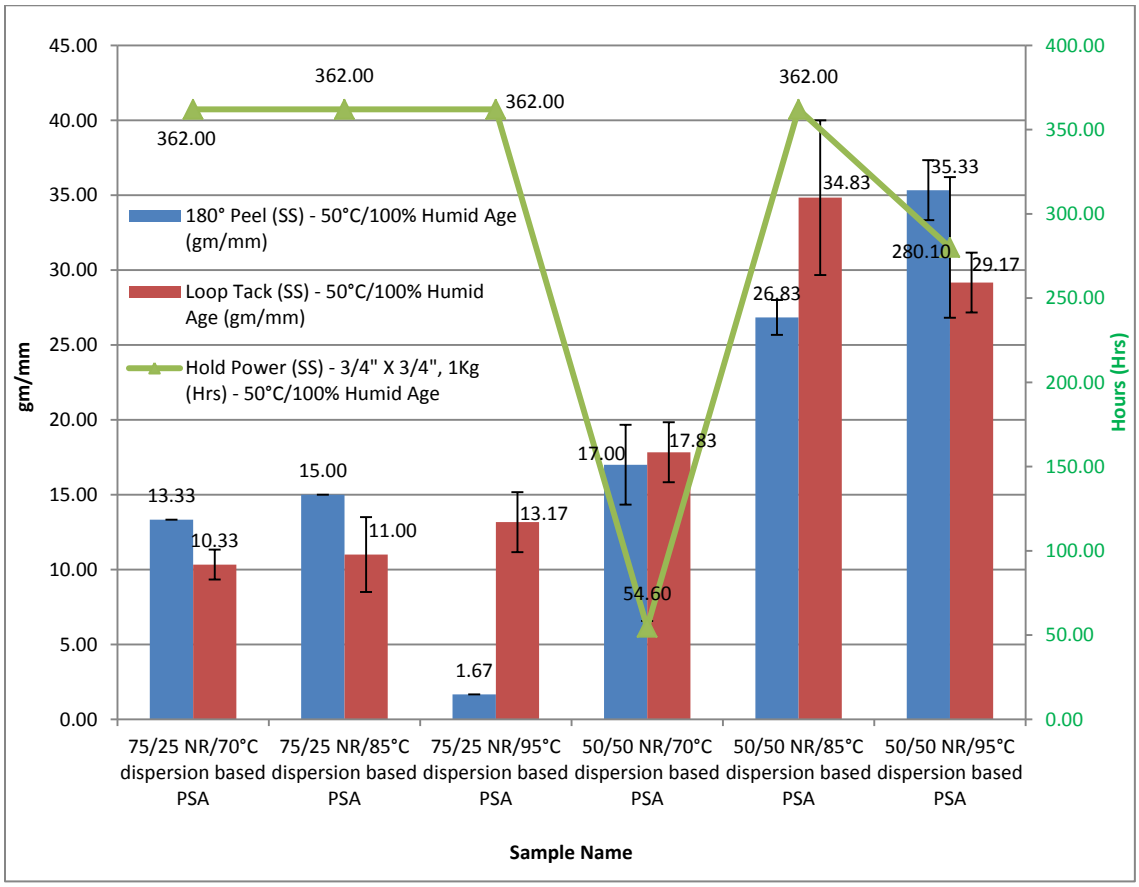

Figure 63. Humid age (50°C and 100% relative humidity) adhesive peel (180° peel), loop tack and shear (hold power) performance of PSAs on stainless steel (SS) substrate

Peel and tack performance for all three PSAs containing 50% tackifier dispersion seem to follow the same trend as room temperature evaluations on LDPE substrate.

Hold power seems to be systematically higher for PSAs containing higher softening point dispersion at 50% addition levels on LDPE substrate.

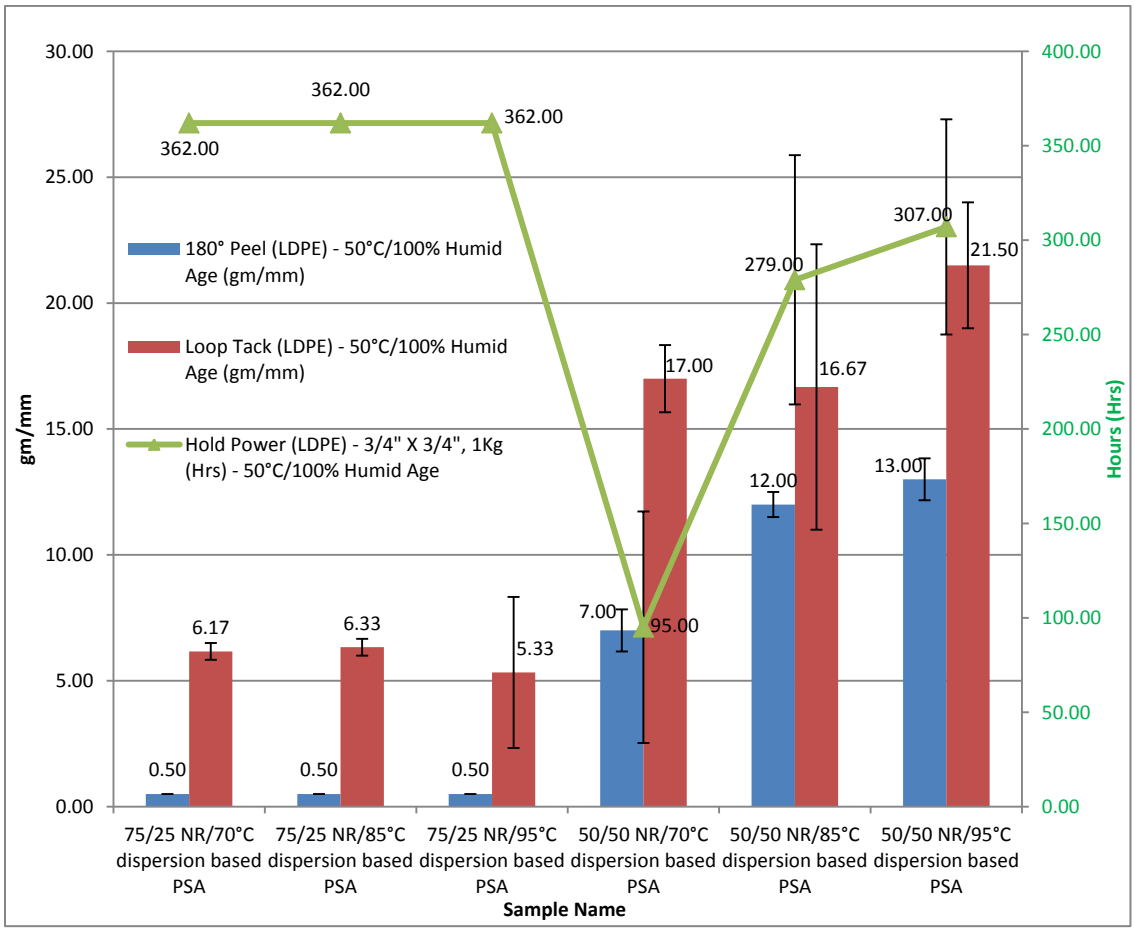

Figure 64. Humid age (50°C and 100% relative humidity) adhesive peel (180° peel), loop tack and shear (hold power) performance of PSAs on low density polyethylene (LDPE) substrate

It should be noted that 95°C tackifier dispersion-based PSAs at 50% resin addition level show the best adhesive and cohesive characteristics on both stainless steel and LDPE substrates, at room temperature and after accelerated humid age evaluations.

Summary and Path Forward

- It was successful in generating a model curve to determine the effect of peel rate (up to 100in/min) on adhesive peel, using universal WLF parameters. Time-temperature superposition experiments revealed that peel rate and temperature have a significant influence on the adhesive peel. It has seen that peel force increases as the peel rate increases for all the water-based PSAs evaluated. Increasing softening point of the tackifier dispersion in the PSA systematically improves the peel.
- 25% addition levels of tackifier dispersion did not show any significant adhesive properties, and the viscoelastic evaluation revealed that the PSA blends containing 25% resin addition level do not satisfy the pressure sensitive adhesive criteria defined by Dahlquist and others. At least 50% tackifier dispersion addition is needed for the PSA blends to meet the defined pressure sensitive adhesive criteria.
- Viscoelastic evaluation also confirmed that all three aliphatic hydrocarbon tackifier dispersions are very compatible up to 50% addition levels with natural rubber latex.
- Adhesive peel, tack and shear property evaluations on a high surface energy substrate (stainless steel) and low surface energy substrate (LDPE) revealed that the time dependent wetting properties of the bulk adhesive are very important in determining the adhesive property characteristics of water-borne PSAs. The PSA containing 95°C tackifier dispersion at 50% resin addition level shows the

optimum adhesive and cohesive characteristics on both stainless steel and LDPE substrates, at room temperature and after accelerated humid aging evaluations.

References

37. W. H. Sheout and H. H. Day, US Patent No. 3965 (1845)
38. D. Satas, *Handbook of Pressure Sensitive Adhesive Technology (2nd Ed.),* Van Nostrand Reinhold, New York (1982)
39. R. G. Drew, GB Patent 312,610 (1930)
40. R. G. Drew, GB Patent 405,263 (1934)
41. T. Sanderson, *Adhesives Age*, 31 (Dec. 1978)
42. W. Demarteau and J. M. Loutz, *Progress in Organic Coatings*, 27, 33 (1996)
43. C. Oldack, R. E. Bloss, *Adhesives Age*, 38 (Apr. 1979)
44. K. F. Gazeley, *1983 Proc. Industry Technical Conference*, *Pressure Sensitive tape Council,* pp. 30-34 (Apr. 1983)
45. I. Benedek and L.J. Heymans, *Pressure Sensitive Adhesive Technology*, Marcel Dekker Inc., New York (1997)
46. D. H. Kaelble, *Physical Chemistry of Adhesion*, pp. 248-254, 471-480, Wiley-InterScience, New York (1971)
47. D. J. Yarusso, in: *The Mechanics of Adhesion*, A. V. Pocius and D. A. Dillard (Ed.), pp. 499-533. Elsevier, New York (2002)
48. C. A. Dahlquist, in: *Hand Book of Pressure Sensitive Adhesive Technology 2nd Ed.,* D. Satas (Ed.), pp. 97-114. Van Nostrand Reinhold, New York (1989)

49. G. Kraus et al., *Journal of Adhesion*, 8, 235 (1977)

50. M. Sheriff et al., *J. Appl. Polym. Sci.*, 17, 3423 (1973)

51. J. B. Class and S. G. Chu, *J. Appl. Polym. Sci.*, 30, 805-842 (1985)

52. S. G. Chu, in: *Hand Book of Pressure Sensitive Adhesive Technology 2nd ed.,* D. Satas (Ed.), pp. 159-203. Van Nostrand Reinhold, New York (1989)

53. *Test Methods for Pressure Sensitive Adhesive Tapes 14th ed***.,** Pressure Sensitive Tape Council (PSTC), Northbrook-IL (2004)

54. D. Satas, in: *Hand Book of Pressure Sensitive Adhesive Technology 2nd ed.,* D. Satas (Ed.), pp. 61-96. Van Nostrand Reinhold, New York (1989)

55. H. J. Kim and H. Mizumachi, *J. Appl. Polym. Sci.*, 56, 201 (1995)

56. C. Derail et al., *Journal of Adhesion*, 64, 123 (1997)

57. H. Lakrout et al., *Journal of Adhesion*, 69, 307 (1999)

58. M. D. Gower and R. A. Shanks, *J. Poly. Sci. Part B: Poly. Phys.*, 44, 1237 (2006)

59. P. M. McGuiggan et al., *International Journal of Adhesion & Adhesives*, 28, 185 (2008)

60. M.L. Williams, R.F. Landel and J.D. Ferry, *J. Am. Chem. Soc.*, 77, 3701 (1955)

61. C.W. Macosko, in: *Rheology Principles Measurements and Applications,* C.W. Macosko (Ed.), pp. 109-126. VCH Publishers Inc., New York (1994)

CHAPTER - 8. OVERLL SUMMARY AND FUTURE WORK

This chapter is divided into two parts. The first part summarizes the interaction of different hydrocarbon tackifier resins with olefinic block polymer-amorphous polyolefin blends, while the second part summaries the effect of different water-based hydrocarbon dispersion on natural-rubber based water-borne pressure-sensitive adhesives.

Part – 1. Olefinic Block Copolymer-Amorphous Polyolefin Blends

Blends of ethylene-octene based olefinic block copolymers with two amorphous polyolefins polymers (atactic propylene homopolymer and ethylene-propylene copolymer) were evaluated at three different ratios. Compatibility and polymer miscibility of the blends was evaluated using Dynamic Mechanical Analysis (DMA), and the morphology of the blends was analyzed using Transmission Electron Microscopy (TEM). Viscoelastic properties of both ethylene-octene olefinic block copolymer blends with amorphous polypropylene polymer, and ethylene-octene olefinic block copolymer blends with amorphous ethylene-polypropylene blends showed incompatibility. Analysis revealed that both blends formed two phase morphologies. The OBC matrix formed the continuous phase, while the amorphous polymers (polypropylene or ethylene-propylene) formed the dispersed phase of the blend morphology. The amount of dispersed phase increased as the amount of amorphous polymer in the blend increased.

Since OBC/PP and OBC/PE-PP polymer blends were immiscible, each exhibiting the T_g of pure blend components and a heterogeneous morphology, a compatibilizing agent is needed to improve the miscibility characteristics of the polymer system. The effect of different low molecular weight hydrocarbon resins was evaluated as compatibilizing and tackifying agents to improve the interfacial adhesion (miscibility) characteristics between the two polymers and also to effectively tackify the polymer system to improve the pressure-sensitive adhesive characteristics. One aliphatic and two aliphatic/aromatic unsaturated resins with varying aromatic content (5% and 14%) were evaluated to understand the effect of aromatic content on blend miscibility as well as a saturated cycloaliphatic hydrocarbon resin and a saturated linear aliphatic-cycloaliphatic hydrocarbon resin were evaluated for this study to understand the structural influence on the blend miscibility (OBC/PP and OBC/PE-PP). A 1:1 polymer blend ratio of OBC/PP and OBC/PE-PP was selected for this study to better understand the influence of resin addition at three different levels 20 wt%, 30 wt% and 40 wt%. Dynamic mechanical analysis and transmission electron microscopy evaluations were performed to determine the blend miscibility characteristics. The fully aliphatic resin seems to improve the miscibility of the OBC/PP blends at higher resin addition levels. No improvement was observed for the OBC/PP/resin blends as the aromatic content of the resin increases. However, OBC/PE-PP blends showed improved miscibility with increasing aromatic content. A ternary phase morphology was particularly observed for both OBC/PP and OBC/PE-PP blends with highly aromatic (14%) unsaturated

hydrocarbon resin, in which OBC formed the continuous phase, and PP, PE-PP and unsaturated hydrocarbon resins formed the dispersed phase.

On the other hand, we did not observe much difference in miscibility characteristics between the two saturated resin chemistries in both blend systems (OBC/PP and OBC/PE-PP). At lower saturated resin addition levels (20 wt%), both blends (OBC/PP and OBC/PE-PP) showed immiscibility behavior irrespective of the resin chemistry, while at higher saturated hydrocarbon resin addition levels OBC/PP and OBC/PE-PP blends showed a single T_g, indicating miscibility with both resin chemistries. A continuous and a dispersed phase morphology were observed for both ternary blends using both saturated hydrocarbon resin chemistries. The Harkins spreading coefficient concept was used to better understand the ternary blend dispersed phase morphology. Spreading coefficients predict that the free unsaturated hydrocarbon resin and saturated hydrocarbon resin is encapsulated by the amorphous PP or amorphous PE-PP polymer in the dispersed phase for the respective blend compositions, as was found in the experiments.

Based on the learning from blend miscibility studies, it has successfully made disposable diaper type pressure-sensitive adhesives with OBC/PE-PP blends, containing unsaturated hydrocarbon resins and saturated hydrocarbon resins. OBC/PE-PP blends based disposable diaper construction adhesives showed good sprayability characteristics, when applied using an air assisted spiral spray equipment, Acumeter Spray Coater. It can be concluded that OBC/PE-PP based PSA formulations can be

applied at lower applications temperature (from viscosity profiles), and these formulations show good formulation latitude with good tolerance for different hydrocarbon resin chemistries (especially saturated aliphatic and slightly aromatic-aliphatic unsaturated resins), with most of them giving good adhesive performance properties, when compared to the comparative SBS based control material.

If this work is extended in the future, it is suggested that some fundamental molecular modeling work be done to better understand the miscibility characteristics and F-H interaction parameters. This may lead to significant learning and predictive possibilities in the interaction between the components of the ternary blend systems. Further work on disposable diaper construction adhesives sprayed at lower temperatures would be beneficial to employ thinner substrates, faster speed and energy savings. An extension of this work would be performed with olefinic block copolymer blends with functionalized polyolefins (such as maleated polyolefins) to obtain better adhesive performance in pressure sensitive adhesive tapes.

Part – 2. Hydrocarbon Tackifier Dispersion Containing NR Based Water-Borne PSAs

The effect of three water borne aliphatic hydrocarbon tackifier dispersions each with different softening points (70°C, 85°C and 95°C) were evaluated with natural rubber latex at two addition levels (25% and 50%) for pressure-sensitive adhesive (PSA) applications. No other additives were incorporated into the PSA formulations so that rheological effects of waterborne aliphatic hydrocarbon tackifier resin dispersions in Natural rubber-based PSAs could be clearly understood. Application of these water

borne PSAs was evaluated, in terms of rheology, since flow parameters have very important influence in the convertibility (coating ability) of such adhesives. Morphological correlations with wet rheology for these water borne PSA formulations and starting materials revealed that the interaction between the latex particle and tackifier dispersion particle has a major influence in determining the viscosity characteristics at low to medium shear rate, where stirring, pumping and filtration processes occur. Tackifier dispersion rheology and morphology are greatly affected by the type and amount of surfactant/dispersing agents employed. A shear thinning effect was also predominant in formulations with lower tackifier dispersion levels. The extent of shear thinning can be correlated well to morphology. Tackifier dispersion rheology and morphology are greatly affected by the type and amount of surfactant/dispersing agents employed.

Correlation of viscoelastic behavior with adhesive properties of theses water-borne PSAs suggests that at least 50% resin addition level is needed to bring the natural rubber-based formulations into PSA criteria as defined by Dahlquist and others. Adhesive property evaluations performed on a high surface energy substrate (stainless steel) and low surface energy substrate (LDPE) suggested that optimum tack, peel and shear properties at room temperature were obtained for a formulation containing a higher softening point dispersion (95°C) at 50% resin addition level. Adhesive peel and tack tend to follow softening point trends as well. Time-temperature superposition analysis using the WLF approximation for adhesive peel has revealed that the adhesives formulated with 50% resin addition level show good adhesive behavior. The application

of the WLF relation was not only useful in modeling adhesive behavior, which appears to be a novel application of the relation, but it may also be useful in predicting likely material performance under other conditions and thus useful in formulating new adhesives and their applications. The time-temperature superposition analysis showed that peel force increases systematically with softening point and peel rate.

It is suggested that further work with hydrocarbon tackifier dispersions containing similar emulsifying systems but with different softening points may be valuable in better understanding the emulsifier effect on the application (wet) rheology of these PSAs.